



# **Bike System**

Senior Design 2

Spring 2021

Group 21

Keegan Van Wyk – EE  
Daniel Birath – EE  
Benjamin Tamayo – EE  
Sandhya Singh – CpE

## Table of Contents

1. Executive Summary	1
2. Project Description	3
2.1 Motivation and Goals	3
2.2 Requirement Specifications	4
2.3 Bike System's House of Quality	7
3. Technology Research & Parts Selection	9
3.1 Parts & Technology Research	9
3.1.1 Power Subsystem	9
3.1.2 Sensors Technology	22
3.1.3 Locking Mechanism	29
3.1.4 Lighting Subsystem	32
3.2. Parts Selection	37
3.2.1 Power Subsystem	37
3.2.2 Sensors Parts Selection	45
3.2.3 Microcontroller Parts Selection	54
3.2.4 LCD Parts Selection	57
3.2.5 LED Parts Selection	60
3.2.6 LED and Locking Mechanism Driver	62
3.2.7 Permanent Magnets	63
3.2.8 Locking Mechanism	65
4. Standards & Design Constraints	68
4.1 Standards	68
4.1.1 LED Standards	68
4.1.2 Supply Voltage Standards	69
4.1.3 Software Standards	70
4.1.4 Communication Standards	74
4.2 Design Constraints	77
4.2.1 LED Array	77
4.2.2 Locking Mechanism	78
4.2.3 Bike System Enclosure	78
4.2.4 Time Constraints	78
4.2.5 Experience Constraints	79
4.2.6 Resource Constraints	80
5. Bike System Design	81
5.1 Hardware Design	81
5.1.1 Power Subsystem Design	81
5.1.2 LED Array Design	93
5.1.3 Microcontroller Design	101
5.1.4 LCD Design	105
5.1.5 Sensors Design	106
5.1.6 RFID Module Design	110
5.2 Bike System Software Design	114
5.2.1 Software Functionality	115
6. Overall Integration	119
7. Administration	122

7.1 Software Tools	122
7.1.1 Communication	123
7.1.2 Development	123
7.2 Project Milestone	122
7.3 Estimated Budgeting and Financing	124
8. Conclusion	126
Appendix	A-1
A.1 References	A-1
A.2 Copyrights	A-2
A.3 Corrections	A-3
A.4 Source Code	A-7

## List of Figures

Figure 1: Block Diagram for Prototype	6
Figure 2: House of Quality	8
Figure 3: Generator (left) and Dynamo (right) <sup>[1][2](2)</sup>	10
Figure 4: Dynamo Rectified & Filtered Output	11
Figure 5: Simplified Linear Voltage Regulator <sup>(1)</sup>	12
Figure 6: Switching Regulator Duty Cycle <sup>[3](3)</sup>	13
Figure 7: Simplified Switching Regulator in a Buck Configuration <sup>(1)</sup>	13
Figure 8: Switching Regulator Voltage Smoothing <sup>[3](3)</sup>	14
Figure 9: Simple Voltage Divider <sup>(1)</sup>	15
Figure 10: Zener Diode I-V Plot <sup>[4]</sup>	16
Figure 11: Example Bandgap Reference IC (LT1004) <sup>[5](4)</sup>	17
Figure 12: Simple Battery <sup>[6](2)</sup>	18
Figure 13: Simple Comparator Operation <sup>[14](2)</sup>	20
Figure 14: Comparator Output Oscillations due to Signal Noise <sup>[17](1)</sup>	21
Figure 15: Hysteresis <sup>[18]</sup>	21
Figure 16: Hall Effect Demonstration	22
Figure 17: Block Diagram of Hardware used in RFID Reader	23
Figure 18: Block Diagram of Hardware used in RFID Tag	24
Figure 19: An example of an active tag (left) versus a passive tag (right)	25
Figure 20: Inductive Coupling Example	26
Figure 21: Typical Backscatter Communication Architecture	27
Figure 22: A typical cam lock	29
Figure 23: Three Options for Delivering Power to LEDs and Automated Lock	34
Figure 24: Simplified Buck-Boost Converter Schematic	35
Figure 25: Simplified Boost Converter Schematic	35
Figure 26: Simplified Direct Power Transfer Schematic	36
Figure 27: Different Bike Dynamo Configurations to Generate Power <sup>[7][8][9]</sup>	38
Figure 28: Lowrider Dynamo Generator <sup>[11]</sup>	39
Figure 29: QFN-20 and TSSOP-8 Packages (Not to Scale) <sup>[12][13]</sup>	41
Figure 30: Clip-on Bike Thermometer	52
Figure 31: Bimetallic strip functionality	52
Figure 32: Standalone Thermometer-Clock	53

Group 21  
EEL 4915

Figure 33: TI MSP430G2553 (Courtesy of Texas Instruments Inc.)	55
Figure 34: TI MSP430FR6989 (Courtesy of Texas Instruments Inc.)	55
Figure 35: Arduino ATmega328P	56
Figure 36: LCD-20x4Y display	58
Figure 37: SunFounder 1602 LCD Module	58
Figure 38: HiLetgo IL19341 Touch Display	59
Figure 39: Configuration 1 of LTPL-P00DWS57 High Power LED	60
Figure 40: Configuration 2 of LTPL-P00DWS57 High Power LED	61
Figure 41: Configuration of 158301240 Ceramic LED	61
Figure 42: Axially and Diametrically Magnetized Magnets Differences	63
Figure 43: Magnetic Field Visualization	64
Figure 44: Inertial Reel Assembly	66
Figure 45: Top Release Lock Assembly	66
Figure 46: Side Release Lock Assembly	66
Figure 47: OSHA Requirements for Illumination Levels	68
Figure 48: Lux Values for Surfaces Illuminated by Different Surfaces	68
Figure 49: Software Development Life Cycle	71
Figure 50: MFRC522 MC Detecting Digital Comm Interfaces Pinout	74
Figure 51: Typical UART packet reception and transmission diagram	76
Figure 52: Typical SPI communication frame	77
Figure 53: Power Subsystem Diagram <sup>(1)</sup>	81
Figure 54: Power Input Stage Circuit <sup>(1)</sup>	82
Figure 55: Dynamo Output	82
Figure 56: Voltage Rectification <sup>[15]</sup>	83
Figure 57: Input Voltage After Regulation	84
Figure 58: Power Switching Stage Circuit	85
Figure 59: Charging and Battery Stage Circuit	87
Figure 60: Power Output Stage Circuit <sup>(1)</sup>	90
Figure 61: Power Subsystem Board Layout	91
Figure 62: Breadboard Testing	91
Figure 63: Assembled Power Subsystem Testing	92
Figure 64: LED Schematic	93
Figure 65: n X m LED Array with m Parallel Strings of n LED's in Series <sup>(1)</sup>	94
Figure 66: Ideal LED Array Configuration 1 <sup>(1)</sup>	95
Figure 67: Buck Boost Converter <sup>(1)</sup>	99
Figure 68: Integrated Buck-Boost LED Driver <sup>(1)</sup>	99
Figure 69: Common-Gate Amplifier	100
Figure 70: Duty Cycle comparison	101
Figure 71: Microcontroller Circuit	102
Figure 72: Example of parallel transmission vs serial transmission	103
Figure 73: LCD Schematic	105
Figure 74: LCD Breadboard testing	106
Figure 75: Temperature Sensor Schematic	107
Figure 76: Hall Sensor with actuating permanent magnet present	108
Figure 77: Terminal Output When Magnet was Present vs. Not Present	109
Figure 78: Schematic of RFID Module Design	110

Figure 79: MFRC522 Pin Map	111
Figure 80: User being prompted to scan a Master Tag	113
Figure 81: Setting a Master Tag	113
Figure 82: Denial of access	113
Figure 83: Adding a tag after the Master Tag is scanned	114
Figure 84: Algorithm Logic Flowchart	115
Figure 85: Use Case UML Diagram	116
Figure 86: Prototype of Welcome message	117
Figure 87: Prototype of Home Screen	117
Figure 88: Bike System Block Diagram <sup>(1)</sup>	119
Figure 89: Bike System Main Board Overall Schematic	120
Figure 90: Bike System Secondary Board Overall Schematic	121

## **List of Tables**

Table 1: Tiers of specifications/goals for the Bike System	4
Table 2: Demonstratable Requirements	5
Table 3: Voltage Regulator Technology Comparison	14
Table 4: Voltage Reference Comparison	17
Table 5: Comparison of operable RFID frequency ranges	28
Table 6: Locking Mechanism Comparison Impact	31
Table 7: Lighting Comparison Using 60w Incandescent as Reference	34
Table 8: LED Power Delivery Comparison Impact	36
Table 9: Lock Mechanism Power Delivery Comparison Impact	37
Table 10: Dynamo Parts Comparison	38
Table 11: Battery Technology Comparison	39
Table 12: Power MUX Part Comparison	40
Table 13: First Voltage Regulator Stage Parts Comparison	43
Table 14: Second Voltage Regulator Stage Parts Comparison	43
Table 15: Voltage Reference Parts Comparison	44
Table 16: Battery Charging IC Parts Comparison	44
Table 17: Reed Switch Parts Comparison	46
Table 18: Hall Sensor Parts Comparison	48
Table 19: RFID Module Parts Comparison	50
Table 20: RFID Tag Parts Comparison	51
Table 21: Temperature Sensor Comparison	54
Table 22: Microcontroller Parts Comparison	57
Table 23: LCD display comparison	59
Table 24: Comparison Table for Different LEDs	62
Table 25: Driver Comparison	63
Table 26: Magnate Comparison	65
Table 27: Push Solenoid Comparison	67
Table 28: Power Mux Logic Table	86
Table 29: LED Configurations	94
Table 30: Milestones	122
Table 31: Financial Budget and Expenses	124



# **1. Executive Summary**

The bicycle is a vital form of transportation for millions of people around the world today. Many security systems already exist to secure bicycles to bicycle racks or fixed objects, but they are not always sufficient. Additionally, bicycle owners who do not own or choose not to wear a smartwatch, such as an Apple Watch or Fitbit, have no way to track metrics such as calories burned, distance traveled, or the speed at which they are traveling when they are cycling. The solution to this need is the Bike System.

The Bike System will be designed to maximize portability, such that it will fit most, if not all, popular bicycle designs. The Bike System also aims to maximize on convenience for its users. By maximizing convenience, the user will save time every time they want to lock or unlock their bicycle. In order to achieve this design goal, an RFID scanner will be available so that the user can swipe an RFID card across an RFID reader to have the locking mechanism lock or unlock in seconds – much faster than traditional bicycle locking systems already on the market. In the odd event that the Bike System is out of power, the user is provided a key to manually unlock and lock their bicycle. Metrics such as calories burned, distance traveled, and speed for the current trip will be displayed continuously on the LCD display once the bicycle is unlocked and in motion. The user will also be able to choose which metric is displayed on the LCD display by using one of three buttons on the electronics housing. By allowing the user to cycle through which metric is being currently displayed on the LCD display, the information is displayed larger, thus taking the user less time to interpret the displayed information and as a result, not become distracted while riding. This is one of the many features on the Bike System that prioritizes safety.

This Bike System also includes the addition of lights as another safety measure that will be mounted on the bike frame itself. If the user chooses to ride his/her bicycle at night, he/she would need to be visible to both pedestrian and motor traffic. With lights mounted to the bike frame itself, the bicycle will be visible from hundreds of feet away. To make the Bike System circuitry as reliable as possible, rubber washers will be installed between the bike frame and the electronics in order to minimize vibrations that will eventually cause wear and tear on the system. The system will also be battery powered and will emphasize long lasting battery life by making the circuitry as energy efficient as possible.

Should time permit, there are many other features that can be implemented to the Bike System to offer the user more convenience and reliability. For example, making the electronics housing waterproof and thermal resistant is currently listed as advanced features under the engineering specifications listed in Section 2.2. Having an electronics housing that is both waterproof and thermal resistant will add to the overall reliability of the Bike System since water can cause short circuit conditions and high temperatures can cause solder joints to melt. If both of these sources of error were to be eliminated, or minimized, by a secure electronics housing, the Bike System would become more reliable and would need very

minimal maintenance. Another advanced feature to be implemented is the ability to unlock and lock the system with the user's fingerprint. This feature is a failsafe in the rare case that the user does not have the RFID tag or the key to manually unlock or lock the system. This serves a perfect failsafe since the user would always have their fingerprint.

A stretch feature that would offer the most convenience to the user would be the implementation of an alternate power source that would allow for the on-board battery to be charged while the user is cycling. The alternate power source would be a generator that will generate power from the mechanical energy transferred from the user. If the battery is fully charged, the power from the generator could be used to take over the most power draining features such as the lights mounted on the bicycle frame or the LCD display. This alternate power source will allow the user to go for longer periods of time without having to remove and charge the battery. Ideally, the battery, in conjunction with the alternate power source, should last for weeks at a time without needing to be removed from the electronics housing to be charged.



## **2. Project Description**

This section provides an overview of the Bike System's requirements and the motivation behind the project. Also, there is an overall diagram of the Bike System's major function blocks to help illustrate the idea.

### **2.1 Motivation and Goals**

There are many options for high-tech bicycles these days. Many of these bikes include the use of some form of electric propulsion that can greatly ease or even eliminate the need for the rider to pedal. However, most of these solutions are rather expensive, and such are only appealing to those who have a specific need for them. For instance, someone with the intention of using a bike for exercise would not really benefit from an electric bike. This then begs the question, what about all the other people?

The motivation behind this project is to improve the experience of riding a bike in a way that is simple and inexpensive. Improving the experience for the rider can be done by adding a few features to an existing bike, such as a speedometer and odometer. By making the system simple to where it can easily attach to an existing bike frame and eliminate the need to buy an expensive specialized bike. By doing this, the design team hopes to expand the possible customer base, as compared to electric bikes.

Table 1 summarizes our goals. The Bike System specifications have been broken down into tiers based on importance/vitality of the Bike System. The basic goals such as the RFID module and manual key module are fundamental to the Bike System's claim of convenience to the user. The manual key module also serves as a secondary security measure that most people are familiar with. This ensures that power failure does not leave the user and his/her bicycle vulnerable and unrideable. Although the added lights to the bicycle frame are a small feature, the lights would give the user added visibility that traditional bicycle reflectors do not provide. In an effort to extend the life of the Bike System and minimize wear and tear, rubber mounted washers will be utilized. Sensors attached to the wheels to measure distance and speed which would be displayed on the mounted LCD display are the barebones of the Bike System design.

The fingerprint module will be added as an advanced feature since two different modes for unlocking/locking the bicycle have been discussed. This is the ultimate failsafe (power permitting) since the user always has their fingerprints with them (unlike a key or RFID tag). The ambient temperature is an advanced feature since it is not a vital part of the Bike System design, but it may be useful to the user to know this information due to Florida's daily fluctuating temperatures. Waterproofing and insulating the electrical system is directly tied into the types of weather experienced in Florida. The unexpected rains will not be a concern to the user if all the electricals are waterproofed. Similarly, the outside high temperatures

may affect the Bike System's equipment and damage certain sensors if not considered.

*Table 1: Tiers of specifications/goals for the Bike System*

<b>Basic Goals</b>	<b>Advanced Goals</b>	<b>Stretch Goals</b>
RFID module as the main locking/unlocking method	Fingerprint locking/unlocking method as a failsafe	GPS tracking module added to system to locate the bike
Alternate mechanical method of unlocking/locking the bicycle in the event of power failure	Thermometer added to Bike System to measure the ambient temperature as an additional metric	Creation of mobile app to save the metrics being measured during each trip via a Bluetooth module
Added lights to frame for safety precautions	Waterproofing/Insulation of the box housing the electrical components	Generate power/charge from the bicycle itself, instead of having replaceable batteries
Rubber mounting washers for shock resistance	-	-
Mounted LCD on handlebars to display metrics	-	-
Sensors attached to the bicycle's wheels to measure distance travelled and calculate average speed	-	-

## 2.2 Requirement Specifications

- Inclusive bike locking system that can be attached to a pre-existing bike frame:
  - The locking mechanism will be housed in a box which can be attached and secured to the bike frame via a clamping lock.
  - The Steel cord will extend from the housing at one end and will be secured in the opposite end.
  - The housing will contain all circuitry.
- Main marketed method of locking/unlocking via RFID module:
  - RFID tag will be housed/attached to a keychain to make this "key" more user-friendly.
- Failsafe method of locking/unlocking via fingerprint:
  - A fingerprint module will be easily accessible on the housing. Once the fingerprint is processed, the locking mechanism will release allowing the user to stow the tethered cable.

- Alternate unlocking mechanism in the case of low power:
  - A key will be supplied to unlock the system in the event of low battery.
- LCD Display:
  - Display speed, ambient temperature, and distance traveled on LCD will be mounted on the handlebars of the bicycle for easy viewing.
  - The current battery level of the internal battery pack will be displayed.
- Measure revolutions of wheel and tire assembly:
  - Sensor mounted to the frame to measure the revolutions of the wheel and tire assembly to calculate speed and distance traveled.
- Additional lights mounted on bicycle frame as a safety measure.
- Rubber mounting washers will be used for shock resistance.
- Waterproofing and insulation of the entire electrical box system to make the system weatherproof and extend the lifespan of the entire Bike System.
- GPS module added to Bike System to help locate bike in event of theft.
- Creation of a mobile app to save the metrics (health data, ambient temperature, distance, and average speed) from each trip.
  - Metrics can be sent/saved to the app by a Bluetooth module.
  - Possible Google Maps integration to give more insight on the location of the user's trips.
- Generator:
  - A DC power generator with drive pulley will be fixed to the frame of the bike to charge the battery.
    - Drive pulley will connect to the existing drive chain on the bicycle.
  - In the event there is not enough power to operate the system, riding the bike will supply enough power to bring the system back online.

Table 2 shows a list of the engineering requirements listed above with three of the requirements that will be demonstrated at the end of Senior Design highlighted.

*Table 2: Demonstratable Requirements*

Requirement	Required Metric
RFID Lock Unlock Time*	<5s
Odometer*	±1ft
LED Light*	>50 Lux
Weight	<5 lbs.
Cost	<\$150
Power	≤3W
Installation time	<30 Min

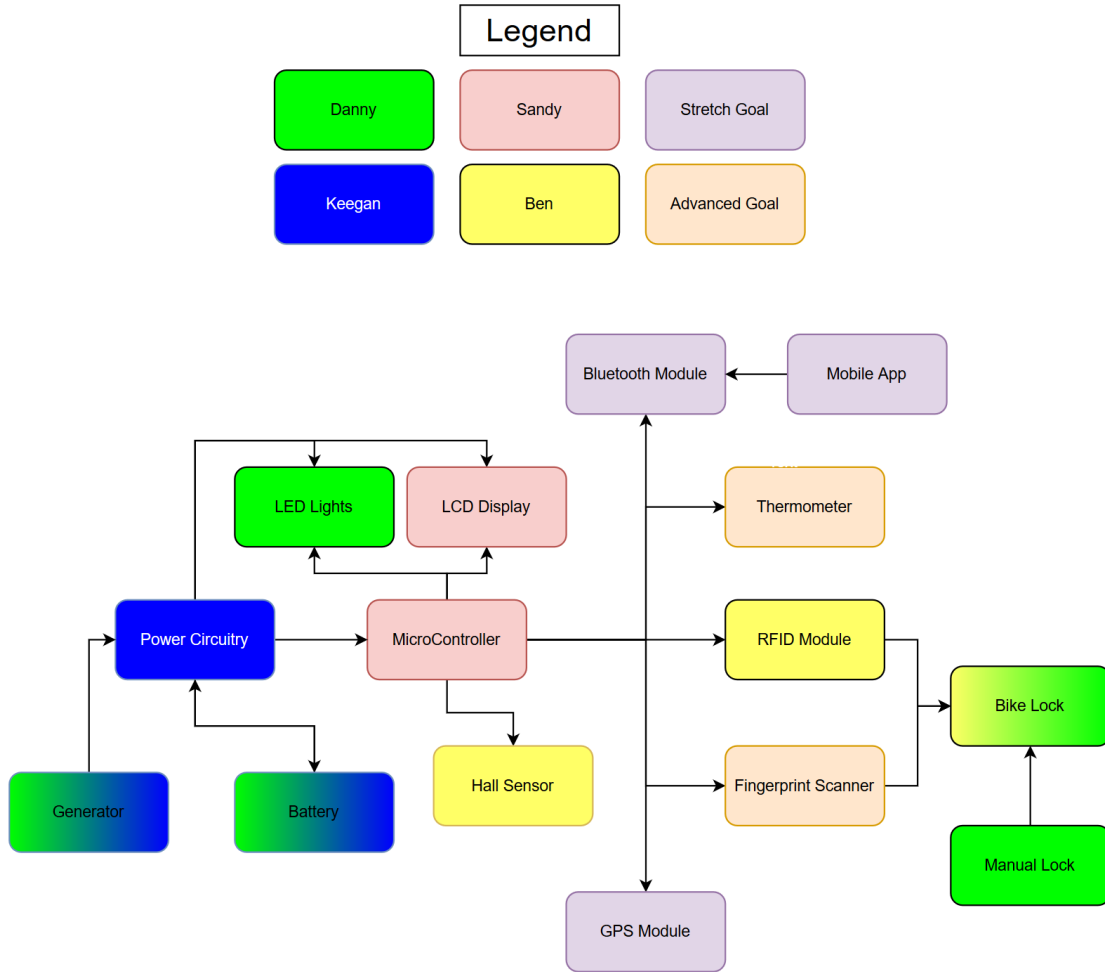


Figure 1: Block Diagram for Prototype

## 2.3 Bike System's House of Quality

The house of quality designed will describe in a systematic way, all the critical engineering requirements as well as the critical marketing requirements. To bring this product to market, several key areas must be met to make it desirable. Looking deeply into the customers interests, five areas were found that the project team wanted to meet. Engineering requirements are the main focus relating to how the marketing requirements will be met. There are seven key areas within the engineering requirements that need to be addressed to entice consumer interest.

It is desirable for the product to be attractive to the consumer and have employed methods to attain this goal. First, the focus is on user convenience. If the product is easy for the user to understand and use, it will be more attractive to them. This can be achieved by incorporating an easy-to-use LCD to display the information that utilizes three buttons at most. Making the product more convenient also includes installation and setup. It is desired to include a primary system, secondary system, and emergency system to lock or unlock the system. Including a seamless method for securing the box to the bike will also be a key task for development.

Next, the box is to be molded to the bike to provide a streamline, aerodynamic casing that will not impede on the riders' natural motion. Designing an aerodynamic case will reduce drag and frustration by the rider. Included in the marketing requirements, the user's upkeep for the product will be kept minimal. By reducing the maintenance of the lock system, the attractiveness of the product increases. Lastly, the battery life is ensured to be long lasting and reliable. A low-power mode will be utilized to save energy while the bike is not in use.

The engineering requirements is where all the magic happens. First, a power generation system will allow the user to continuously charge the batter and power the system in the same way an alternator does in a vehicle. Overall, it is to be expected a minimal draw of power within the lock system providing opportunity for a long battery life. Next, it is desired that power is saved where applicable and design an energy efficient system. This means reducing the loss of power when the user is on the bike and not moving. Lastly, the box dimensions and install time are crucial to the success of this product. By providing the user a way to easily mount and unmount the bike system is as important as giving the user the illusion that the system is not even there.

The design team believes that the mix of marketing requirements will make this product attractive enough to warrant attention and the engineering requirements will pave the path for future bike systems. Incorporating this system into an existing bike will provide a convenient and reliable way for the user to upgrade their status in an ever-changing world.

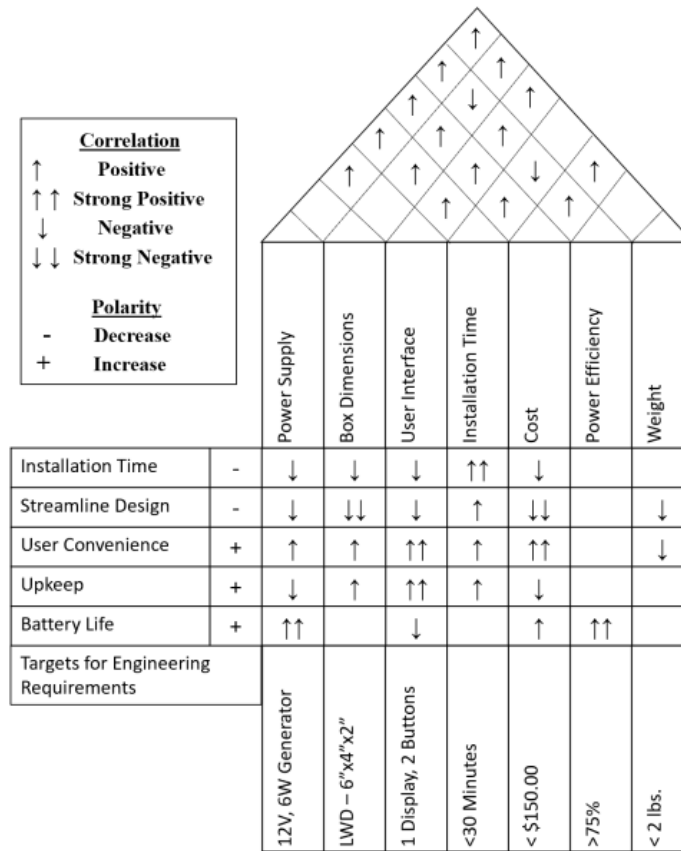


Figure 2: House of Quality

## 2.4 Senior Design II Changes

During the course of Senior Design II, it was decided that some of the Bike System’s requirements and specifications would change in order to best address the needs of the project. One change was the removal of any real specifications or requirements that were more mechanical in nature, such as mounting rubber shock absorbers, waterproofing, etc. This was done to allow the group to focus more on the electrical and computer related aspects of the bike, to better demonstrate the group’s skills and knowledge obtained while in pursuit of their degree. Also, there were some additions to the specifications and requirements. One addition was to make the LED lights dim depending on the ambient light. A photoresistor was used in an operational amplifier circuit to dim the lights according

to the sensitivity at which the photoresistor receives photons. Due to the design of the photoresistor, an operational amplifier was needed to inverse the characteristics of the device. This was needed because as the light intensity decreased, the resistance of the photoresistor increased. For the LED's to turn on when it is dark, the photoresistor was used in a voltage divider which was connected to the non-inverting terminal of the operational amplifier. Next, due to the EMI generated from an electromagnet and the proximity to the antenna for the RFID, we used a servo motor to rotate an arm 90 degrees to lock or unlock the locking mechanism. The power requirements of the two devices are almost identical and was an easy replacement for the electromagnet.

### **3. Technology Research & Parts Selection**

Before parts can be acquired, let alone assembled, for the Bike System, careful research into various technologies and parts much be done. This is to ensure that the technologies and parts researched and selected will work together, while mitigating the need for redesign and repurchasing parts. This section details this process for the Bike System design.

## **3.1 Parts & Technology Research**

This section covers the research done into a variety of different parts and technologies that are to be utilized in the Bike System. This section is broken up into major subsystems of the Bike System, and then those sections are further broken down into various subsections.

### **3.1.1 Power Subsystem**

This section details the relevant technologies that were considered for the design of the Bike System's power subsystem. See Section 3.2.1 for the part selection for the power subsystem.

#### **3.1.1.1 Generator/Dynamo**

In order for the various electronics on the bike system to work, there is a need for a power source. The Bike System will be using a battery to power the system; however, to keep upkeep to a minimum, the system will introduce a method charging the battery via mechanical energy. Since there is an abundance of mechanical energy generated by the rider, it would be an excellent source for additional power.

A way to harness mechanical energy and convert it into electrical energy is with the use of generators. The conversion of mechanical energy to electrical energy can be accomplished by taking advantage of the relation between magnets and electricity, or Faraday's Law of Electromagnetic Induction. When a conductor is in the presence of a moving magnetic field (or vice versa), a voltage and current are induced in the conductor. Generators work by rotating a conductor in a stationary magnetic field, while a dynamo works by rotating a magnet in the presence of

conductors (see Figure 3). The output voltage and current of these devices are varying, so if a load needs steady values, such as most electronics, there will need to be some form of rectification and regulation.

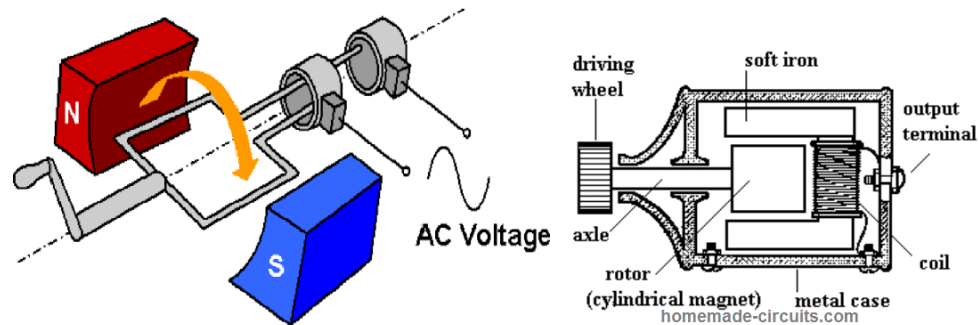


Figure 3: Generator (left) and Dynamo (right)<sup>[1][2](2)</sup>

These technologies can be utilized to take the rotational energy inherent to the operation of riding a bike and convert it into usable electric power. This electric power can then be used to power the Bike System's electronics and charge the batteries when the bike is in use.

### 3.1.1.2 Voltage Regulation

As electronics get smaller and more precise, the need for a steady source of power is needed. This is due to the fact that slight variations in the supply voltage to an electronic component or circuit can propagate through and greatly affect the output of that component/circuit. To address this issue, equal advancements in the methods of voltage regulation have kept in step with the need for more steady input power.

Most power is generated with varying or alternating current, which results in vary unsteady power. After rectification and smoothing, the instantaneous voltage value will vary from the average value (usually referred to as the DC value). The amount of this variation is called the ripple. The main goal of voltage regulators is to mitigate this ripple as much as possible. By doing so, the voltage regulator output becomes very steady, which is needed for sensitive electronics.

The need for a regulator for this project is crucial. This is because the power generated from a generator or dynamo will not be steady, and a steady voltage is needed to power the electronics of the Bike System and to charge the battery. Figure 4 shows the dynamo's rectified output under load. A significant ripple voltage (about 500 mV) can be seen for the shown ~7.5V output, which clearly demonstrates the need for a voltage regulator.



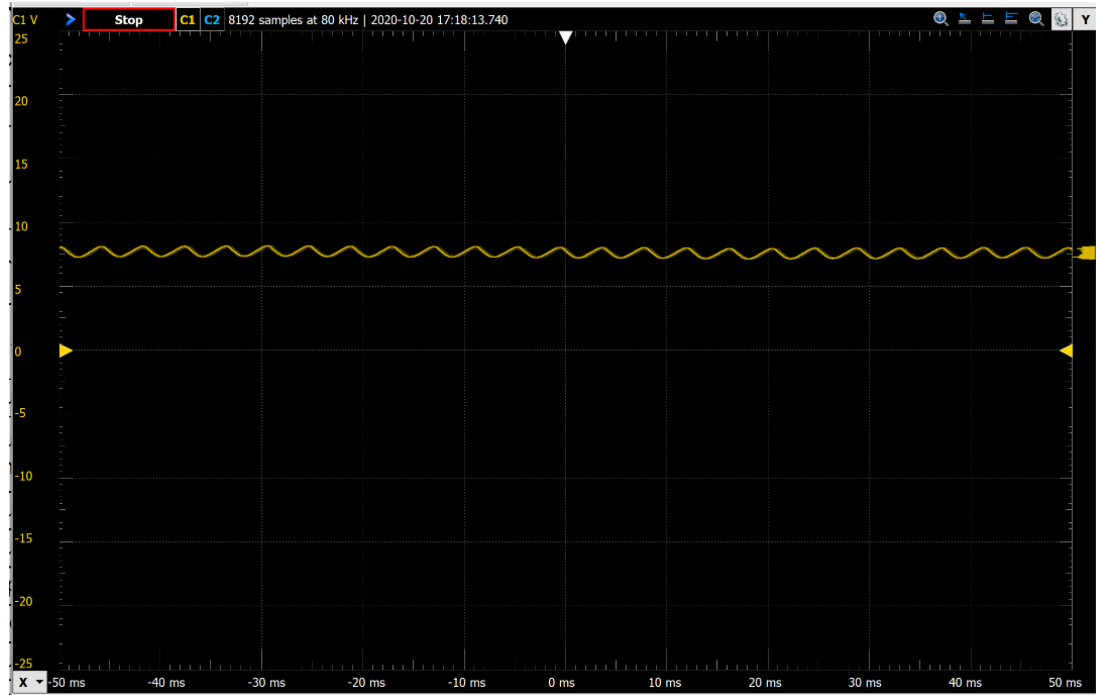


*Figure 4: Dynamo Rectified & Filtered Output*

While it is clear that voltage regulation serves a vital purpose, it does not come without some drawbacks. One drawback is power losses caused by the voltage regulator. While some regulators can achieve percent power efficiencies in the high 90s, there will always be some power lost due to the regulation. In addition to this, most regulators need to receive a higher voltage at their input than their regulated output. The lowest voltage that the regulator can receive while still producing the regulated output is referred to as the drop-out voltage (since regulators output will “drop-out” below that voltage).

There are two main categories of voltage regulators, linear and switching. To achieve a better understanding to the differences of these two regulator types, both the linear and switching regulators are discussed in Sections 3.1.1.2.1 and 3.1.1.2.2, respectively.

### **3.1.1.2.1 Linear Regulators**

The operation of a linear regulator is fairly straight forward. What a linear regulator does is continuously control the flow of current from the source to the load, and by doing so, control the voltage at the load. This simple concept is built on the foundations of Ohm’s Law:  $V = IR$ . As it can be gathered from Ohm’s Law, a change in the current results in a proportional change in voltage. Thus, if the voltage at the load begins to dip, the regulator increases the flow of current to the load to compensate, and the opposite for a voltage spike. A simplified circuit diagram is shown in Figure 5 to help illustrate this operation.

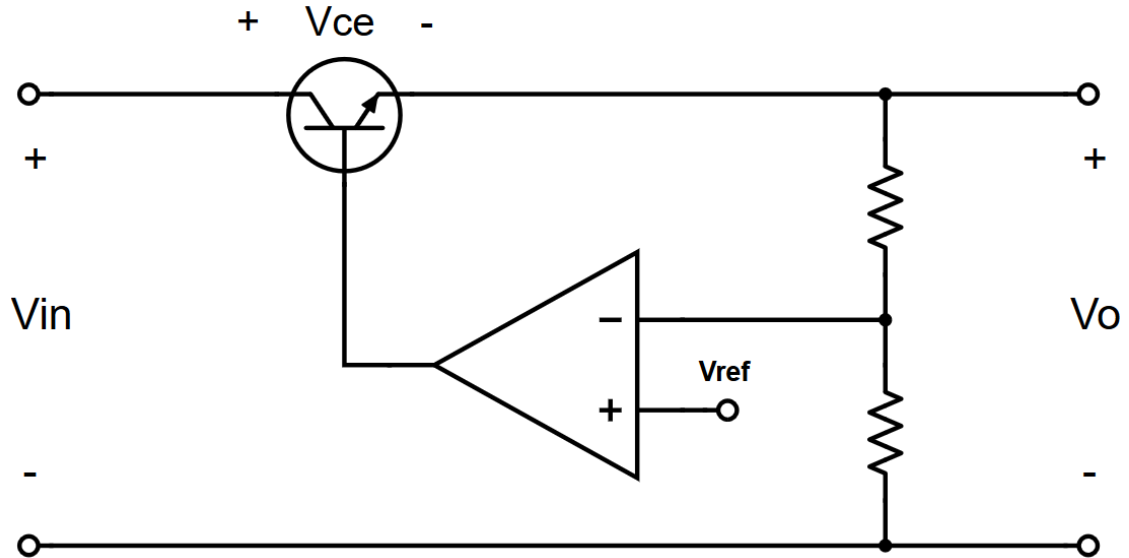


Figure 5: Simplified Linear Voltage Regulator<sup>(1)</sup>

In Figure 5 a bipolar junction transistor (BJT) and an operational amplifier (OPAMP) are used to control current flow. The resistor divider serves to take a sample of the output so that the OPAMP can compare it to the voltage reference ( $V_{ref}$ ). If the output voltage is too high, the OPAMP will decrease its output, which causes the current to the base of the BJT to decrease. This decrease in base current in the base of the BJT decreases the amount of current that can flow through it. This decrease in current results in a low voltage, by Ohm's Law, and thus the voltage has been regulated. The same reasoning is used for when the output voltage gets too low.

The biggest disadvantage of linear regulators is their efficiency. The process of regulation consumes power, and whatever power is consumed by the regulator cannot be used by the output load. Since power efficiency is the ratio of output power to input power, any losses of power in between input and output will decrease power efficiency. In linear regulators, the biggest offender for power losses is usually the current controlling device (in Figure 5 it is the BJT). This is because of the voltage difference across the current controlling device, shown as  $V_{ce}$  in Figure 5. Since there is a voltage difference across the device, and current flowing through it, there is power being dissipated by it. The larger the difference between the input and the output, the larger the power dissipated, and less the efficiency. To compound on this, the power dissipated by the current controlling device is transformed into heat, which then must be dealt with. This can make a circuit much harder to implement when heat dissipation becomes nontrivial.

### 3.1.1.2.2 Switching Regulators

Switching regulator operations is based on a different concept than linear regulators. As the name suggests, the basis of switching regulators is switching. How switching regulators work is by switching (done by a BJT in the simplified

buck regulator circuit in Figure 7) the input power on and off very quickly, essentially chopping the voltage into smaller parts. What this accomplishes is lowering the average voltage at the output (for a buck converter, see Figure 7). The average output can then be further controlled by changing the ratio of the time when the switch is on versus when the switch is off; this ratio is referred to the duty cycle (D). For example, if a DC input of 12V is applied, and the duty cycle is 50% (the switch is on for half the time, and off for the other half), then the average voltage at the output would be 6V. This is governed by the simple equation  $V_o = DV_{in}$ . However, the real trick with switching regulators is the speed at which they do this switching, which can approach a switching frequency in the MHz. The switch in question is usually some sort of transistor and is switched rapidly by applying a pulse width modulated (PWM) square wave to its base/gate (see Figure 6). The benefit of this operation is that the switching device is off for some period of time, and during this time no power is being dissipated (ideally). Because of this, the percent efficiencies of switching regulators can approach into the high 90s, even if the input voltage is much higher than the output voltage. This high efficiency results in higher power utilization and less wasted power (heat) to deal with.

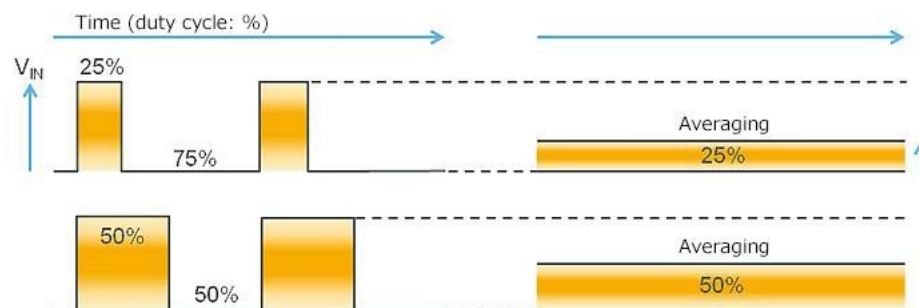


Figure 6: Switching Regulator Duty Cycle<sup>3](3)</sup>

However, most electronics cannot accept a chopped-up voltage as described above. The voltage needs to be smoothed or averaged out before it can be used by other devices and circuits. This smoothing is accomplished by an LC circuit, as shown in a simplified switching regulator depicted in Figure 7. This LC circuit takes the chopped-up voltage and smooths it into a more useful voltage, as shown in Figure 8.

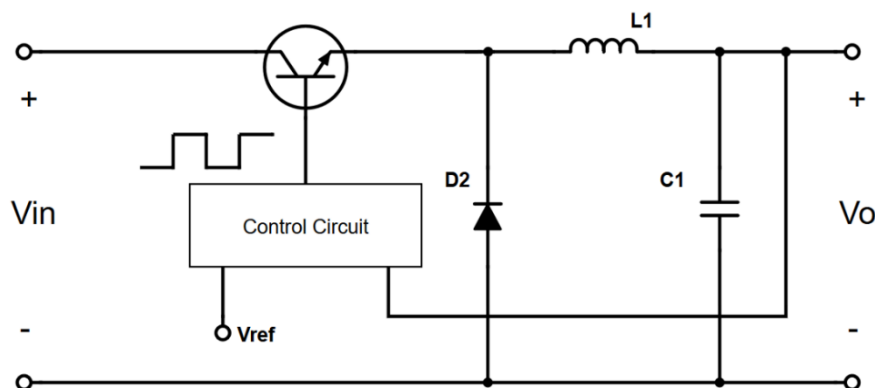


Figure 7: Simplified Switching Regulator in a Buck Configuration<sup>(1)</sup>



Figure 8: Switching Regulator Voltage Smoothing<sup>[3][3]</sup>

There are three main types of switching regulators (also called DC-DC converters, since they take a DC voltage and convert it into another DC voltage): buck, boost, and buck-boost converters. Buck converters have an output that is lower than the input (the example of a switching regulator used in this section), boost converters have an output that is higher than the input, and buck-boost converters have an output that is either higher or lower than the input.

The main disadvantage of switching regulators is their complexity, size, and cost. Switching regulators require a special control circuit to compare the output to a reference and create a PWM signal corresponding to that comparison to regulate the output. Also, even after the smoothing done by the LC circuit integral to the switching regulator, additional filtering may be necessary depending on the application and switching frequency of the regulator, which adds to complexity and cost. Switching regulator circuits are often larger than their linear counterparts due to the need of an inductor, which size is hard to minimize for certain values of inductance.

### 3.1.1.2.3 Voltage Regulator Technology Comparison

Table 3 summarizes the comparison between the two voltage regulator technologies, with the chosen regulator technology highlighted.

Table 3: Voltage Regulator Technology Comparison

	Linear	Switching
<b>Voltage Regulation</b>	Yes	Yes
<b>Efficiency</b>	Fair/Poor	High
<b>Cost (including necessary surrounding passive circuitry)</b>	Less Expensive	More Expensive
<b>Introduces High Frequency Noise</b>	No	Possible (but preventable with good circuit design)
<b>Simplicity</b>	Simple	Complex

The Switching regulator was chosen because of its high efficiency. The cost is not appreciably more than a linear regulator for our small volume application, and issues with complexity and noise are remedied with tools that can be used to design switching regulators, see Section 3.2.1.4.

### 3.1.1.3 Voltage References

Observant readers may have noticed that in both regulator types there is a need for a reference voltage, and thus a need in the Bike System. As the name would

imply, a voltage reference is a device that holds a constant voltage that can be compared to other voltages in various applications. Specifically, for voltage regulation, having a stable voltage reference is important in order to have a stable and accurate output voltage. Three types of voltage references will be considered here: a resistor divider, the Zener diode, and the band-gap reference.

### 3.1.1.3.1 Voltage Divider

The simplest form of a voltage reference is the use of a voltage divider, made from a set of resistors. A voltage divider works by using the voltage drops of resistors to set the reference voltage between the resistors. This is usually accomplished with 2 resistors set up in series, with the reference voltage being the voltage drop of the second resistor. The equation for the voltage of drop of the second voltage ( $V_{out}$ ) is given as follows:

$$V_{out} = \frac{R_2}{R_1 + R_2} V_{in}$$

Where  $R_1$  is the resistance of the first resistor,  $R_2$  is the resistance of the second resistor, and  $V_{in}$  is the voltage at the first resistor with respect to ground (see Figure 9). The advantage of such a method is the simplicity of the circuit and the ease at which it can be implemented.

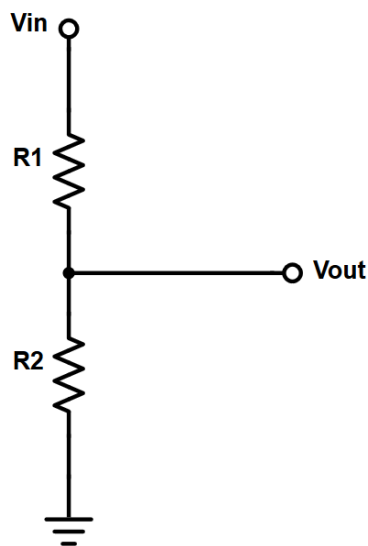


Figure 9: Simple Voltage Divider<sup>(1)</sup>

While this can provide a reference voltage, it is directly dependent on the input voltage,  $V_{in}$ . This means any fluctuations in  $V_{in}$  will be directly transferred to the output,  $V_{out}$ . Additionally,  $V_{out}$  is directly dependent on the resistance values of the resistors, which can vary widely from component to component and from changes in temperature. This makes for a very unstable, and thus poor, voltage reference.

A voltage divider should only be used when the stability of  $V_{in}$  can be ensured, and the tolerances of deviation for the resistance values are within the tolerances needed for the reference voltage.

A more common use for voltage dividers is for taking samples of an output to be used for comparison to a more stable voltage reference, such as in Figure 5 where the output voltage is reduced by the voltage divider and compared to a stable voltage reference via an OPAMP. The need to take a sample of the output is because, in most applications, the output voltage is higher than the voltage reference. The voltage divider serves to take a sample of the output by reducing it to a voltage close to that of the voltage reference. The sample output value is adjusted by the resistor values used in the voltage divider. For example, if a 12V output was to be compared to a 2V reference voltage,  $R_1$  could be chosen to be 5k $\Omega$  and  $R_2$  to be 1k $\Omega$  to result in a 2V output sample. Here the direct relation of voltage input to output works in favor of operation, as if the 12V output goes up or down, the 2V output sample will change proportionally with negligible delay. This method is commonly used in linear regulation, as described in Section 3.1.1.2.1.

### 3.1.1.3.2 Zener Diode

A Zener diode works as a voltage reference by leveraging the concept for the Zener breakdown region. As shown in Figure 10, while past a certain point in the breakdown region, the voltage drop across a reversed biased Zener diode (also referred to as the Zener voltage,  $V_z$ ) is not a strong function of the current passing through it. This means that the Zener voltage will be relatively steady over a range of current, and thus be a decent voltage reference.

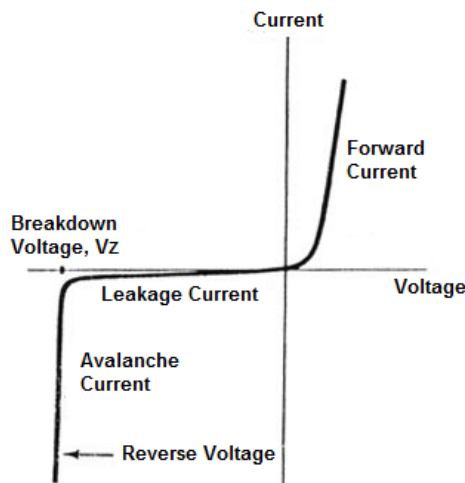


Figure 10: Zener Diode I-V Plot<sup>[4]</sup>

The disadvantages of using a Zener diode as a voltage reference is that, for certain applications, they may be too unstable. While the Zener voltage may not be a *strong* function of reverse current, it still may be too strong for sensitive applications. Also, Zener diodes are sensitive to variations in temperature, which translates to variations in the voltage. Additionally, Zener voltages only come in select values and may need a high overhead voltage.

### 3.1.1.3.3 Bandgap Reference

Bandgap references are more elaborate than simple Zener diodes, as they are an entire integrated circuit rather than a single component. Bandgap references are based on the characteristics of BJTs. Essentially, bandgap references use the voltage drop across the base emitter junction ( $V_{be}$ ) of complementing BJTs to accurately produce a voltage reference that is compensated for temperature variations (see Figure 11, which shows theoretically zero temperature variation to voltage). A more rigorous treatment of the theory behind bandgap references is beyond the scope of this document. In practice, a bandgap reference functions as a more accurate Zener diode (maintains a set voltage for a range of currents passing through it), which is why it often share the same circuit symbol as a Zener diode.

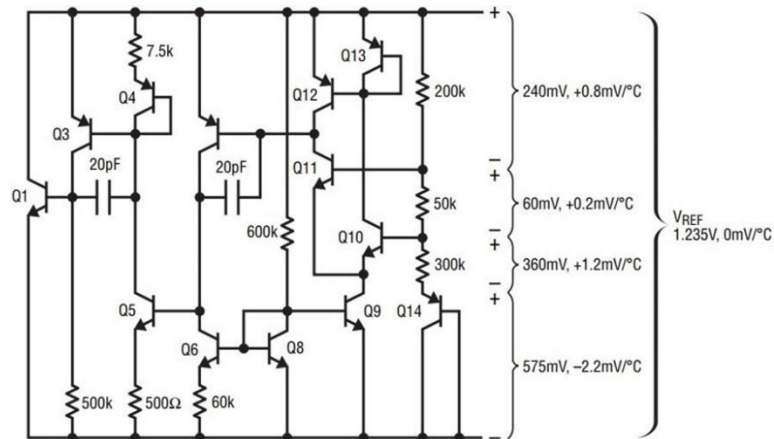


Figure 11: Example Bandgap Reference IC (LT1004)<sup>[5](4)</sup>  
(Courtesy of Analog Devices, Inc.)

The main disadvantage of a bandgap reference would be cost and implementation.

### 3.1.1.3.4 Voltage Reference Comparison

Table 4 summarizes the different voltage reference technologies discussed in Section 3.1.1.3, with the chosen technology highlighted.

Table 4: Voltage Reference Comparison

	Voltage Divider	Zener Diode	<b>Bandgap Reference</b>
<b>Susceptibility to Input Voltage Variation</b>	High	Low	Low
<b>Sensitivity to Changes in Temperature</b>	High	Average	Low
<b>Voltage Reference Accuracy</b>	Low	Low	High

<b>Cost</b>	Very Low	Low	Low
<b>Power Dissipation</b>	High	Low	Very Low

The bandgap reference was chosen because it was purpose built for this specific application and has most benefits and fewest downsides.

### 3.1.1.4 Battery Technologies<sup>[10]</sup>

While the Bike System will support power being generated from the bike itself, there needs to be a continuous source of power available for when the bike is not in motion. The solution to this is the humble battery. Most all batteries operate on the principle of the conversion of chemical energy to electrical energy. In general, this is accomplished by using two dissimilar metals and an electrolyte. The two dissimilar metals are referred to the anode and cathode of the battery, where the cathode holds a positive charge and the anode hold a negative charge. The electrolyte facilitates the chemical reactions that produce excess electrons for the anode and a shortage of electrons for the cathode. This results in the difference in charge of the metals, and the flow of electrons, see Figure 12 for a simple example of a battery. In addition to the nominal voltage between the cathode and anode, batteries are rated by their capacity. A battery's capacity is usually measured in milliamp-hours (mAh), which is how much current a battery can sustain over one hour before being depleted (theoretically). For example: a 2000 mAh battery should be able supply 2A of current for 1 hour, or the same battery can supply 200 mA for 10 Hours.

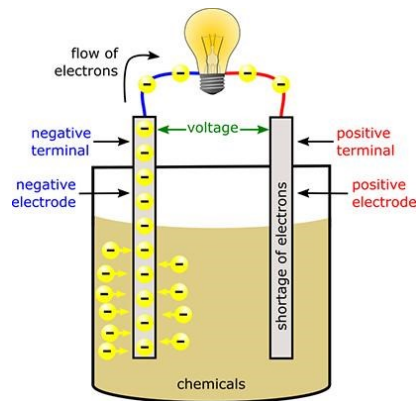


Figure 12: Simple Battery<sup>[6](2)</sup>

However, there are many different battery technologies. Some of these technologies are rechargeable. For this project, rechargeable battery technologies were looked into. These technologies were lithium-ion/-ion polymer (Li-ion/-Po), Nickel-Cadmium/-Metal Hydride (Ni-Cd/-MH), and Lead-acid batteries. While an in-depth treatment of battery chemistry and theory is beyond the scope of this document, below are some key differences and features of each battery technology considered.



#### **3.1.1.4.1 Li-Ion/Li-Po**

Both Li-ion and Li-Po are combined together is because the only difference between the two is that the Li-Po uses a gel polymer electrolyte instead of a liquid electrolyte. Li-ion batteries are light weight, have a high-power density, and a high cell voltage (3.7V). The higher cell voltage means a higher voltage can be achieved with less battery cells, which leads to a reduction in space occupied by the batteries.

The main disadvantages of this technology are the cost, and the safety concern. The concern for safety is due to the fact that if there is a malfunction of the battery, such as a short across the terminals of the Li-ion battery, the battery could explode. However, this risk can be mitigated by proper circuit design and testing.

#### **3.1.1.4.2 Ni-Cd/Ni-MH**

Again Ni-Cd and Ni-MH batteries are considered together since they have similar properties, with the difference lying in the different chemical composition (cadmium vs metal hydride). Ni-Cd have a slightly lower power density and nominal voltage (1.2V vs 1.25V for Ni-MH). One major advantage of these batteries is that they are available in most standard sizes (AA, AAA, C, etc.), so they can often be used as direct replacements for non-rechargeable alkaline batteries. Additionally, they are rather cheap, which makes them ideal for high production of products where price is the main concern

For Ni-Cd batteries, the main disadvantage is the environmental impact since cadmium is a toxic metal. For both batteries, the power densities are lower than that of lithium-based technologies and have a lower nominal cell voltage.

#### **3.1.1.4.3 Lead-Acid**

Lead-acid batteries are the same type of batteries that are in most vehicles. These batteries are cheap, come in a variety of voltages (such as 2V, 6V, 12V, or 24V), and have a high output power capability.

The disadvantages are that they have very low power density, which means that these batteries are very bulky and weigh a lot. Lead-acid batteries are typically used when space and weight are not much of an issue.

#### **3.1.1.4.4 Battery Technology Comparison**

Table 11 in Section 3.2.1.2 summarizes the comparison of the battery technologies presented in Section 3.1.1.4.

#### **3.1.1.5 Voltage Comparison**

In electronic circuits it is often very useful to compare between voltages. This is usually done to see when one voltage becomes higher than the other or to monitor a voltage level. The Bike System is no exception to this. Using two different power

sources requires needing to change between those two sources. To do this the voltages of the two sources must be monitored and compared against each other. One device that can be used to do this is a comparator. A comparator works by taking two inputs into its noninverting (denoted by a “+” on its schematic symbol) and inverting (denoted by a “-” on its schematic symbol) terminals, then outputting high (where high is equal to the supply voltage) when the voltage at the noninverting terminal is at higher potential than that inverting terminal, and low (where low is the lower supply voltage, or ground) when the inverting terminal is at a higher potential than the noninverting terminal. Figure 13 shows an example of a comparator in operation. With a triangular input at the noninverting terminal, the output is only high when the triangular voltage becomes higher than the voltage set by the voltage divider ( $V_{CC}/2$ ). This point when the voltage at the noninverting terminal is either just above or below the voltage at the inverting terminal, where the comparator’s output switches between states, is known as the threshold voltage.

In this example, the second supply input (at the bottom of the comparator symbol in Figure 13) is what determines what the “low” of the output. In Figure 13, the second supply is connected to ground (0V), so the “low” for the output is also ground. Note that a comparator shares a circuit symbol with an OPAMP; this is due to the fact that a comparator is a specialized OPAMP that is designed to have an output voltage that is, or very close to, the supply voltage (also known as rail-to-rail output).

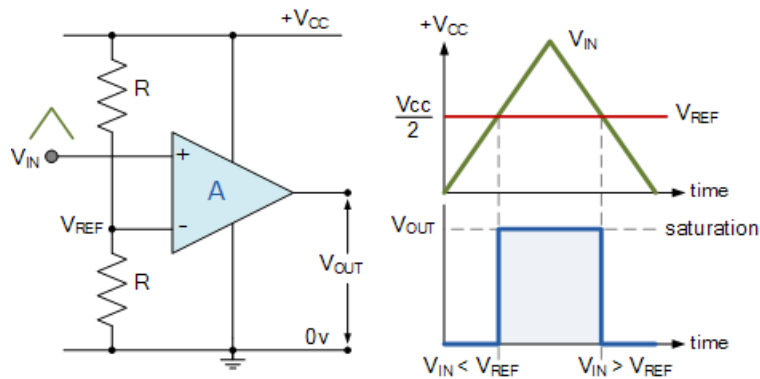


Figure 13: Simple Comparator Operation<sup>[14](2)</sup>

As it can be seen, the comparator takes two analog voltages, compares them, then outputs a discrete output (either high or low). In the Bike System, a comparator can be used to check which one of the power sources are higher than the other, and send an output to change which input to use. Comparators can either be discrete, standalone, devices that send a high or low signal to another device, or comparators can be integrated into a device to aid in its function (such as the BQ24076, see Section 3.2.1.4).

The simple comparator circuit shown in Figure 13 has a fatal flaw, however. As Figure 13 shows, the comparator's output switches states *exactly* at the threshold voltage. In other words, as soon as the voltage at the noninverting input goes above or below the voltage at the inverting input, even by a very small number, the state will change. This means that noise imposed on a signal could cause erroneous switching at the output of the comparator, as shown in Figure 14. In Figure 14 the blue trace is the input signal, while the red trace is the output signal for a comparator like the one pictured in Figure 13. Figure 14 (red trace) also shows how these erroneous switching events cause oscillations that could result in incorrect readings from a device connected to the comparator's output, or even damage it.

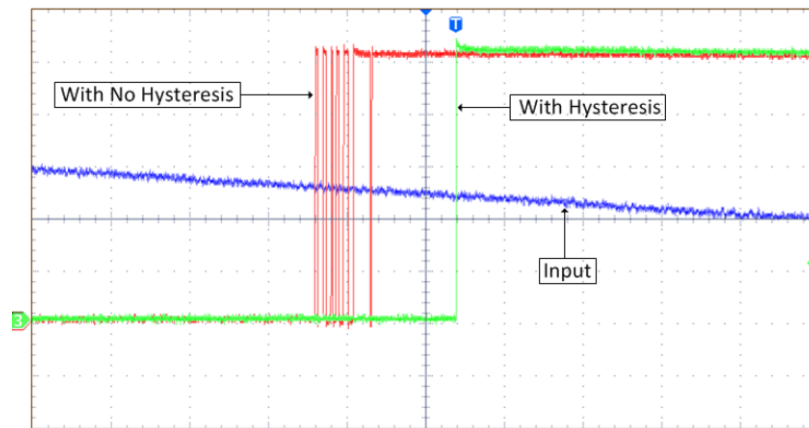


Figure 14: Comparator Output Oscillations due to Signal Noise<sup>[17](1)</sup>

The solution to this problem is hysteresis, as shown in Figure 14 with the green trace. In essence, hysteresis is where the voltage threshold, that serves to trigger the change in the state of the comparator's output, is shifted depending on the state of the output. The hysteresis curve shown in Figure 15 is used to help illustrate this, where the "X" axis is the input voltage, while the "Y" axis is the voltage of the output. The curve can be interpreted by starting at the bottom of the curve (near "LOGIC "0"") and following the arrows on the line to the left, corresponding to an increase in the input voltage. Once it reaches the first voltage threshold (shown as the leftmost vertical line) the output jumps to "LOGIC "1"". However, once the input voltage begins to decrease and follow the arrows on the lines to the right, the first threshold voltage will be passed until the input voltage reaches the second threshold voltage (shown as the rightmost vertical line). Once the second threshold voltage has been reached, the voltage output drops to LOGIC "0".

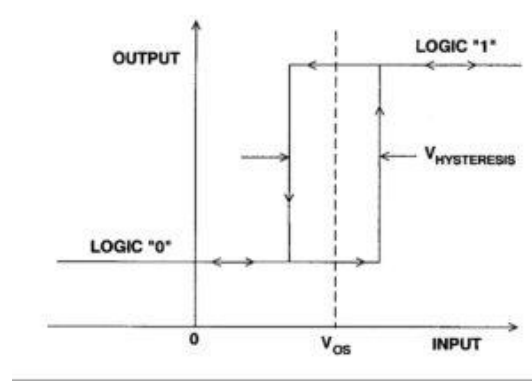


Figure 15: Hysteresis<sup>[18]</sup>

By having a “dead-zone” (shown in Figure 15 as  $V_{HYSTERESIS}$ ) the noise shown on the blue trace in Figure 14 does not reach the new threshold once the first has been reached. This is how the green trace has a clean transition without oscillations.

### 3.1.2 Sensors Technology

This section covers the technologies that relate the to the various sensors that will be needed for the Bike System.

#### 3.1.2.1 The Hall Effect

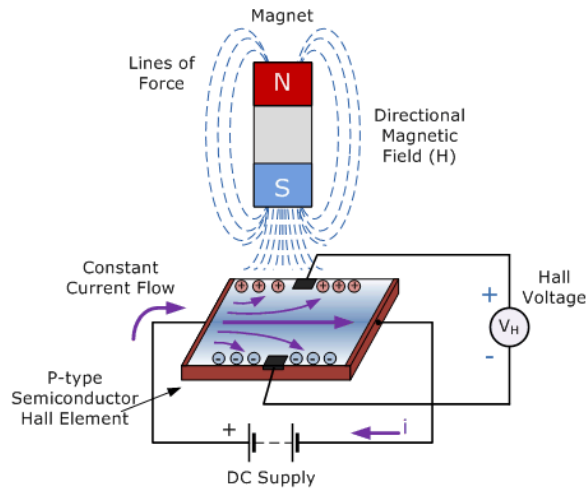


Figure 16: Hall Effect Demonstration

The Hall Effect is a situation where a magnetic field pushes flowing electrons in a conductive material in such a way that a potential difference (voltage) is developed.

$$\text{Hall Voltage} = -\frac{IB}{ept}$$

Hall voltage is influenced by five things: the amount of current flowing through the conductive material ( $I$ ), the magnetic field intensity ( $B$ ), the charge of an electron ( $e$ ), the thickness of the conductive material ( $t$ ), and the number of electrons per unit volume ( $p$ ). In applications today, the conductive materials used are usually indium antimonide (InSb), indium arsenide (InAs), or gallium arsenide (GaAs). Because of their properties, the aforementioned compounds are called Hall elements.

The Bike System will use the Hall Effect Sensor as the means to calculate speed and distance traveled. By attaching a small permanent magnet to either the front or back bicycle tire, the Hall Effect Sensor will be able to count the number of revolutions of the bicycle tire. In order for this method to be implemented, at least one permanent magnet will need to be attached to either the front or back bicycle tire, but more permanent magnets may be attached to either tire for better accuracy in measuring both speed and distance. For example, if four permanent magnets are attached equidistant from one another on the front wheel of the bicycle, the speed and distance calculations would have less error because of the more accurate measure of how far the bicycle tire actually turned.

### 3.1.2.2 RFID Technology

RFID, which is an acronym for Radio-Frequency Identification, is a system made up of two components: a reader and a tag.

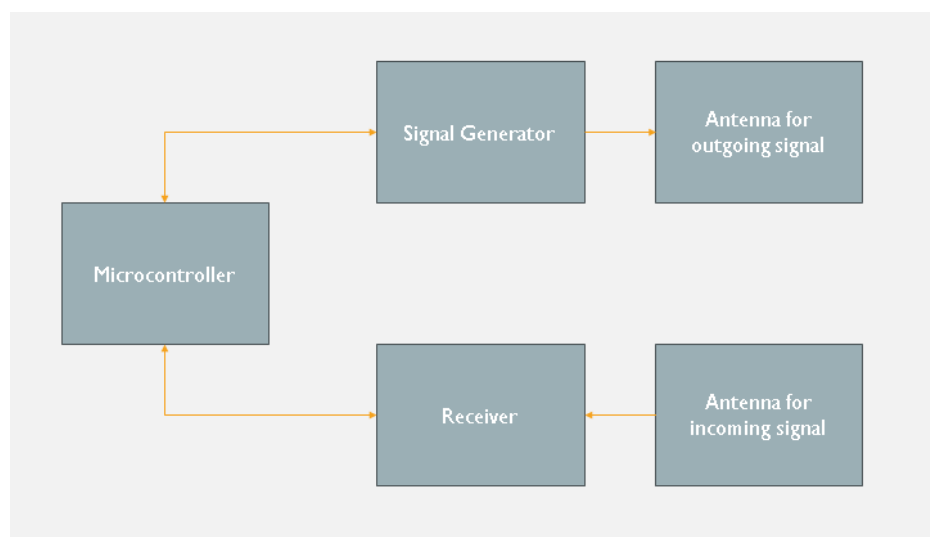


Figure 17: Block Diagram of Hardware used in RFID Reader

The RFID reader consists of a signal generator, signal receiver, two antennae, and a microcontroller. Depending on the type of RFID tag being used, the signal generator will send out a signal that has a frequency somewhere in the range of 20 kilohertz to just less than 1 gigahertz. RFID systems can generally be categorized into three operating frequencies: low frequency, high frequency, and ultra-high frequency. Each range of operable frequency has benefits and disadvantages associated with the behavior of the radio wave at that specific

frequency. For example, the low frequency range, which varies from 30 kilohertz to 300 kilohertz, is very resistant to electromagnetic interference, but the disadvantage is that the reader is only able to read the tag on this frequency range from a distance of about 10 centimeters maximum. Due to established standards, most low frequency RFID systems operate at either 125 kilohertz or 134 kilohertz. Low frequency signals have the ability to propagate through metals and liquids with minimal electromagnetic interference. Low frequency RFID systems generally have lower data transfer rates as compared to the two other operable frequency ranges, typically between 4 and 8 kilobits per second.

The next operable frequency range is the high frequency range. This frequency range describes signals with frequencies between 3 megahertz to 30 megahertz. Due to established standards, most high frequency RFID systems operate at 13.56 megahertz. While high frequency readers and tags are more sensitive to electromagnetic interference, the benefits to high frequency systems are higher data transfer rates and a greater distance that the tag is able to be read by the reader. Most high frequency RFID systems have a read range of up to 1 meter. This is why high frequency RFID systems are used for applications such as automatic toll ticketing.

The last operable frequency range is the ultra-high frequency range. This frequency range describes signals with frequencies between 30 megahertz to 3 gigahertz. When compared to RFID systems that operate in the two previously mentioned operable frequency ranges, the RFID systems that operate in the ultra-high frequency range are the newest and are most sensitive to electromagnetic interference. The technology that makes ultra-high frequency RFID possible is currently the fastest growing in the industry. Most ultra-high frequency systems operate between 900 and 950 megahertz. The maximum range that a tag is able to read in an ultra-high frequency system is 12 meters.

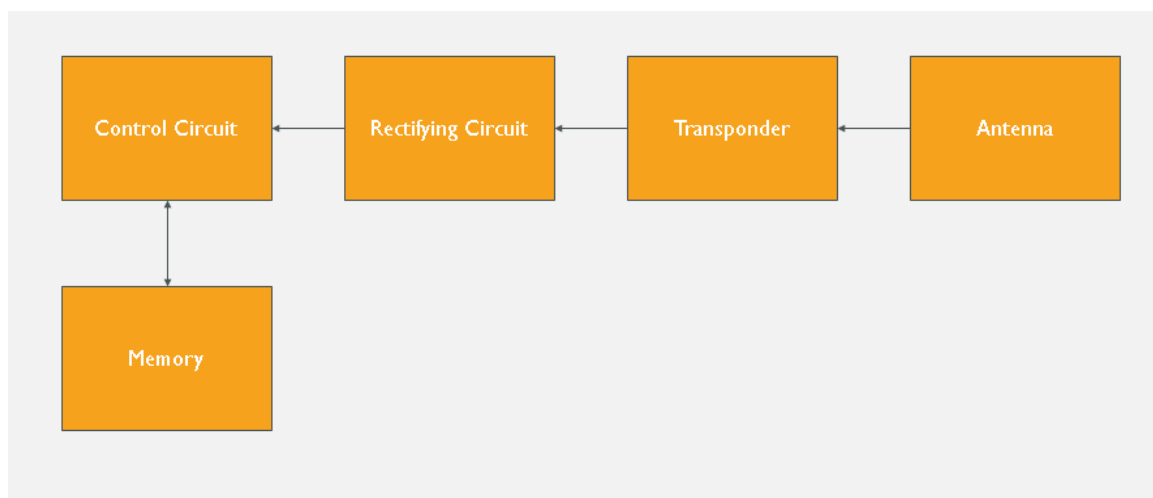


*Figure 18: Block Diagram of Hardware used in RFID Tag*

As can be seen above, most RFID tags contain an antenna, a transponder, a rectifying circuit (or battery), memory, and a controller. Since passive tags do not have their own power supply, the rectifying circuit is used to capture the energy from the received radio waves and then feed it to the controlling circuit/element. There are three types of RFID tags, active, semi-passive, and passive tags.

Passive tags are defined as tags that use the concept of inductive coupling or electromagnetic coupling, as known as near-field coupling or far-field coupling respectively, to power itself. Passive tags are only turned on when they receive energy from a RFID reader. Because tags are only turned on when they are being read, they require very little maintenance and have an almost indefinite lifespan. Passive tags tend to be the most cost-effective option when considering RFID tags, but this is because passive RFID tags have the least amount of memory available as well as the lack of software available to assist with data allocation.

Semi-passive tags are defined as integrated circuits that feature a battery and antenna. The addition of a battery allows for semi-passive RFID tags to feature sensors and tracking hardware, but do not improve the range from which the tag can be read. The piece of hardware responsible for extending the range from which an RFID tag can be read is a transmitter, and this is the sole difference between a semi-passive RFID tag and an active RFID tag.

Active tags are defined as integrated circuit that features an antenna, transmitter, and a battery. The transmitter is powered by the battery and is responsible for sending a signal back to the RFID reader which is how the transmitter extends the range from which the RFID tag can be read. Because active RFID tags can feature a number of sensors, tracking technology, and logic, they tend to be the largest of the three tags in terms of physical space occupied. Furthermore, active RFID tags must include an embedded power source, which is in most applications a battery. This embedded power source only adds to physical space occupied by the RFID tag itself. When compared to the other RFID tags, the active RFID tag has the shortest lifespan because of the power consumed by the transmitter.



*Figure 19: An example of an active tag (left) versus a passive tag (right)*

As can be seen in Figure 19, the size contrast between active and passive RFID tags can be large. Not only are the active RFID tags larger, but they require maintenance in the form of periodic battery changes.

The Bike System will use RFID as the primary method of locking/unlocking the locking mechanism on the bicycle. Because of application specificity and cost, The Bike System will be using a passive RFID tag likely in the form of a key fob or RFID card.

### **3.1.2.2.1 Inductive Coupling**

Inductive coupling, also known as near field coupling, is a phenomenon where the electromagnetic wave, in the Bike System's case a radio wave, is used to energize circuitry through a shared magnetic field. Near fields are mostly magnetic in nature. In the case of RFID, the antenna in the RFID reader transmits a signal; the transmitted signal will be in either the low or high frequency range. Once this transmitted signal is picked up by the RFID tag, the circuitry in the RFID tag is powered by the energy in the captured transmitted signal.



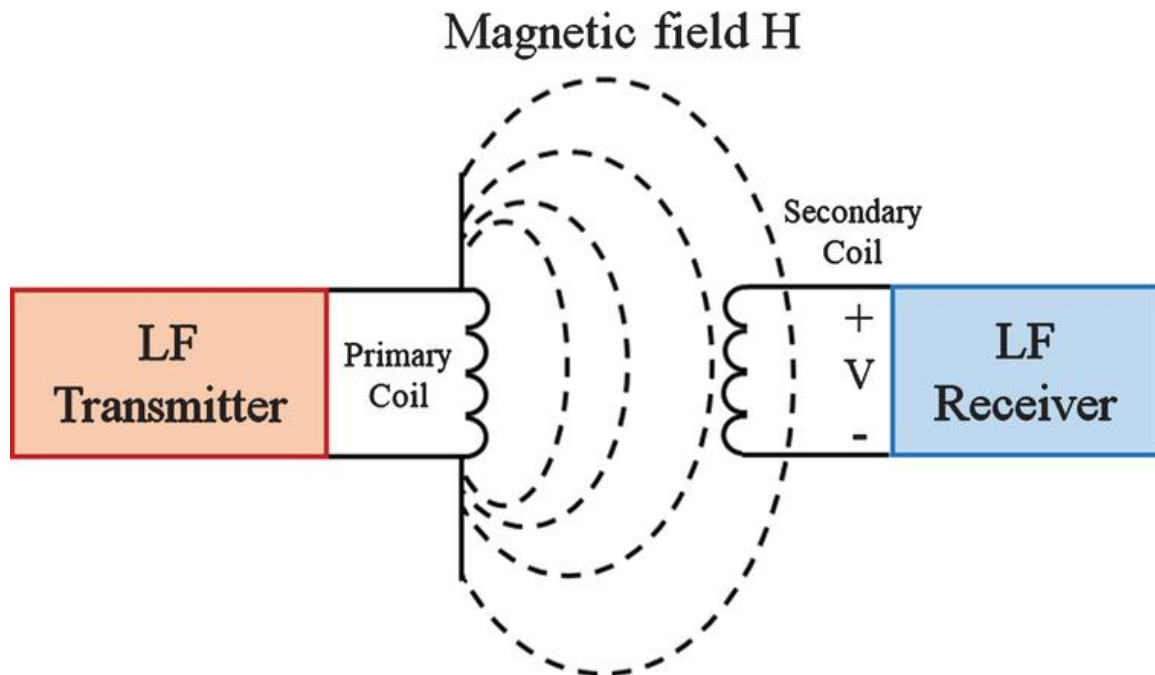


Figure 20: Inductive Coupling Example

In Figure 20, it can be observed that the transmitted electromagnetic field is captured by a coil in the RFID tag. The transmitted electromagnetic field induces a voltage in the RFID tag. The induced voltage in the receiver is then rectified and is used to power the receiver. Also, the transmitter and receiver are labeled 'LF' for low frequency, but inductive coupling is the working principle for both low frequency and high frequency ranges.

### 3.1.2.2.2 Electromagnetic Coupling

Electromagnetic coupling, also known as far field coupling, is very similar to inductive coupling in that the result of the working principle is that circuitry in the receiver uses the energy from the transmitted electromagnetic wave to power itself. The key difference is that electromagnetic waves transmitted over a distance greater than one meter have significantly different characteristics than electromagnetic waves transmitted over a distance less than one meter. Once the electromagnetic wave is emitted from the reader, it travels until it is absorbed and reflected by the antenna in the tag. The amount of energy absorbed and reflected by the tag depends on both the frequency of the emitted electromagnetic wave and the orientation of tag when it is struck. The phenomenon of reflecting electromagnetic waves in the exact direction that they were emitted from is called backscatter. Backscatter can also be used to transmit data from the tag to the reader. By modulating the property of the antenna that reflects the electromagnetic wave, data in the form of bits can be transmitted from the tag to the reader; this form of backscatter is called modulated backscatter. In order to make modulated backscatter possible, the modulation of the antenna in the tag would need to happen synchronously with a clock in the reader. It is important to note that while

far field coupling has both electric and magnetic field components, the power intensity of both these field components decrease inversely with respect to the distance from the transmitter squared. Another key difference between near field coupling and far field coupling is that far field coupling is used only for ultra-high frequency range applications.

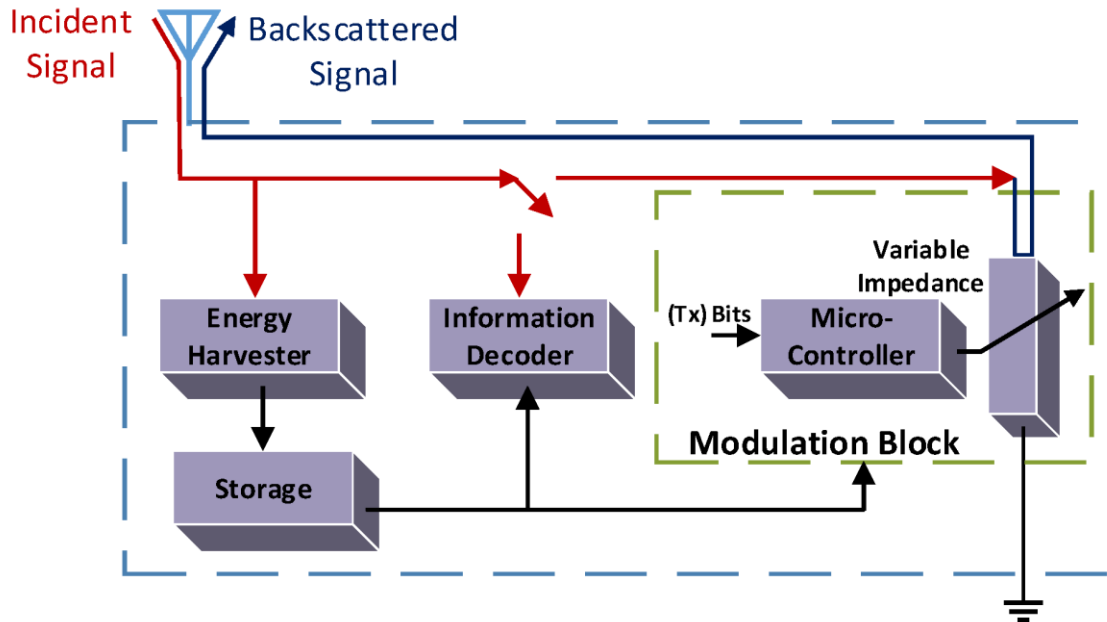


Figure 21: Typical Backscatter Communication Architecture

In Figure 21, it can be observed that the typical architecture of an RFID tag that uses the modulated backscatter principle. The emitted electromagnetic wave from the RFID reader, in Figure 21 called the incident signal, is captured by an antenna, and is then used to power the tag. Depending on the amount of time that the emitted electromagnetic signal is absorbed by the antenna on the RFID reader, the energy captured by the rectifying circuit may or may not be stored in a battery component on the RFID tag. If there is encoded information in the emitted electromagnetic wave from the RFID reader, it will be decoded in the 'Information Decoder' block seen in Figure 21. If the RFID tag needs to send data back to the RFID reader, it will do so by modulating the emitted electromagnetic signal by varying the impedance the received signal sees on its path back to the antenna. In Figure 21, it can also be observed that there is a 'Microcontroller' block. For RFID tags with memory, this is necessary as the RFID tag needs to decide which data to emit back to the RFID reader. For simpler applications, this would not be necessary as the tag would only need to be encoded with a single piece of information to represent a single user.

Table 5: Comparison of operable RFID frequency ranges

Frequency Range Classification	Frequency Range	Working Principle	Typical Range of Detection	Price Comparison
--------------------------------	-----------------	-------------------	----------------------------	------------------

<b>Low Frequency Range (LF)</b>	30 – 300 kHz	Inductive Coupling	Less than 1 meter	Low
<b>High Frequency Range (HF)</b>	3 MHz – 30 MHz	Inductive Coupling	Less than 1 meter	High
<b>Ultra-High Frequency Range (UHF)</b>	300 MHz – 3 GHz	Electromagnetic Coupling	Greater than 1 meter	Highest

As can be observed in Table 5, the most suitable technology for this project will be an RFID module operating in either the low frequency or high frequency range. While RFID modules operating in the ultra-high frequency range are within the scope of this project, the purpose of the RFID module, in the application of this project, would be to unlock the locking mechanism when a user swipes their RFID transponder from the distance of 0 centimeters to 10 centimeters away from the antenna embedded on the RFID module. Furthermore, RFID modules operating in the low frequency and high frequency ranges are much cheaper when compared to those operating in the ultra-high frequency range.

### 3.1.2.3 Temperature Sensor/Thermometer

As an additional feature of the Bike System, a thermometer or temperature sensor will be implemented to give the user some insight about the current weather conditions that the user is currently experiencing. The temperature sensor or thermometer can be implemented as a part on the microcontroller or as a standalone accessory on the handlebars of the Bike System.

The standalone temperature accessories are common in the motorcycle world and most are just as cost effective as the temperature sensors. The main downfall of the standalone thermometers we have considered are not perfectly accurate since it utilizes a bimetallic strip and displays the temperature on an analog face showing both Celsius and Fahrenheit which is indicated by a small red arrow. Displaying the temperature with an almost perfect accurate reading is not a top priority since the difference of a one or two degrees will not be a noticeable change in the weather for the user to notice.

The purpose of the thermometer or temperature sensor is to provide insight or an estimation of how hot or cold it currently is without utilizing another device such as a smart watch or smart phone. If a standalone, ready to use accessory will be utilized, there is only the issue of mounting it permanently so it cannot be removed by malicious means.

If a temperature sensor is to be utilized instead, the final decision will be made based on the constraints of the microcontroller and the power supply being used. Since these sensors do not have an accompanying display, the temperature

values will be processed by the microcontroller and displayed on the LCD display that will be mounted on the handlebars.

A possible constraint of using an onboard temperature sensor is the possibility of receiving incorrect temperature readings. This possibility would arise from the temperature sensor being stored inside the housing for the Bike System's main electrical system, and as a result, the temperature sensor could be reading a much higher temperature from the box housing the other electricals than the outside ambient temperature. This possible constraint is being taken into consideration when choosing an appropriate housing for the Bike System's electronics.

### 3.1.3 Locking Mechanism

The locking mechanism which secures the bicycle to the place where the user chooses to leave it has proved difficult to research. The locking mechanism must be able to operate both electrically and mechanically in the absence of power to the electrical actuator, in the Bike System's case a servo motor. A potential option for a locking mechanism would be to use a cam lock in conjunction with a servo motor and a modified bicycle chain.



*Figure 22: A typical cam lock*

In Figure 22, it can be observed that the typical cam lock used in filing cabinets and anything with a sturdy flange. It is proposed to mount this type of lock onto the electrical housing and position the cam lock in such a way that when the cam lock is in the locked position, the metal tab attached to the lock itself is directly beside the entry for the key, that it to say directly beside the keylock on either the right or the left, whichever is more convenient for the construction of the electrical housing. Next, a cut into the electronics housing is made just large enough for the end of the modified bicycle chain to fit through. The end of the modified bicycle chain should be a screw with threads that fit the threading on a nut held on the other side of the metal tab of the cam lock in the locked position by a servo motor. In this

configuration, the locking mechanism will be operable with or without supplied power. The servo motor will turn the nut mounted onto its shaft according to the direction specified by the microcontroller to either lock or unlock the bicycle. In the case the system is without power, a key will be used to turn the metal tab holding the modified bicycle chain in place to allow it to either lock or unlock. This is a viable option for the locking mechanism as it is cost effective. It requires only a cam lock, servo motor, and screw.

### **3.1.3.1 Cable and Reel**

The best material to secure the bike with is steel cable. The steel cable will be wound in an inertial reel which will be fixed to the housing. The inertial reel provides an easy solution for storing the steel cable while not in use and a seamless delivery system for the user. It will also reduce the amount of cable exposed which in turn increases the difficulty of theft. When the user inserts the male end of the steel cable into the housing, the inertial reel will lock providing additional security. Once the male end of the cable is secured to the housing, the inertial reel will lock and not allow the cable to be pulled out of the housing until it is unlocked.

### **3.1.3.2 Spring Loaded Lock**

Research into the physics of a spring is required to gather enough understanding to design the automated locking mechanism with a manual override. The idea behind this lock is the user can pull a steel cable with the male connecting adapter away from the housing to secure the bike to a fixed object. Pulling the cable from the stowed position will compress the spring and open the latch for the lock. Once the male connector is pressed inside the housing, the spring will release the latch and secure the cable. The male adapter can be inserted into the housing where the spring will release the locking mechanism to secure the cable and lock the inertial reel.

### **3.1.3.3 Servo Driven Rotating Lock**

A servo motor will be used to lower the locking mechanism when the male end of the cable is pressed into the housing. The motor will be driven by the microcontroller utilizing a pulse width modulated signal to reduce power consumption. When the RFID is authenticated, the servo will unlock and release the cable. The manual release system for this design will use a key and lock. If in the event there is no power to the bike system, the user can use the key to manually turn the lock to release the cable.

### **3.1.3.4 Seat Belt Assembly**

A seat belt assembly will be used to simulate the steel cable and reel discussed above. The assembly consists of an inertial reel that will behave similar to the design envisioned for the bike system. The assembly will be mounted in the housing with the buckle protruding from a narrow opening. The user can pull the buckle to secure the bike to a fixed object and the buckle can be inserted into the

housing where it will lock in place by the seat belt locking mechanism. The locking mechanism is spring loaded and requires a certain amount of force to release the buckle.

### 3.1.3.5 DC Linear Push Solenoid

A linear push solenoid is required to release the lock which secures the buckle. The amount of force required to release the locking spring will be measured to ensure a solenoid is obtained with the proper ratings. When the user uses the RFID to unlock the bike, the solenoid will press the release button to release the buckle. Many solenoids use a range of input voltages and a DC/DC boost converter will likely be needed to supply the voltage and current specifications on the device. A small hole will be used to manually open the lock in the event there is no power to the bike system. The user would insert a key into the hole which will actuate a lever and release the lock.

### 3.1.3.6 Comparison

The seat belt assembly appears to be the most practical design for this system. Due to the mechanical engineering involved in designing a custom locking mechanism, the fabrication of the mechanism is not feasible. At first glance, the servo driven rotating lock does not seem to provide the rigidness the spring-loaded lock would provide, and component failure would seem likely. The seatbelt assembly is an inclusive design with the inertial reel and belt properly fitted to the locking mechanism. The locking mechanism is actuated by pressing the release button with a force equal to the tension of the spring within the mechanism. The seat belt assembly will be less expensive and less time consuming. Implementing the seat belt assembly will require the locking mechanism to be mounted a distance away from the solenoid and the inertial reel would be mounted to the enclosure.

Table 6: *Locking Mechanism Comparison Impact*

Device	Seat Belt Assembly	Custom Lock Assembly
Design	Low	High
Cost	Low	High
Implementation	Low	High

## 3.1.4 Lighting Subsystem

This section details the lighting subsystem that will be used as a safety feature for the Bike System, as covered in Section 2.

### 3.1.4.1 LED V. The Others:

Dating back to the first humans that were able to control fire, the necessity of a having light when the Sun dipped below the horizon and darkness consumed the

land was not only integral in the ability to see in the darkness but was also a key of survival. Fast forwarding a hundred thousand years, oil lamps were primarily used until candles were invented. Candela is the base unit of luminous intensity and received its name from the candle. One candlepower was defined as the light produced by a pure spermaceti candle. The next breakthrough came when the incandescent light bulb was invented. The incandescent light bulb which is a big resistor that dissipates energy as heat is still used today and will not be considered for use in this lighting system. The halogen light bulb and the light emitting diode will be used in the technology comparison to find the best quality of light using efficiency as the reference for the comparison.

### **3.1.4.1.1 Halogen Light Bulb**

Overview:

A halogen lamp is an incandescent lamp which contains a tungsten filament and is encased in a mixture of inert gases and a halogen such as iodine or bromine. This allows for improved luminous efficacy and color temperature over the standard incandescent lamp as well as a much smaller package size.

Lifespan:

The tungsten filament evaporates over time and is rated for a certain voltage range. The inert gas mixture and halogen additive allows the evaporated tungsten to deposit back onto the filament, thus increasing the life span of these lamps.

Spectrum:

Halogen lamps produce a wide range of light spanning from ultraviolet to the infrared region. Due to the mixture of gasses surrounding the filament, the lamp can operate at a higher temperature than traditional incandescent lamps which causes the light spectrum to shift towards the blue region. The shift in the spectrum produces light with a higher effective color temperature and higher power efficiency.

Power:

In Table 7, a traditional 60W incandescent lamp is used as the baseline for several different measurements including but not limited to power, lumens, and luminous efficiency. Halogen lamps are about 19.56% more efficient than incandescent lamps.

### **3.1.4.1.2 Light Emitting Diode:**

Overview:

A light-emitting diode (LED) is a semiconductor light source that will emit light when a predefined current flow's through it. During the recombination process within the semiconductor device, electrons recombine with holes and photons are emitted. A diode requires a minimum forward voltage to 'turn on' and allow current to flow through the device. The luminous intensity is a function of the current flowing through the device under a constant voltage model. The LED has a high luminous

efficiency at low current value's, but the efficiency drops rapidly at high currents and temperatures. Oleg Losev created the first LED in 1927 and it took about 70 years of refining the technology before becoming relevant in consumer electronics.

**Lifespan:**

The lifespan of a LED is roughly 25,000 hours and ranges from about a 163-300% increase over halogen lamps making them widely popular in a wide variety of applications. They are sensitive to high current and temperature and the lifespan can be extended or shortened based on these parameters.

**Spectrum:**

The LED emits light within a narrow band of wavelengths which is dependent on the materials used for the semiconductor and doping impurities. Certain materials emit light with a measured intensity at specific wavelengths. This realization allows for the design of a LED which emits light as single color. The LED is limited to a 120-degree viewing angle and must be taken into consideration when designing a circuit where LEDs are used for lighting.

**Power:**

The power and efficiency of a LED is dependent on materials used for the semiconductor and doping impurities. A shorter wavelength corresponds to an increase in the forward voltage of the LED due to the increase of energy needed for an electron to move into the conduction band. In Table YY, a LED lamp that emits light at an intensity comparable to a 60W incandescent lamp, consumes 6.5W and is roughly 158% more efficient.

### 3.1.4.1.3 Comparison

LED's have the best luminous efficiency, lifespan, and control of the device as opposed to halogen lamps. Their fast-switching speed allows for the use of a pulse width modulated signal from the microcontroller to control brightness and save energy. Halogen lamps provide better spherical light fields and have more flexible input power constraints. The LED does not have a complete luminous intensity at all angles like the halogen lamp does and the viewing angle must be accounted for when using LEDs to light an area. To preserve the lifespan of the LED, current through the device must be regulated closely and proper heat dissipation is critical to prevent failure of the LED.

Table 7: Lighting Comparison Using 60w Incandescent as Reference

Device	LED	Halogen Lamp	Incandescent Lamp
Power (watt)	9.5	43	60
Luminous Flux (lumen)	815	750	860



<b>Efficiency (lumen/watt)</b>	85.8	55.4	14.3
<b>Lifespan (hour)</b>	25,000	1,000	1,000

### 3.1.4.2 LED and Automated Lock Driver

The three options illustrated in Figure 23 will be explored to drive power to the LED array and automated locking mechanism. Minimizing the power requirement is essential to optimize and maintain the power budget of the entire system. The load at the output of the schematics shown below will be either the LED array or the automated lock. A pulse width modulation signal from the microcontroller will be integrated into the final design of both systems to reduce power consumption and maintain a high level of efficiency.

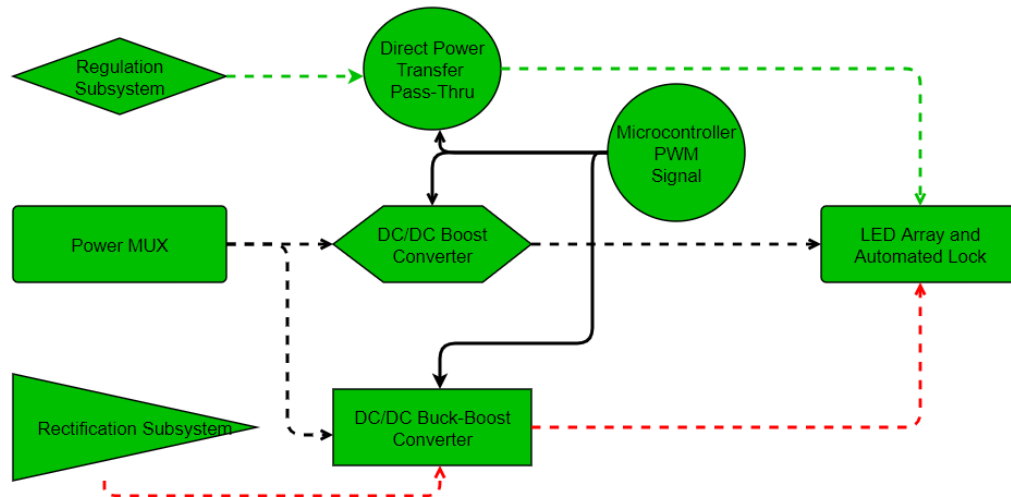


Figure 23: Three Options for Delivering Power to LEDs and Automated Lock

#### 3.1.4.2.1 Buck-Boost Converter

A buck-boost DC/DC converter, which would accept input from the AC to DC rectification stage and battery, was researched to drive the LED array and/or the automated lock. The step-down buck section of the converter would take a range of input voltages from the rectification stage and output the desired voltage level required by the LEDs and/or automated lock. The boost section would then take the reduced voltage and boost the current to be able to supply enough power to adequately supply the LEDs and/or the automated lock. The schematic shown in Figure 24 is a simplified buck-boost DC/DC converter. The switching device is a NMOS transistor in enhancement mode which will receive input from the PWM signal from the microcontroller. When the bike is not in motion, the input source must be switched from the generator to the battery to ensure the LEDs remain illuminated.

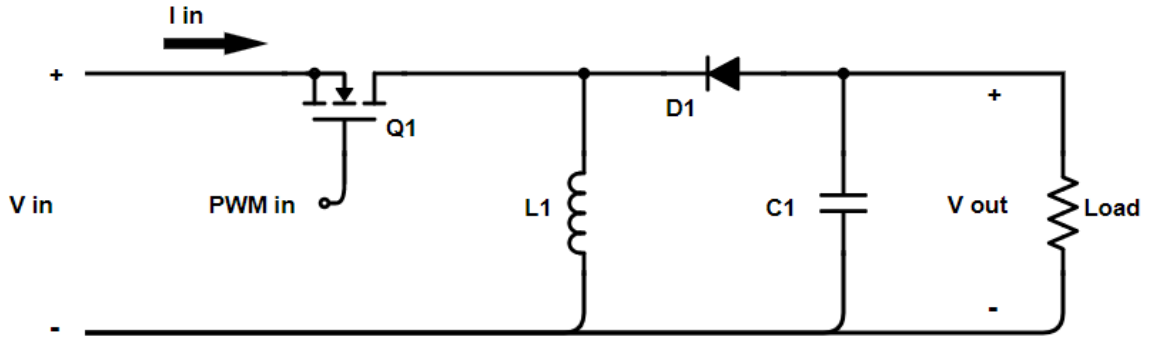


Figure 24: Simplified Buck-Boost Converter Schematic

### 3.1.4.2.2 Boost Converter

A boost DC/DC converter, which would accept input from the output of the power subsystem in Section 3.1.1, was researched to drive the LED array and/or automated lock. The boost converter would need to be configured into a voltage controlled current source to maintain proper current at the input of the LEDs and/or automated lock. The output of the power subsystem has a rectified voltage level and voltage source switching implemented into the design. The boost converter would regulate and deliver the voltage and current characteristics required by the LEDs and automatic lock. The switching device shown in Figure 25 is a NMOS transistor in enhancement mode which will receive input from the PWM signal from the microcontroller.

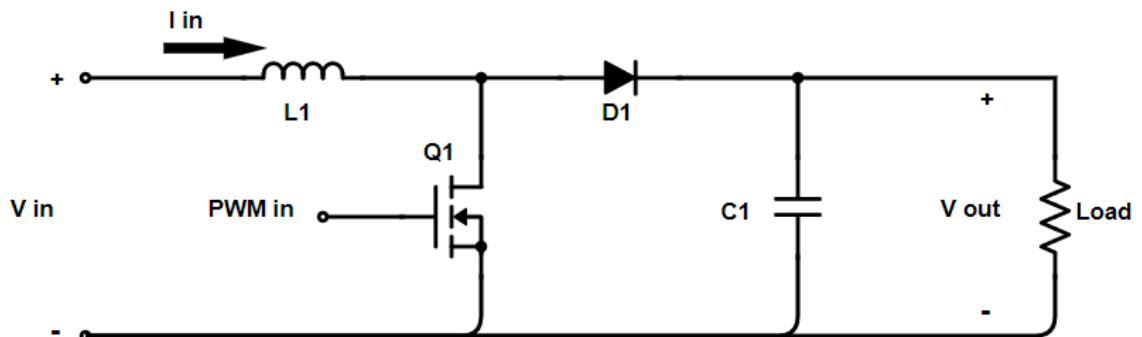


Figure 25: Simplified Boost Converter Schematic

### 3.1.4.2.3 Feed from Output of Rectification Stage

The output from the regulation stage of the power subsystem has been limited to 3.3V at 1A to provide power to different systems. As described in Section 3.1.1, this system will be in place and is required to regulate voltage levels and switch from the generator to the battery and vice versa. As long as the maximum current at the output is not exceeded, the output pin can be tapped into to drive the LED array and/or the automated lock. The switching device shown in Figure 26 is a NMOS transistor in enhancement mode which will receive input from the PWM signal from the microcontroller.

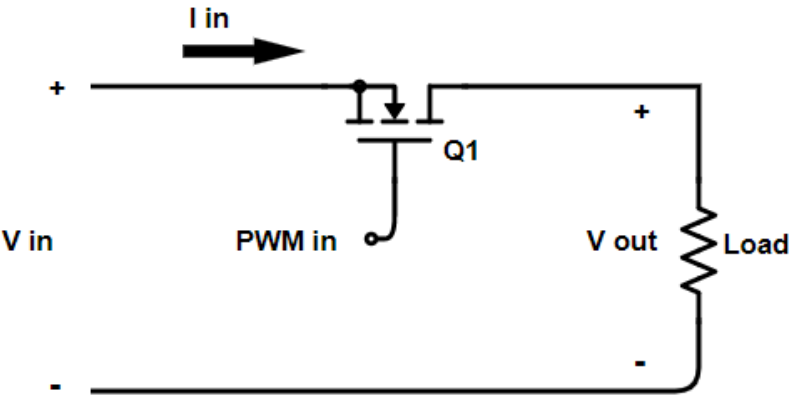


Figure 26: Simplified Direct Power Transfer Schematic

**3.1.4.2.5 Comparison**

The LED does not need additional voltage or current from the regulation stage of the power subsystem. Power from the generator and battery runs through a rectifier and the buck-boost converter will attempt to regulate an already regulated output. These DC/DC converters are widely used as drivers for LED circuits but do not seem to be applicable to this system. The direct power transfer from the output pin of the rectification stage seems to be the most realistic approach to drive the LED array. A MOSFET would be used to switch on and off the LEDs and provide an additional layer of security to ensure over-voltage or over-current conditions are avoided but have additional design parameters. Using the output pin of the rectification stage would appear to be the most straight-forward method to drive the LED array.

Table 8: LED Power Delivery Comparison Impact

Driver	Buck-Boost	Boost	Direct Power
Complexity	High	Mid	Low
System Integration	High	High	Low
Efficiency	High	High	Mid

The solenoid for the locking mechanism requires additional power from the power subsystem. Most solenoids operate within a range of input voltages and corresponding current values. A buck-boost converter does not seem applicable for the same reason mentioned above for the LEDs. The output of the regulation stage will not be able to support enough power to the solenoid as it can supply 3.3 volts at 1 amp for a total of 3.3 watts. A DC/DC boost converter will be required to increase the voltage or the current at the output to be able to acuate the solenoid.

Table 9: Lock Mechanism Power Delivery Comparison Impact

Driver	Buck-Boost	Boost	Direct Power
Complexity	High	Mid	Low

<b>System Integration</b>	High	High	Low
<b>Efficiency</b>	High	High	Mid

## 3.2. Parts Selection

This section builds from Section 3.1 by taking the discussed technologies and looking into practical parts that can be used to actualize the Bike System. The breakdown for this section will be similar to that of Section 3.1.

### 3.2.1 Power Subsystem

This section deals with the selection of part for the Bike System's power subsystem. For the relevant technologies that these parts represent, refer to Section 3.1.1.1.

#### 3.2.1.1 Power Generation

There were many options for ways to generate power for the Bike System. The essence of this process is to take some of the energy that is being produced by the rider of the bike and convert it into electrical power that can be used by the electronics of the Bike System. While power generation all focuses on taking the mechanical energy from the bike and transforming it into electrical energy, there are many different ways to go about it. Three methods of energy harvesting that were considered are: a dynamo attached to the frame harvesting the energy from the bike tire's rotation (Figure 27, top left), a dynamo built into the hub of a bike tire to take advantage of the rotational energy at that point (Figure 27, top right), and a dynamo attached to the frame of the bike to utilize the movement of the bike chain to spin a gear to generate electrical energy (Figure 27, bottom). A comparison of the key features of each type of dynamo are highlighted in Table 10.



Figure 27: Different Bike Dynamo Configurations to Generate Power<sup>[7][8][9]</sup>

Table 10: *Dynamo Parts Comparison*

	<b>Tire Dynamo</b>	<b>Wheel Hub Dynamo</b>	<b>Chain Dynamo</b>
<b>Power</b>	3W	3W	1000 mAh
<b>Mounting Method</b>	Bike Frame	Wheel Hub	Bike Frame
<b>Energy Harvesting Method</b>	Contact/Friction (rotational)	Wheel rotation about the hub	Moving bike chain

The tire dynamo is the option that was chosen for this project. This is because the tire dynamo generates sufficient power and is easy to install. While the wheel hub dynamo operates under the same premise (tire/wheel rotation), it requires special hardware (such as a whole new wheel), or special installation (such as needing re-spoking the wheel). Also, many of the wheel hub dynamo solutions were rather expensive (over \$50) while the tire dynamo solution is much cheaper (under \$25). For the chain powered dynamo, the power is more unreliable since the chain can stop moving even while the bike is still moving. Also, the chain can move considerably during riding from gear shifting and from increasing/decreasing the tension on the chain. This introduces a point of failure that is not shared by the other types of dynamos considered.

The part chosen was the Lowrider Dynamo Generator (Figure 28). In addition to the previous reasoning, this part was chosen because of its advertised 12V/6W rating and the plastic head. Similar dynamos use a metal head, which might not get the best traction on a rubber tire versus that of one made of a plastic material. Although the part is advertised as being able to provide 6W, it will be shown later

that only around 3W can be practically produced. However, this is still a sufficient amount of power for the purposes of the Bike System.



Figure 28: Lowrider Dynamo Generator<sup>[11]</sup>

### 3.2.1.2 Battery

Three different battery technologies were presented in Section 3.1.1.4 Key features of each battery technology is summarized below in Table 11.

Table 11: Battery Technology Comparison

	Li-ion/Li-Po	Ni-Cd/Ni-MH	Lead-Acid
<b>Rechargeable</b>	Yes	Yes	Yes
<b>Nominal Voltage Per Cell</b>	3.7V	1.2V/1.25V	2V/6V/12V/24V
<b>Power Density</b>	126 Wh per Kg	60 Wh per Kg / 100 Wh per Kg	7 Wh per Kg
<b>Additional Advantage</b>	Many Charging Solutions	Standard Sizes	High Power Capacity
<b>Disadvantage</b>	Higher Risk of Danger to User	Cadmium is a Toxic Metal	Extremely Bulky and Heavy

For a small and portable system, such as the one the Bike System describes, a lead-acid battery is clearly not a valid solution. This is mainly due to the size and weight of the battery technology, and high-power capability is not needed for the Bike System's hardware. This leaves the Ni-Cd/Ni-MH or Li-ion/Li-Po as possible considerations for use on the Bike System.

For the Bike System, the battery technology chosen was Li-ion/Li-Po. This choice was made because Li-ion/Li-Po have higher power densities and a higher nominal voltage per cell. This means less battery cells are needed to achieve a specific voltage, and they will take up less space for the same amount of power. Also, since Li-ion/Li-Po is a popular technology, there are many different charging solutions available with a wide range of support.

### 3.2.1.3 Power Multiplexer

A multiplexer (MUX) is a device that can electrically switch between inputs to outputs, where the number of inputs to outputs are represented as a ratio. For example, a 3:2 MUX takes one of the 3 inputs and maps them to one of the 2 outputs. What determines which input goes to which output is a control signal, usually a binary input via control lines. The key feature of a MUX vs using a physical switch is the fact that it can be controlled via electrical signals, which means circuits can be designed to control these devices automatically.

A power MUX operates under the same principles as a traditional signal MUX, where power inputs are selected between to be connected to an output. The main difference between a power MUX and a traditional MUX is the power rating of the devices. The need for a power MUX in the Bike System is to switch between the power generated by the dynamo and the power from the battery. This switching needs to be done automatically to ensure that the power to the electrical devices of the Bike System do not shut down when the dynamo is not producing enough power, such as when the bike is temporarily stopped. To keep the devices functioning correctly, a seamless transition between these two supplies is also needed, which cannot be provided by a manually operated switch.

Three power MUXs were considered. The key characteristics and features of the three devices are tabularized in Table 12.

*Table 12: Power MUX Part Comparison*

	<b>TPS2115A</b>	<b>TPS2124</b>	<b>BQ24076</b>
<b>Device Type</b>	Power MUX	Power MUX	Battery Charger w/ Power-Path Management
<b>Current Handling</b>	1.6A	2.5A	1.6A
<b>Input Voltage</b>	2.8V – 5.5V	2.8V – 22V	4.35V – 26V
<b>Package</b>	TSSOP	VQFN	VQFN
<b>Switching Method</b>	Externally (using a comparator)	Automatically	Automatically
<b>Features</b>	Adjustable current limit	Adjustable current limit and voltage switchover threshold	Adjustable current limit and battery charging capabilities

All three of these parts fulfil the requirements of the project. The BQ24076 has the most features and serves as an all-in-one solution for the power circuit. This is because of the included battery charging circuitry that allows the battery to charge when the input power is able supply both the load and battery charging current, and the device will automatically switch from input power to battery power once the input power falls too low.

The TPS2124 does not contain any power charging circuitry, but it has the ability to automatically switch between two inputs. This is done by a resistor network that sets the voltage threshold for when the inputs are switched. This is important because of the nature of the battery charging voltage and nominal battery voltage, more details in the following paragraph.

The TPS2115A also does not have any battery charging capabilities, and while it can automatically change inputs, it only changes when one input becomes lower than the other. This method of switching will not work because the charging voltage of the battery is higher than the battery's voltage. When the input fall below the battery charging voltage, the inputs will switch, turning off the battery charger. When this happens, the battery voltage will drop from the charging voltage to the nominal voltage, which could be lower than what the input voltage is at that time. This could result in undesirable oscillations as it switches between the inputs. These means an external circuit is needed to control when the MUX switches inputs.

One important factor in component selection is the physical package that it comes in. Both the BQ24076 and the TPS2124 come in only VQFN packages, similar to the QFN package (a QFN-20 is pictured in Figure 29, left; for reference). However, the TPS2115A is available in a TSSOP package (not to scale example shown in Figure 29, right). While small size is usually advantageous in most designs, monetary and time constraints dictate a package size that can be easily 'breadboarded' and tested for the Bike System. As shown in Figure 29, left; the small sizes of these components make them very difficult to build a test circuit for that can be used to ensure the component will work for this project purposes.

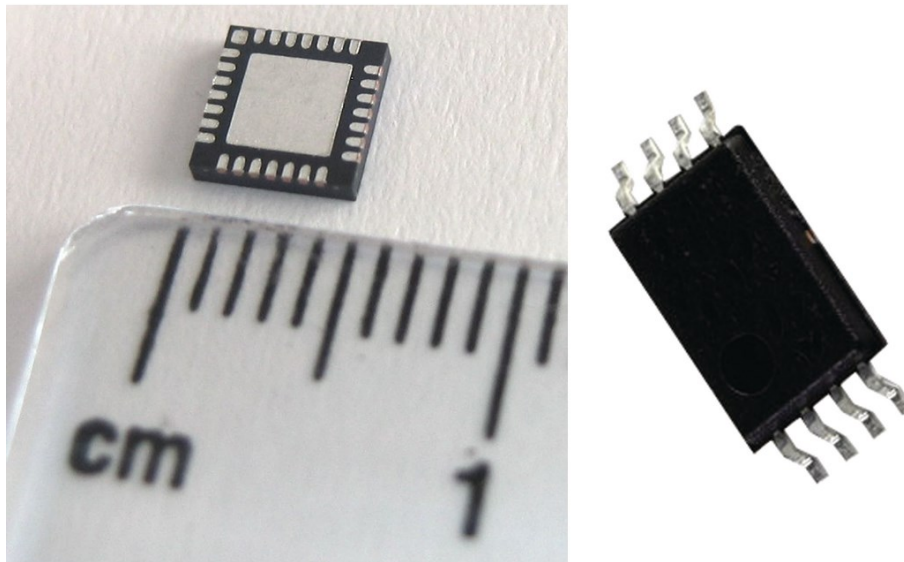


Figure 29: QFN-20 and TSSOP-8 Packages (Not to Scale)<sup>[12][13]</sup>

While the BQ24076 and TPS2124 are clearly the better choices performance wise, the TPS2115A is the best option in a package that can be put into a test circuit. As



discussed previously, the disadvantage of this part is the need for external circuitry for both setting the voltage threshold and for charging the battery.

### 3.2.1.4 Voltage Regulators

For this project two voltage regulators will be needed. The first voltage regulator will take the dynamo's rectified output voltage from the full-wave rectifier, and regulate it down to a steady 5V. Since the dynamo's rectified output ranges from around 7V – 15V and has a significant ripple voltage (see Figure 4) during operation, a voltage regulator is needed to make a steady and usable voltage for use by the following circuitry. The other voltage regulator will be at the final stage of the power circuitry to take either the regulated 5V provided by the first regulator, or the battery voltage (the two supplies are switched between by a power MUX). The reason for second this regulator is twofold. The first is for the variation in the battery voltage over time. A battery's voltage will change depending on its state of charge or discharge. To address this, a voltage regulator is needed to keep a constant output in the presence of this varying voltage. Secondly, when the power MUX switches between the different inputs, there will be variations in the voltage during the transition between the inputs. These variations are caused by both the voltage dip during the transition period and transients generated from the process of switching.

The design of a voltage regulator is no easy task, and involves many factors that need to be consider. Thankfully tools have been made that make this process much easier. One such tool is Texas Instruments' (TI) Webench® Power Designer<sup>(1)</sup>. This tool allows a designer to input key values such as max/min input voltage, output voltage, and max output current. After inputting these values, the tool generates a list of designs that fit the criteria given by the designer. Included is a schematic and all the required parts and values to build the circuit. Also, this tool allows for the export of the designs to many different schematic software tools so that the designs provided by Webench® can be easily incorporated into another board design. The generated designs provide the designer great flexibility, as they come in a variety of different configurations. Some of these differences in configurations are the switching frequency, topology, and power efficiency. Other useful information provided is the bill of materials (BOM) cost, number of components, and approximate area that the circuit will occupy. For these reasons, the Webench® tool was chosen to aid in the selection of a voltage regulator design that would be suitable for the Bike System project.

Since the working input voltage from the dynamo would be around 7V – 15V, the minimum and maximum input voltages chosen to be inputted into the Webench® tool were 6V and 20V, respectively. The working power will be around 3W, and the first stage of regulation will need 5V, so a maximum output current of 1A was chosen to accommodate this. Below in Table 13 are some of the generated designs that were considered.

*Table 13: First Voltage Regulator Stage Parts Comparison*

	<b>LMR36510FA</b>	<b>LMR36510A</b>	<b>TPS56339</b>
<b>Efficiency</b>	92.8%	92.8%	94.9%
<b>BOM Cost</b>	\$2.44	\$2.44	\$3.03
<b>BOM Count</b>	12	12	11
<b>Footprint</b>	326 mm <sup>2</sup>	326 mm <sup>2</sup>	244 mm <sup>2</sup>
<b>Topology</b>	Buck	Buck	Buck
<b>Switching Frequency</b>	400 kHz	400 kHz	543.55 kHz

One of the driving factors in the selection of the voltage regulators is the efficiency of the regulator. Of the three regulators considered, the TPS56339 has the highest efficiency. This component also has a smaller footprint and the lowest BOM count. These advantages do come at a price, however, the BOM cost is slightly higher. Even with a slightly higher BOM cost, the TPS56339 is the better option of the three regulators. This is why this component was chosen for the design.

For the second state of voltage regulation will take a minimum and maximum voltage of 3.5V and 6V, respectively. Again, the power would be around 3W, and with an output voltage of 3.3V, the maximum output current was chosen to be 1.5A to accommodate this requirement. Below in Table 14 are some of the generated designs that were considered for the second stage.

*Table 14: Second Voltage Regulator Stage Parts Comparison*

	<b>TPS62913</b>	<b>TPS54388-Q1</b>	<b>TPS62912</b>
<b>Efficiency</b>	96.4%	97.9%	95.7%
<b>BOM Cost</b>	\$2.67	\$4.15	\$2.17
<b>BOM Count</b>	12	14	12
<b>Footprint</b>	127 mm <sup>2</sup>	735 mm <sup>2</sup>	140 mm <sup>2</sup>
<b>Topology</b>	Buck	Buck	Buck
<b>Switching Frequency</b>	1 MHz	302.34 kHz	1 MHz

Just as with the first regulator stage, the driving factor for regulator selection was the efficiency. From Table 14, it can be seen that the TPS54388-Q1 has the highest efficiency of the three regulators considered. This higher efficiency comes at a steeper cost than that of the first regulator, however. The TPS54388-Q1 has a higher cost than the other two, and occupies a significantly larger amount of board space. Despite these tradeoffs, the component chosen was the TPS54388-Q1. The highest efficiency is needed to make the most use of the limited amount of power being generated by the dynamo, and the power being used by the battery. Limiting the losses in power from both of these sources is important to long battery life for the system.

### 3.2.1.5 Voltage Reference

The Bike System design requires a voltage reference to be used for the comparison of voltages. Voltage comparison is needed to switch between the

different input voltages as the input voltage from dynamo changes. In order to do this the input voltage from the dynamo must be compared against to a known voltage to tell when the input voltage dips below a certain level. What the input voltage from the dynamo is compared against is a voltage created by a voltage reference. In Section 3.1.1.3.1 it was made clear that a voltage divider wouldn't serve as adequate voltage reference. This leaves the possible voltage references to be considered are the Zener diode and a bandgap reference. Table 15 shows a part comparison between one of each type of component.

*Table 15: Voltage Reference Parts Comparison*

	<b>1N4615-1 (Zener)</b>	<b>TL4050A25 (Bandgap Reference)</b>
<b>V<sub>z</sub></b>	2V	2.5V
<b>Initial Voltage Accuracy</b>	5%	1%
<b>Operating Current</b>	250μA	60μA
<b>Temperature Coefficient</b>	$-7.5 \cdot 10^{-4}$	$5 \cdot 10^{-5}$
<b>Price</b>	\$3.68	\$2.58

From Table 15, it can be seen that the bandgap reference is better in every way, and for less of the cost. This is because the bandgap reference has been made specifically for the task of voltage regulation, while the Zener diode can be used in a wider set of applications. For the reasons stated above, and based on Table 15, the TL4050A25 was chosen as the component for voltage regulation.

### 3.2.1.6 Battery Charging IC

In Section 3.2.1.2 the battery decided for the Bike System design was a Li-ion Battery, which is a rechargeable battery. The Bike System will also implement a method of charging the battery when it is not in use. While a discrete solution can be designed to charge the Li-ion battery, it can be rather complex to do it effectively and safely. This is mainly related to ensuring that the battery doesn't get over charged and create an unsafe situation. For these reasons it is usually more preferable to go with an "off-the-shelf" solution. This is supported by the vast amount of consolidated battery charging IC that are available on the market. Two of the parts consider are compared in Table 16.

*Table 16: Battery Charging IC Parts Comparison*

	<b>LTC4056</b>	<b>BQ21040</b>
<b>Input Voltage</b>	4.5V – 6.5V	3.5V – 28V
<b>Max Quiescent Current</b>	600μA	125μA or 1mA
<b>Number of Battery Cells</b>	1	1
<b>Can Set Current Limit</b>	Yes	Yes
<b>External Components Needed</b>	4	3

Both of these parts have the ability to charge a single cell Li-ion battery, and can utilize the regulate input voltage generated by the dynamo (5V). While the LTC4056 has a lower quiescent during charging, but the BQ21040 has a standby

mode that only draws 125 $\mu$ A of current. One key feature for the charging IC is the ability to limit the charge current. This is important because if the battery charging takes too much current, the rest of the Bike System's electronics might not be getting enough current for them to function correctly. One downside for the LTC4056 is the need for an external PNP BJT transistor. This PNP transistor is used to control the charge current that flows through the battery. The BQ21040 does not need an external transistor to control the flow of current to the battery, as it is controlled internally.

Although both parts are valid solutions, the BQ21040 was chosen because of the low standby current draw and does not need the additional PNP transistor.

## **3.2.2 Sensors Parts Selection**

This section details the selection of parts that were considered for the sensors that are needed in the Bike System.

### **3.2.2.1 Magnetic Reed Switch**

A Magnetic Reed Switch is viable candidate for detecting speed because of the dependability and cost of the part. Ideally, this part will be used in conjunction with a generic permanent magnet that has a strong enough magnetic field to both stick to the rim of the bicycle tire and can active the contacts inside the Reed Switch itself. The Reed Switch has an advantage over the Hall Sensor because it requires less pins to operate and does not draw power while in the normally open state, meaning that it will be the more power effective option. The working principle behind the Reed Switch is that two contacts inside the switch, which can be in the normally open (NO) or normally closed (NC) position, will either close or open, respectively, depending on the normal orientation of the contacts when a magnetic field comes close enough to the switch.

Typical specifications that differentiate Reed Switches include the size of the Reed Switch itself and the amount of voltage that can flow through the contacts of the Reed Switch. Since the Bike System's application emphasizes low power consumption, the smallest Reed Switches were chosen for consideration. Also, every Reed Switch considered has an operating temperature range of at least -40°C to 105°C.

#### **3.2.2.1.1 59145 Flange Mount Reed Sensor**

This Reed Switch is considered for its availability, price, and the wide variety of options available from the manufacturer. At the time of creation of this document, over 18,000 units are available to ship immediately. Furthermore, Littelfuse Inc. offers a wide range of configurations for this part include the package size, mounting types, and connector types. Also, this part is hermetically sealed meaning that the contacts are sealed in an airtight enclosure; this adds to the longevity of the part and ensures that the part will not need to be serviced in the

near future. This Reed Switch is a flange mount type meaning that it can be secured to the frame of the bicycle with screws or bolts that fit through the flange holes. The specifications in the datasheet are given for when the 59145 Flange Mount Reed Sensor is used in conjunction with the 57145 Actuator, which is a flange mount permanent magnet with retentivity of 11,000 Gauss.

### 3.2.2.1.2 59010 Sub-Miniature Firecracker Reed Sensor

This Reed Switch is considered primarily for its small package size; it requires only a 3 millimeter hole in the bike frame to be securely mounted. This part is hermetically sealed meaning that the contacts are sealed in an airtight enclosure; this adds to the longevity of the part and ensures that the part will not need to be serviced in the near future. At the time of creation of this document, only 400 units are available to ship immediately. The specifications in the datasheet are given for when the 59010 Sub-Miniature Firecracker Reed Sensor is used in conjunction with the 57020 Actuator, which is a cylindrical permanent magnet with retentivity of 11,000 Gauss.

### 3.2.2.1.3 59070 M8 Plastic Threaded Barrel Reed Sensor

This Reed Switch is considered for both its mounting type and price. The 59070 M8 Plastic Threaded Barrel Reed Sensor can be mounted in a tapped hole of the same screw type, meaning that this Reed Switch has little chance of falling off the bicycle or failing because of misalignment with the permanent magnet on the rim of the bicycle tire. At the time of creation of this document, only 400 units are available to ship immediately. This part is hermetically sealed meaning that the contacts are sealed in an airtight enclosure; this adds to the longevity of the part and ensures that the part will not need to be serviced in the near future. The specifications in the datasheet are given for when the 59070 M8 Plastic Threaded Barrel Reed Sensor is used in conjunction with the 57070 Actuator, which is a threaded permanent magnet of the same dimensions as the 59070 M8 Plastic Threaded Barrel Reed Sensor with retentivity of 11,000 Gauss.

*Table 17: Reed Switch Parts Comparison*

Part Number	Price per part	Max Voltage VDC	Dimensions (L, H, W) or (L, Diameter)	Mount
<b>59145-010</b>	\$2.90	200	28.57mm, 19.05mm, 6.35mm	Flange
<b>59010-010</b>	\$10.53	170	9.0mm, 3.0mm	NA
<b>59070-010</b>	\$3.71	200	38mm, 8mm	Threaded

After consideration, the part selected for this project will be the 59145 Flange Mount Reed Sensor because of the low cost of the part and the amount of readily available parts. The hardware in consideration for the speed calculation of the bicycle is still under review. The speed calculation hardware will either consist of a Reed Switch or a Hall Sensor to be used in conjunction with either a permanent magnet or magnetic actuator from Littelfuse Inc.

### **3.2.2.2 Hall Sensor**

In researching what type of Hall Sensor would be best for the application of detecting a passing permanent magnet, the Threshold Hall Switch is the best fit. This type of Hall Switch will output either a digital signal or analogue signal depending on the part. Similar to the Reed Switch, the ideal application of this part would be in conjunction with a permanent magnet that is both strong enough to adhere to the rim of the bicycle tire and will activate the Threshold Hall Switch as the bicycle tire rotates. One significant downside to the Threshold Hall Switch versus the Magnetic Reed Switch is that the Threshold Hall Switch requires a constant power supply when the system is active, even if the bicycle is not moving making the Threshold Hall Switch a less power effective option. The working principle behind the Threshold Hall Switch is that while power is supplied to the part, it will output a signal once the measured Gauss exceeds a defined threshold, thus why this part is called the Threshold Hall Switch. Hall Switches can be unipolar or bipolar, meaning that it can measure both positive and negative values of Gauss, corresponding to which pole of the permanent magnet is passing the sensor at a given time. This is a significant benefit as it allows for user error when attaching the permanent magnets to the inside of the bicycle rim.

#### **3.2.2.2.1 55100 Miniature Flange Mounting Proximity Sensor**

This Hall Sensor is considered for both its size and low threshold value, meaning that it will be sensitive to any passing permanent magnets. The 55100 Miniature Flange Mounting Proximity Sensor is unipolar in that it only detects the south pole of passing permanent magnets. The 55100 series of Hall Sensors are flange mounted sensors, meaning that they can be attached to the frame of the bicycle with either screws or an adhesive without affecting the performance of the part. The threshold of the 55100 series of Hall sensors is typically around 130 Gauss. The activation distance listed on the datasheet is 12.5 millimeters, but depending on the strength of the permanent magnet used, this distance can be extended. The 55100 Miniature Flange Mounting Proximity Sensor has options for both digital and analogue outputs, but the part in consideration is the one with the digital output. The 55100 Miniature Flange Mounting Proximity Sensor has an operating temperature range of -40°C to 100°C.

#### **3.2.2.2.2 55310 Flat Pack Digital Hall Sensor**

This Hall Sensor is considered for both its size and ultra-low threshold value, meaning that it will be sensitive to any passing permanent magnets. The 55310 Flat Pack Digital Hall Sensor is unipolar in that it only detects the south pole of

passing permanent magnets. Similar to the 55100 Miniature Flange Mounting Proximity Sensor, the 55310 Flat Pack Digital Hall Sensor also has a flange mount. This flange mount will allow for the part to be attached to the frame of the bicycle with either screws or adhesives without affecting the performance of the part. The 55310 Flat Pack Digital Hall Sensor has a digital output. The 55310 Flat Pack Digital Hall Sensor has an operating temperature range of -40°C to 105°C.

### 3.2.2.2.3 APS11700 Micropower Hall Effect Switch

This Hall Sensor is considered for both its size, price, and ultra-low threshold value, meaning that it will be sensitive to any passing permanent magnets. The APS11700 Micropower Hall Effect Switch is the smallest and cheapest of the considered options. It is also the most sensitive Hall Effect Switch considered. One particular downside to this part is that the only available packaging options are surface mount and through hole configurations meaning that the part will need to be secured to the frame of the bicycle by alternative means such as adhesives. The APS11700 Micropower Hall Effect Switch comes in both unipolar and omnipolar configurations meaning that the Hall Effect Switch will be sensitive to both the north pole and south pole of the permanent magnet passing in front of it; however, for both the unipolar and omnipolar configurations, the magnet must pass by the Z-axis of the part in order for it to operate correctly. The Z-axis of the part is clearly defined in the datasheet. The APS11700 Micropower Hall Effect Switch has an operating temperature range of -40°C to 165°C, which is the largest range of the considered Hall Effect Sensors. Also, the APS11700 Micropower Hall Effect Switch draws as little as 6 microamps when in operation making it a viable option in terms of power consumption when compared to the Magnetic Reed Switches. Unlike the other Hall Effect Switches considered, the APS11700 Micropower Hall Effect Switch is the only considered option with only an analogue output as the indicator of a passing permanent magnet. This will require the use of an analogue to digital converter on board the microcontroller to detect when the output voltage of the APS11700 Micropower Hall Effect Switch exceeds a defined limit to indicate that a permanent magnet has passed.

*Table 18: Hall Sensor Parts Comparison*

Part Number	Price per part	Supply Voltage in VDC	Dimensions (L, H, W) or (L, Diameter)	Threshold
<b>55100-3M</b>	\$9.68	3.8-24	25.5mm, 11.00mm, 3.00mm	130 Gauss
<b>55310-00-02-A</b>	\$7.24	4.75-24	28.5mm, 20.4mm, 6.35mm	55 Gauss
<b>APS11700</b>	\$1.08	3.3-24	4.09mm, 3.02mm, 1.52mm	40 Gauss

### **3.2.2.3 RFID Module**

The RFID module will be used to encode/decode information onto, or from, specific RFID transponders. This method will be the primary mechanism that either locks or unlocks the bicycle. Only RFID modules with integrated antennas were considered as for the Bike System as the RFID module to read/write onto, or from, the RFID transponder is only from a distance of a few centimeters away.

#### **3.2.2.3.1 RC522 RFID Module 13.56MHz**

The RC522 RFID Module is the cheapest RFID module considered and it has a significant advantage over the other RFID modules solely because of its price. Furthermore, the RC522 RFID Module has large amounts of reference material available for use when integrating this part into the Bike System's design. Included in this reference material are libraries of code that execute in the Energia IDE, and while the Energia won't be used IDE for the software development environment used in the Bike System's design, there exists a working example of the RC522 RFID Module reading and writing onto RFID transponders. The RC522 RFID Module can communicate with a host PC with the following communication protocols: RS232 (Serial UART), SPI, and I2C. The RC522 RFID Module has a low power mode and power down feature, which is good for the Bike System since maximizing the efficiency of the power system in the Bike System's design in order to maximize the time the user will need to go without having to charge the system with an external power source. The maximum power dissipation of the RC522 RFID Module is 200mW. Lastly, RC522 RFID Module has an operating temperature range of -25°C to 85°C and has a moisture sensitivity rating of this package is level one.

#### **3.2.2.3.2 Proximity Reader Module RFID RW01**

The Proximity Reader Module RFID RW01 module operates in the low frequency band which makes it very resistant to noise when reading from, or writing to, an RFID transponder. The Proximity Reader Module RFID RW01 module has a maximum power dissipation of 300mW which is 100mW more than the RC522 RFID module, but it still good overall because a power dissipation of 300mW is good as compared to other RFID modules that exist today. The Proximity Reader Module RFID RW01 has an integrated antenna as well has ports for another antenna which will be useful in case the need to implement a stronger antenna is required to meet the stretch goals defined in Table 1. The Proximity Reader Module RFID RW01 module has the longest read range of all the modules considered and can interact with a host PC via RS232 (Serial UART). The Proximity Reader Module RFID RW01 module has an operating temperature range of -25°C to 70°C.

#### **3.2.2.3.3 Proximity Reader Module RFID RW01L.AB-A**

The Proximity Reader Module RFID RW01L.AB-A module is very similar to the Proximity Reader Module RFID RW01 module made by the same company, Feig Electronics. The difference between them is that the Proximity Reader Module



RFID RW01L.AB-A module sacrifices some features available on the Proximity Reader Module RFID RW01 module for the sake of size and power consumption. The Proximity Reader Module RFID RW01L.AB-A module is optimized for embedded use as it has a 200mW power consumption rating and has the smallest dimensions of all the RFID modules considered. Similar to the Proximity Reader Module RFID RW01 module, the Proximity Reader Module RFID RW01L.AB-A module operates in the low frequency band meaning that it is very resistant to electromagnetic interference. The Proximity Reader Module RFID RW01L.AB-A module communicates with a host PC via RS232 (Serial UART). The operating temperature range of the Proximity Reader Module RFID RW01L.AB-A module is -25°C to 70°C.

### 3.2.2.3.4 13.56 MHz RFID Handheld Reader Module

The Gao RFID handheld reader module, like the Proximity Reader Module RFID RW01L.AB-A module, is optimized for embedded application with its small dimensions and low power consumption. Unlike the Proximity Reader Module RFID RW01L.AB-A module, the Gao RFID handheld reader module operates in the high frequency band, which makes it a little more susceptible to electromagnetic interference. The Gao RFID handheld reader module communicates to the host PC via Serial TTL which has to be converted to RS232 (Serial UART). The Gao RFID handheld reader module has a maximum read range of 4 centimeters and has an operating temperature range of -20°C to 80°C.

*Table 19: RFID Module Parts Comparison*

Part Number	Price	Supply Voltage VDC	Dimensions (L, W, H)	Communication Protocol	Maximum Read Range
<b>RC552</b>	\$12.95	2.5-3.6V	60mm × 39mm	UART, SPI, I2C	3cm
<b>ID RW01</b>	\$295.17	5V	90mm, 47mm, 11.6mm	UART	12cm
<b>ID RW01L.AB-A</b>	\$171.43	5V	45 mm, 40 mm, 16 mm	UART	8cm
<b>713002R (on website)</b>	\$195	5V	60mm, 30mm, 6mm	UART	4cm

After consideration, the RFID module selected is the RC522 RFID Module 13.56MHz because of the large cost contrast of all the RFID modules considered. Furthermore, the RC522 RFID Module 13.56MHz only requires a 3.3V power source and has the most options for communication with the microcontroller. The RC522 RFID Module 13.56MHz also has large amount s of reference material available; this reference material will be vital during the integration phase of the

project. Although the RC522 RFID Module 13.56MHz has the shorted read/write range of all RFID modules considered, this will not be an impeding issue since the user is expected to touch the RFID module with the RFID transponder during use. Lastly, the RC522 RFID Module 13.56MHz has an average size when compared to the other RFID modules considered. The dimensions of the RC522 RFID Module 13.56MHz are considered because the electronics housing that will house this RFID module needs to be minimized in terms of size as to not disrupt the user while they are riding the bicycle.

### 3.2.2.4 RFID Tags

RFID tags, also called RFID transponders, are to be used in conjunction with RFID readers to verify that the user with the RFID tag has access to the information or function the RFID reader is associated with. In the Bike System's case, the RFID tag verifies that the user who is trying to unlock the bicycle is the person who owns the bicycle. Each RFID tag can be encoded with a specific identification number, thus making it the sole key to unlocking the system via radio frequency modulation methods.

#### 3.2.2.4.1 MIKROE-1475

The MIKROE-175 is a transponder in the form of a key fob. This transponder should be used if the RFID reader that is chosen operates in the high frequency band.

#### 3.2.2.4.2 MIKROE-779

The MIKROE-779 is a transponder in the form of a keycard. This transponder should be considered if the RFID reader that is chosen operates in the low frequency band. This is the lightest of the RFID transponders considered and is also the cheapest.

#### 3.2.2.4.3 HT2DC20S20/F/RSP

The HT2DC20S20/F/RSP is a transponder in the form of a key fob. This transponder should be considered if the RFID reader that is chosen operates in the low frequency band. This transponder is the heaviest and most expensive of the low frequency transponders considered.

*Table 20: RFID Tag Parts Comparison*

Part Number	Price	Weight	Standard	Frequency
<b>MIKROE-1475</b>	\$2.08	5 grams	ISO14443-A	13.52MHz
<b>MIKROE-779</b>	\$1.77	2 grams	ISO14443-A	100-150 kHz
<b>HT2DC20S20/F/RSP</b>	\$2.91	8 grams	ISO14443-A	125kHz

After consideration, the MIKROE-1475 is selected for use in this project because of its operable frequency range. The MIKROE-1475 is a key fob shaped RFID transponder that can be attached to any keychain or zipper. The MIKROE-1475 was selected for its price and weight also.

### 3.2.2.5 Temperature Sensor Parts Selection

This section covers the different temperature sensor parts that were considered for use in the Bike System.

#### 3.2.2.5.1 Sun Company Clip-on Bike Thermometer

The Sun Company Clip-on Bike Thermometer shown in Figure 30 is a ready to use accessory that features a dial thermometer than be easily clipped on or off of the handlebars of the Bike System. This thermometer has an operation range of -20 C to 120 C. This device is discreet and requires no batteries for operation which does not put additional strain on to the Bike System's power supply.



*Figure 30: Clip-on Bike Thermometer*

This device will be not closely accurate to the nearest degree like some of the other options listed here in this section simply due to the nature of its design. Similar to other dial thermometers or even some applications of fire alarms, this thermometer contains a bimetallic strip that expands and bends at the temperature increases. As the bimetallic strip expands, it pushes the red pointer. Similarly, as the temperature drops, the bimetallic strip shrinks or tightens which causes the red pointer to fall. This can be seen in the Figure 31 below.

Since this device uses the bimetallic strip mentioned, it would not be requiring or using any power from the Bike System. It also can be viewed as a standalone device since it is separate from the Bike System circuitry.

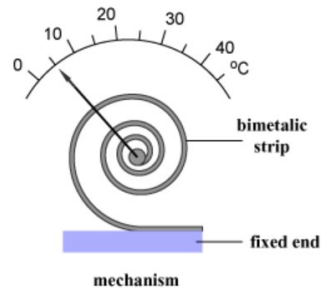


*Figure 31: Bimetallic strip functionality*

### **3.2.2.5.2 AOZBZ Motorcycle Thermometer Clock**

This AOZBZ Motorcycle Thermometer Clock, shown in the Figure below, provides two functionalities: the current ambient temperature and the current time. This device utilizes a battery and displays these values digitally. It is made to be small and compact. This is a similar standalone, ready to use accessory like the Sun Company clip-on bike thermometer mentioned above.

It can be attached to the Bike System via the adhesive pads supplied with the device. The device is housed in a waterproof casing and there is a button to illuminate the screen for easier viewing. This button is located at the bottom of the device (Figure 32) for easy accessibility.

These features make it a good design for the outdoor conditions associated with the Bike System. The downside to this particular device is that it cannot be mounted permanently since it would make changing the battery nearly impossible. Without being mounted permanently, this leaves the device open to the chance of being stolen or tampered with.



*Figure 32: Standalone Thermometer-Clock*

### **3.2.2.5.3 Texas Instrument's LM35 Temperature Sensor**

A LM35 temperature sensor with analog output can be integrated into the microcontroller to provide the user with the current ambient temperature. This sensor can measure the temperature within the range of -55 °C and 150 °C. This

is a wide enough range for Florida's ever-changing weather. This device only draws 60  $\mu\text{A}$  and it does not require any external calibration by the user. This LM35 temperature sensor was selected as the best fit choice for this project.

### 3.2.2.5.4 Texas Instrument's TMP75-Q1 Temperature Sensor

A TMP75-Q1 sensor device with digital output is of automotive grade and best suitable for extended periods of temperature measurements. It has wide temperature operation range of  $-40\text{ }^{\circ}\text{C}$  to  $125\text{ }^{\circ}\text{C}$ . This unit has a power draw of 50  $\mu\text{A}$ .

### 3.2.2.5.5 Texas Instrument's TMP235 Temperature Sensor

A TMP235 temperature sensor is very similar to the LM35 temperature sensor, but with a smaller power draw of 9  $\mu\text{A}$ . This sensor has a wider range of  $-40\text{ }^{\circ}\text{C}$  and  $150\text{ }^{\circ}\text{C}$ . This sensor also supplies analog output. This temperature sensor has the smallest power draw of the other alike sensors mentioned in this section.

### 3.2.2.5.6 Temperature Sensor Comparison

Below is a table comparing each thermometer or temperature sensor discussed in this section. In senior design 2, we opted for the TMP235 temperature sensor instead of the LM35 temperature sensor that was chosen in Senior Design 1. This was due to the lower power consumption and because the TMP235 temperature sensor was more easily available.

*Table 21: Temperature Sensor Comparison*

	<b>Clip-on Bike Thermomet er</b>	<b>Digital Motorcycle Thermomet er Clock</b>	<b>LM35 Sensor</b>	<b>TMP75- Q1 Sensor</b>	<b>TMP235 Sensor</b>
<b>Manufactur er</b>	Sun Company	AOZBZ	Texas Instrumen ts	Texas Instrumen ts	Texas Instrumen ts
<b>Cost</b>	\$ 12.99	\$11.99	\$22.67	\$0.69	\$0.58
<b>Operating Temperatur e Range</b>	$-20^{\circ}\text{C}$ - $120^{\circ}\text{C}$	$-10^{\circ}\text{C}$ - $50^{\circ}\text{C}$	$-55^{\circ}\text{C}$ - $150^{\circ}\text{C}$	$-40^{\circ}\text{C}$ - $125^{\circ}\text{C}$	$-40^{\circ}\text{C}$ - $150^{\circ}\text{C}$
<b>Power Draw</b>	Not Applicable	Battery Operated	60 $\mu\text{A}$	50 $\mu\text{A}$	9 $\mu\text{A}$
<b>Standalone Accessory</b>	Yes	Yes	No	No	No

## 3.2.3 Microcontroller Parts Selection

In considering the possible candidates for the microcontroller, we do not expect that the Bike System will be utilizing operations that are computational heavy. As a result, we are considering three microcontrollers for this project, which are the

Texas Instruments MSP430G2553 microcontroller, the Texas Instruments MSPFR6989 microcontroller and the Arduino ATmega328P microcontroller.

The Texas Instruments MSP430G2553 microcontroller and the Texas Instruments MSPFR6989 microcontroller can be easily programmed using the C programming language within the Code Composer Studio (CCS) integrated development environment. Both of these Texas Instrument microcontrollers have already been acquired since we have all used them in one or more past pre-requisite classes. Hence, these two microcontrollers are strong candidates due to the familiarity of working with them for an extensive period in the past.

The third option under consideration is the ATmega328P on the Arduino Uno. Although working with Arduinos is unfamiliar to the team, this type of MCU is used extensively in beginner-level applications. The ATmega328P microcontroller is programmed using the C++ programming language.

### 3.2.3.1 MSP430G2553

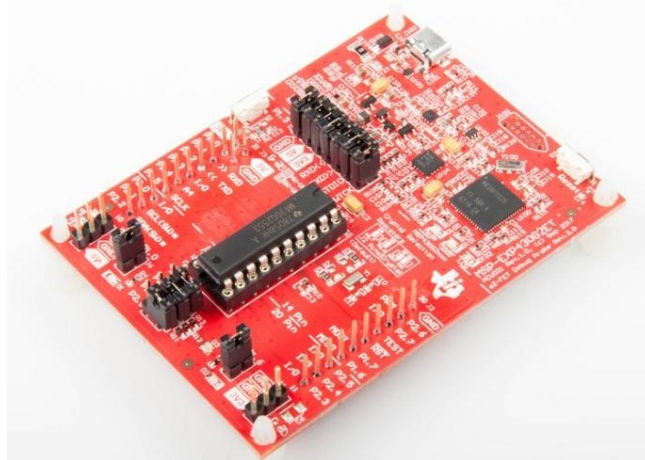


*Figure 33: TI MSP430G2553 (Courtesy of Texas Instruments Inc.)*

The MSP430G2553 utilizes UART and contains 16 KB of flash memory. This device also features a 16-bit RISC architecture and five different low power modes. The low power modes are vital to the Bike System design since we want to minimize or prevent any wasted power. A 32 kHz crystal is one of the basic clock module configurations on this MSP430G2553 microcontroller. In the Figure 8 above, the MSP430G2553 is seen on the MSP-EXP430G2ET Development Kit that will be used for testing purposes. This is the microcontroller that was decided upon for the Bike System.

### 3.2.3.2 MSP430FR6989



Figure 34: TI MSP430FR6989 (Courtesy of Texas Instruments Inc.)

An additional feature that this microcontroller possesses, that the other two options do not, is the onboard LCD. This MSP430FR6869 microcontroller features a 16-bit RISC architecture, 128KB of flash memory and seven low power modes. In addition to the 32 kHz crystals, this microcontroller contains high-frequency crystals; there is a flexible clock system.

### 3.2.3.3 ATmega328P



Figure 35: Arduino ATmega328P

This microcontroller features fourteen digital input/output pins, six analog inputs and a 16MHz quartz crystal. Unlike the two Texas Instruments microcontrollers mentioned above, this Arduino Uno board would be programmed within the Arduino Software Integrated Development Environment. The ATmega328P on this Arduino Uno comes preprogrammed with a bootloader so that the programmer can upload new code to the MCU. The cost of this part from Mouser is approximately \$22. It has an operating supply voltage of 5V, a data bus width of 8 bit and flash memory of 32 KB. Compared to the two other microcontrollers, this ATmega328P

is totally unfamiliar to the programmer so there would be a bit of a learning curve with working with this part.

### 3.2.3.4 Microcontroller Parts Comparison

We opted for the Development Kits when considering each microcontroller to make the preliminary testing phase of the Bike System project faster and much easier. Below is a table comparing each specification discussed of each microcontroller mentioned above.

All three of the microcontrollers considered were capable of entering low power modes so as to avoid wasting any unused power. With all of the auxiliary sensors and devices being implemented in the Bike System, the number of pins available was an important factor.

All three of the microcontrollers discussed in this section have an operating temperature of  $-40^{\circ}\text{C} - 85^{\circ}\text{C}$ . They also all have a clock frequency of 16MHz. These three microcontrollers all contained both digital input and output.

Table 22: Microcontroller Parts Comparison

	<b>MSP430G2553</b>	<b>MSP430FR6869</b>	<b>ATmega328P</b>
<b>Memory</b>	16KB flash 512B SRAM	128KB flash 2 KB SRAM	32KB flash 2KB SRAM 1KB EEPROM
<b>Cost</b>	\$ 9.99	\$20.00	\$ 22.00
<b>Operating Voltage</b>	1.8 V – 3.6 V	1.8 V – 3.6 V	1.8 V – 5.5 V
<b>Power Consumption</b>	200 $\mu\text{A}$ (on) 0.1 $\mu\text{A}$ (off)	100 $\mu\text{A}$ (on) 0.02 $\mu\text{A}$ (off)	200 $\mu\text{A}$ (on) 0.1 $\mu\text{A}$ (off)
<b>Analog I/O</b>	Both I/O	Both I/O	Only Input
<b>GPIO pins</b>	24	83	23
<b>Bit count</b>	16	16	8

### 3.2.4 LCD Parts Selection

A liquid crystal display (LCD) is a vital feature of the Bike System. Metrics such as the speed, distance travelled on the current trip and the ambient temperature will be communicated to the user via an LCD display. This display would be mounted on the handlebars of the bicycle to ensure optimal viewing when the user is riding the bicycle. This ease of accessing information about a trip is the foundation of the purpose behind the Bike System.



The LCD would ideally be backlit so that the user can easily read the speed, distance, and temperature values during his/her trips taken place at nights. The LCD chosen also has to be compatible with the microcontroller chosen. The largest and most important feature to consider in choosing the LCD display is the power draw.

A smaller, but equally relevant consideration was the size of the display. We strive to have the display big enough as to where the user is not struggling to read and possibly decipher the information being displayed, and to be compact enough as to where the screen did not become a distraction to the rider. It is a priority to make the display as less of a distraction as possible so as to avoid any potential safety concerns.

#### **3.2.4.1 LCD-20x4Y**

This module is manufactured by Gravitech and the cost is approximately \$14.59. The dimensions of this display are 98 mm x 60 mm x 14 mm, however the viewing size is 76 mm x 25.2 mm. The display is a yellow/green backlight display color. This device does not have touchscreen capabilities. It has a current draw of 80 mA and  $V_{DD}$  of 5V. This display utilizes the HD44780 driver.

The parallel interface communication of this device is not familiar to the programmer which may hinder the project in the time taken to learn the new communication interface protocols and rules. This interface is also very common – the yellow/green display color can be seen as an unpleasant experience for the user of the Bike System.



*Figure 36: LCD-20x4Y display*

#### **3.2.4.2 SunFounder's 1602 LCD Module**

This module is similar in construction to the Gravitech component discussed above with the 4 lines x 20 characters construction. It is also similar in size. This LCD module does not possess touch display capabilities. It also has the smallest power draw of the three LCD displays being considered.

This 1602 LCD module provides a more appealing appearance due to the white characters on the blue backlight. This small design feature would make it the output metrics on the screen easier to see in both the daytime and nighttime.



*Figure 37: SunFounder 1602 LCD Module*

### **3.2.4.3 HiLetgo IL19341 Touch Display**

The major feature that sets this module apart from the previous two displays mentioned, is that it is a touch display. The part number for this component is 3-01-1433. Although the initial power consumption of this device is high in comparison to the others discussed here, it is a trade-off that will be made for the sleeker design and the touch display capability.

The touch display feature of this module will provide an overall more pleasing experience to the user. Being a touch display, this module allows us to give the user options when it comes to the screen brightness. This is a small customization that the display offers to the user. Ultimately, this touch display was our chosen module for the Bike System.



*Figure 38: HiLetgo IL19341 Touch Display*

### **3.2.4.4 Display Parts Comparison**

The Table 23 serves as a comparison of the displays mentioned and discussed in this section.

Table 23: LCD display comparison

	LCD-20x4Y	LCD-1602	HiLetgo IL19341
<b>Manufacturer</b>	Gravitech	SunFounder	HiLetgo
<b>Cost</b>	\$14.59	\$8.99	\$13.99
<b>Construction</b>	4 lines x 20 characters	4 lines x 20 characters	240 x 320 dots
<b>Backlit</b>	Yes	Yes	Not Applicable
<b>Dimensions (inches)</b>	3.86 x 2.36 x 0.56	4.92 x 1.7 x 0.4	31.5 x 2.17 x 0.1
<b>Current Draw</b>	80 mA	30 mA	150 mA
<b>Power (V<sub>DD</sub>)</b>	4.5 V – 5.5 V	5 V	3.3 V or 5 V
<b>Interface</b>	Parallel	I2C	SPI
<b>Touch Display</b>	No	No	Yes

## 3.2.5 LED Parts Selection

As a portable system, operating voltages and current must be minimized by the LED to ensure there is enough power available for all other operating systems. The size and shape of the main enclosure will not restrict the space required from the surface mount LED and will not be considered for part selection.

### 3.2.5.1 LTPL-P00DWS57 High Power LED

This LED has a maximum forward pulse current of 100mA tested with a PWM signal at 10% duty cycle at a 100 msec pulse width and the maximum forward current the device can handle is rated at 80mA. The maximum continuous current is rated at 75mA and the LED should operate in the range of 40mA to 75mA to preserve the lifespan of the device. The forward voltage required to turn on the LED is 3.2V typical with a minimum voltage of 2.7V and a maximum voltage of 3.8V at 75mA of current flowing through the device. The forward voltage at 40mA is 3.0V typical with a minimum voltage of 2.7V and a maximum voltage of 3.6V. The minimum and maximum power dissipation of the device are as follows:

Test Condition  $I_f = 40\text{mA}$

$$P_{min} = V_{f\ min} \times I_{f\ min} = 108\text{mW}$$

$$P_{max} = V_{f\ max} \times I_{f\ continuous} = 144\text{mW}$$

Test Condition  $I_f = 75\text{mA}$

$$P_{min} = V_{f\ min} \times I_{f\ min} = 203\text{mW}$$

$$P_{max} = V_{f\ max} \times I_{f\ continuous} = 285mW$$

This LED is capable of emitting 21 lumens at a forward current of 40mA with an efficiency rating of 85 typical and 37 lumens at a forward current of 75mA with an efficiency rating of 75 typical. The operating temperature of this device ranges from -40° C to 85° C. This device contains two LEDs per unit providing more flexibility for the design and can be configured in two different designs as shown in Figure 39 and Figure 40. Figure 39 illustrates configuration 1 in which a single resistor is in series with two LEDs in parallel. This configuration reduces the number of resistors required but both LEDs may not be uniformly illuminated. Figure 40 illustrates configuration 2 in which a resistor is in series with each LED. All LEDs will be manufactured with slightly different characteristics and configuration 2 offers the optimal design to ensure equal current is distributed and the device is uniformly illuminated.

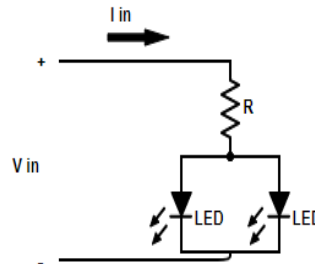


Figure 39: Configuration 1 of LTPL-P00DWS57 High Power LED

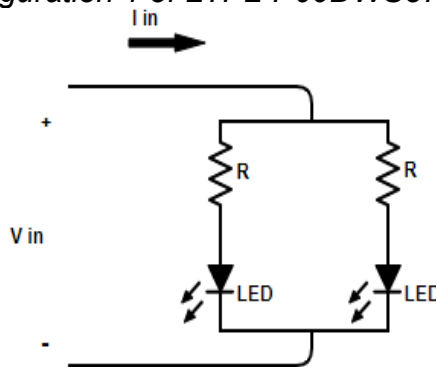


Figure 40: Configuration 2 of LTPL-P00DWS57 High Power LED

### 3.2.5.2 158301240 Ceramic LED

This LED has a peak forward current of 40mA tested with a PWM signal at 10% duty cycle at a frequency of 1kHz. The maximum continuous current is rated at 30mA and the LED can operate in the range of 20mA to 30mA to preserve the lifespan of the device. The forward voltage required to turn on the LED is 3V typical with a max forward voltage of 3.5V at 20mA of current flowing through the device. The minimum and maximum power dissipation of the device are as follows:

Test Condition  $I_f = 20mA$

$$P_{min} = V_{f min} \times I_{f min} = 60mW$$

$$P_{max} = V_{f max} \times I_{f continuous} = 105mW$$

This LED is capable of emitting 8.5 lumens typical at a forward current of 20mA with an efficiency rating of about 80. The operating temperature of this device ranges from -40° C to 85° C. The device contains a single LED and is illustrated in Figure 41.

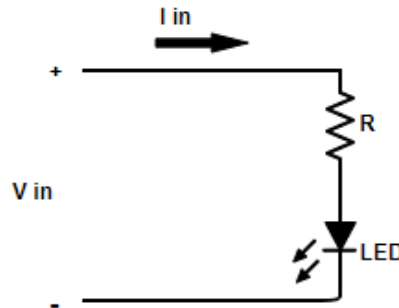


Figure 41: Configuration of 158301240 Ceramic LED

### 3.2.5.3 Comparison

The ceramic LED requires less power to operate than the high-power LED when comparing the voltage to current relationship. The high-power LED operates more efficiently and has a broader range of input voltages. The device contains two LEDs per unit making the high-power LED more flexible than the ceramic LED which only contains one LED per unit. Increasing the number of resistors will use more space on the circuit board but this system does not have space constraints. Depending on the power budget for the entire system, the high-power LED appears to be the better choice for the lighting solution. Table 24 illustrates the differences between the characteristics of the devices.

Table 24: Comparison Table for Different LEDs

Device	High-Power LED	Ceramic LED
Power (TYP)	108-144mW @ 40mA	60-105mW @ 20mA
Forward Voltage (TYP)	3V @ 40mA	3V @ 20mA
Forward Current (TYP)	40mA	20mA
Luminous Flux (TYP)	21 lumens @ 40mA	8.5 lumens @ 20mA
Luminous Efficiency (TYP)	85 lumens/watt @ 40mA	80 lumens/watt @ 20mA

### 3.2.6 LED and Locking Mechanism Driver

The LED array will connect to the output pin of the regulation stage of the power subsystem. A resistor will be used to control the current through the LEDs and a MOSFET will be used for switching.

The locking mechanism solenoid will require a boost converter to supply enough power to operate. Different integrated chips offer an increase in voltage, an increase in current, or a combination of the two at the output terminals and will be discussed below.

#### 3.2.6.1 TPS61021A

This integrated circuit will amplify the current at the output. It is capable of accepting a range of input voltages from 0.5 volts to 4.4 volts and will output from 1.8 volts to 4.0 volts. When the input voltage is greater than 1.8 volts, this IC will output a current of at least 1.5 amps at 3.3 volts. It is 95.3% efficient with a \$1.52 price tag.

#### 3.2.6.2 TPS61230A

This integrated circuit will amplify the current and voltage at the output. It is capable of accepting a range of input voltages from 2.5 volts to 4.5 volts and will output from 2.5 volts to 5.5 volts. When the input voltage is greater than 2.5 volts, this IC will output up to 2.4 amps at 5 volts. It is 93.9% efficient with a \$1.20 price tag.

#### 3.2.6.3 Locking Mechanism Driver Comparison

Both integrated chips offer high efficiency rating and a low price tag. The TPS61230A offers better output and current ratings with a slightly lower efficiency rating. Due to the additional flexibility with the output voltages, the TPS61230A is preferred over its competitor.

Table 25: Driver Comparison

Device	TPS61021A	TPS61230A
Input Voltage	>1.8V	2.5V – 4.5V
Output Voltage	1.8V – 4.0V	2.5V – 5.5V
Output Current	>1.5A @ 3.3V	<2.4A @ 5V
Efficiency	95.3%	93.9%
Cost	\$1.52	\$1.20

### 3.2.7 Permanent Magnets

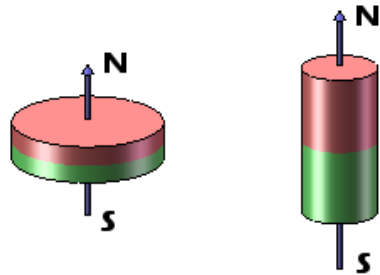
A permanent magnet will be needed should we choose not to use the specified actuators with the Magnetic Reed Sensor and will be needed if we choose to use

the Hall Effect Switch. In either case, the following configurations must be specified when considering the correct magnet to buy for our application. They are:

- Magnetization Direction
- Physical Size
- Magnetic Field Strength
- Cost

Permanent magnets come in two different magnetization directions: axially and diametrically.

#### Axially Magnetized



#### Diametrically Magnetized

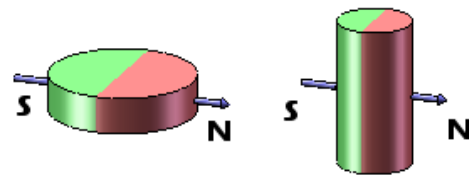


*Figure 42: Axially and Diametrically Magnetized Magnets Differences*

As can be seen in Figure 42, the north and south poles of the magnet in the axially magnetized configuration are such that they bisect the magnet itself with respect to the z axis and the diametrically magnetized magnets bisect the magnet with respect to the x-y plane. The difference between the magnetization direction is that it changes the shape of the magnetic field around the magnet and will change the way the magnet needs to be mounted in order for it to serve its purpose, in our case this will be to activate either a Reed Switch or Hall Effect Switch.

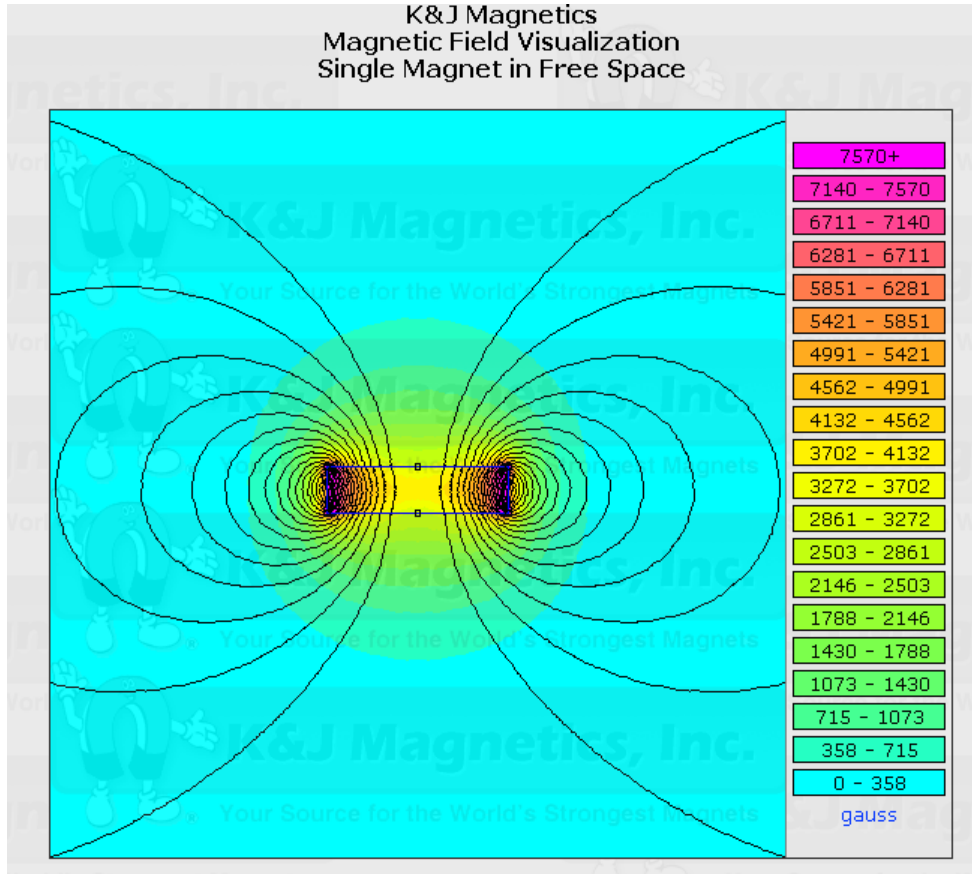


Figure 43: Magnetic Field Visualization

From Figure 43, we can observe that the magnetic field intensity is the greatest around the left and right edges of the axially magnetized disk. This is because this is the area where the magnetic field has to travel the least amount of distance to flow to the south pole and thus incurs less loss. In order for the axially magnetized disk in Figure 43 to be used with the Hall Effect Switch, the correct pole must be facing towards the Hall Effect Switch of the Hall Effect Switch must be omnipolar.

### 3.2.7.1 D81AD-P

This part is an axially magnetized disk. Its dimensions are comparable to that of a penny. What separates this part from other permanent magnets is that it come with a 3M 467MP adhesive strip on the backside of it, that is the adhesive strip is on the south pole of the magnet. This is also the largest permanent magnet considered and depending on where the permanent magnets are mounted, it should have more than enough magnet field strength to activate either the Hall Effect Switch or Reed Switch.

### 3.2.7.2 D42DIA

This part is a diametrically magnetized disk. It is smaller and has less magnetic field strength than D81AD-P when considered from the same distance. This part was considered because depending on the location of either the Hall Effect Switch



or Reed Switch, the diametrically magnetized disk will offer an advantage when being secured to the bicycle frame. Specifically, this advantage is that this permanent can be mounted in such a way that the adhesive being used will have maximum surface area contact with the permanent magnet when being mounted to the bicycle frame.

### 3.2.7.3 D12-N52

This part is an axially magnetized disk and is both the smallest and cheapest of all the permanent magnets considered. Since the exact mounting place of either the Hall Effect Switch or the Reed Switch are unknown, permanent magnets with various magnetic field strengths need to be considered as the Hall Effect Switch has a maximum rating for the amount of magnetic field strength that it can experience before lagging in performance. This magnetic field strength depends largely on the amount of distance between the permanent magnet and the orientation of the magnet with it is mounted to the bicycle.

*Table 26: Magnate Comparison*

Part Number	Price	Magnetization Direction	Dimensions (Diameter, Thickness) in inches	Magnetic field strength
D81AD-P	\$1.37	Axial	1/2", 1/16"	148.2
D42DIA	\$0.38	Diametric	1/4", 1/8"	96.9
D12-N52	\$0.14	Axial	1/16", 1/8"	7.4

After consideration, the permanent magnet selected for this project is D81AD-P. Although this part is the most expensive of all the parts considered, it has an adhesive pad attached to the back of it that will greatly assist the team during the integration phase of the project. Also, the D81AD-P is the strongest of all permanent magnets considered. The hardware in consideration for the speed calculation of the bicycle is still under review. The speed calculation hardware will either consist of a Reed Switch or a Hall Sensor to be used in conjunction with either a permanent magnet or magnetic actuator from Littelfuse Inc.

## 3.2.8 Locking Mechanism

The seat belt assembly and locking mechanism can be acquired from an automotive scrap yard or purchased online. Due to the complexity of designing and building a custom locking mechanism, the seat belt assembly is the only part in this section.

### 3.2.8.1 Cable and Reel

The assembly contains the belt with a buckle attached, inertial reel assembly, and mounting plate. The price of the assembly is roughly \$22.



Figure 44: *Inertial Reel Assembly*

### 3.2.8.2 Spring Loaded Locking Mechanism

There are two versions of the locking mechanism available. The first will have the spring-loaded release on the top on the unit and the second will have the spring-loaded release on the side of the unit. Testing the spring force is required to obtain an accurate calculation of the force required to press the button and release the lock. The distance the button travels will also be measured on both units to find the unit that requires the least amount of force to actuate the lock. The price of the assembly is roughly \$8.

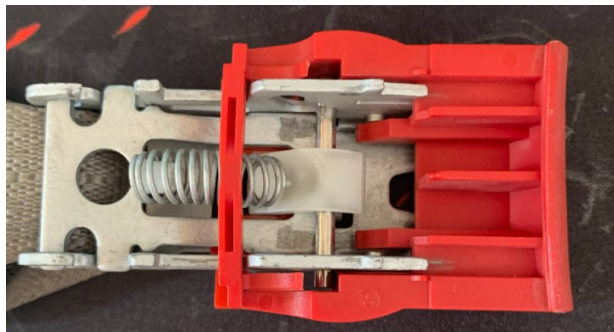


Figure 45: *Top Release Lock Assembly*



Figure 46: *Side Release Lock Assembly*

### 3.2.8.3 DSOS-0416-03D 3V Open Frame Push Solenoid

This is an open-frame push solenoid capable of exerting up to 300 grams of force with a very short stroke. The amount of force this device exerts on an object decreases exponentially with an increase in distance. It can accept an input voltage of 3 volts at 1.28 amps for an intermittent push consuming 3.8 watts. The DC resistance of the solenoid is 2.33 ohms.

### 3.2.8.4 DSOS-0416-05D 5V Open Frame Push Solenoid

This is an open-frame push solenoid capable of exerting up to 300 grams of force with a very short stroke. The amount of force this device exerts on an object decreases exponentially with an increase in distance. It can accept an input voltage of 5 volts at 0.66 amps for an intermittent push consuming 3.3 watts. The DC resistance of the solenoid is 7.55 ohms.

### 3.2.8.5 DSOS-0416-09D 9V Open Frame Push Solenoid

This is an open-frame push solenoid capable of exerting up to 300 grams of force with a very short stroke. The amount of force this device exerts on an object decreases exponentially with an increase in distance. It can accept an input voltage of 9 volts at 0.4 amps for an intermittent push consuming 3.6 watts. The DC resistance of the solenoid is 22.6 ohms.

### 3.2.8.6 Solenoid Comparison

All of the solenoids are manufactured from the same company and differ in the input voltage the unit accepts. The 5V model consumes the least amount of energy with a low DC resistance. Once the power budget of the entire system is evaluated, a solenoid with a higher input voltage and lower current may be required.

*Table 27: Push Solenoid Comparison*

Device	DSOS-0416-03D	DSOS-0416-05D	DSOS-0416-09D
Input Voltage	3V	5V	9V
Current	1.28A	0.66A	0.4A
Power	3.8W	3.3W	3.6W
DC Resistance	2.33 $\Omega$	7.55 $\Omega$	22.6 $\Omega$

## 4. Standards & Design Constraints

This section details the standards and design constraints that guided the Bike System’s features, parts selection, and design.

### 4.1 Standards

Standards are an important parameter that must be considered whenever undertaking the design of any system. The purpose of this section is to highlight some of the important standards that are applicable to the design of the Bike System.

#### 4.1.1 LED Standards

The LEDs must supply enough lighting to be visible by motor vehicles and to provide a lighted path for the rider. Figure 47 provides a reference for the minimum light intensity in different environments required by OSHA. The intensity of light emitted from an LED decreases at the inverse of distance squared ( $\frac{1}{d^2}$ ). Figure 48 illustrates the lux values measured by different light sources acting on a surface. These values will be used as a reference when designing the LED array and choosing which part to use in the system.

Lumens (foot-candles)	Area or operation
3.....	General areas on vessels and vessel sections such as accessways, exits, gangways, stairs, and walkways.
5.....	General landside areas such as corridors, exits, stairs, and walkways.
5.....	All assigned work areas on any vessel or vessel section.
5.....	Landside tunnels, shafts, vaults, pumping stations, and underground work areas.
10.....	Landside work areas such as machine shops, electrical equipment rooms, carpenter shops, lofts, tool rooms, warehouses, and outdoor work areas.
10.....	Changing rooms, showers, sewer toilets, and eating, drinking, and break areas.
30.....	First aid stations, infirmaries, and offices.

**Note to table F-1 to § 1915.82:** The required illumination levels in this table do not apply to emergency or portable lights.

Figure 47: OSHA Requirements for Illumination Levels

Illuminance (lux)	Surfaces illuminated by
0.0001	Moonless, overcast night sky (starlight) <sup>[4]</sup>
0.002	Moonless clear night sky with airglow <sup>[4]</sup>
0.05–0.3	Full moon on a clear night <sup>[5]</sup>
3.4	Dark limit of civil twilight under a clear sky <sup>[6]</sup>
20–50	Public areas with dark surroundings <sup>[7]</sup>
50	Family living room lights (Australia, 1998) <sup>[8]</sup>
80	Office building hallway/toilet lighting <sup>[9][10]</sup>
100	Very dark overcast day <sup>[4]</sup>
150	Train station platforms <sup>[11]</sup>
320–500	Office lighting <sup>[8][12][13][14]</sup>
400	Sunrise or sunset on a clear day.
1000	Overcast day; <sup>[4]</sup> typical TV studio lighting
10,000–25,000	Full daylight (not direct sun) <sup>[4]</sup>
32,000–100,000	Direct sunlight

Figure 48: Lux Values for Surfaces Illuminated by Different Surfaces

## 4.1.2 Supply Voltage Standards

This section covers some of the most common voltage standards that are used in electronic devices and systems. There is a wide array of official and unofficial (or *de facto*, Latin for “of fact”) standards that establish the voltage levels that are to be used as supply voltages for electronic components, such as 48V for phone lines or 120V<sub>rms</sub> for the outlet voltage in the US. However, only three standards that are the most relevant to the Bike system will be discussed here.

### 4.1.2.1 TTL 5V Standard

TTL, or transistor-transistor logic, is an old and long-standing standard that defines the use of 5V for supplying logic circuits and driving circuits, and was based on bipolar junction transistor technology. The transistor part comes from the fact that logic circuits are mainly comprised of transistors that interact directly with one another. The logic portion for this standard comes from the defined logic levels. The thresholds for these voltage levels for inputs are defined for logic high as being 5V – 2V, and logic low as being 0.8V – 0V. For outputs, the voltage levels are 5V – 2.7V and 0.5 – 0V for logic high and low, respectively. The reason for this difference in voltage is because of the noise margin. This margin is used to ensure that a circuit will not output a signal that might be interpreted incorrectly. This standard became prevalent in computing components, microprocessors, and computing peripherals.

This standard was defined for logic circuits; however, this resulted in a *de facto* standard for power supply voltages. This *de facto* standard came about with the increase of the integration of TTL circuits and ICs in electric systems. Because of the need for 5V in TTL circuits, designers would naturally design their circuits to use a supply voltage of 5V. Even though this standard was developed in the 1960s, this standard still persists due to the use of TTL components in today’s market. Many logic circuits, microcontrollers, and peripherals are still able to use either 5V, or the more modern 3.3V voltage level. The 3.3V standard is discussed in Section 4.1.2.2.

### 4.1.2.2 JESB8C.01 3.3V Standard

The JESB8C.01 defines the standard of using 3.3V ±0.3V for the supply voltage ( $V_{dd}$ ) for digital logic circuits and their corresponding driving circuits. The input voltage threshold is defined to be  $V_{dd} + 0.3V - 2V$  for logic high, and 0.8V – -0.3V for logic low. The output voltage is defined as either a minimum of 2.4V or  $V_{dd} - 0.2V$  for logic high, and either maximum of 0.4V or 0.2V for logic low. This standard came about because of the advancement of transistors and the need for faster switching times. The old standard, described in Section 4.1.2.1, used a higher voltage at 5V, while this newer standard uses 3.3V. Since a lower voltage takes less time to transition from logic high to logic low, this reduction in voltage led to an increase in switching speeds and performance.

As with the TTL 5V standard discussed in 5.1.2.1, the JESB8C.01 3.3V standard resulted in another *de facto* standard for power supply options for circuits. Again, this was due to the increase in popularity of using logic circuits and ICs that use the JESB8C.01 3.3V standard. As the use of these circuits became more prevalent, the need for supplying power at 3.3V increased as well. This is again supported by the plethora of electrical systems and devices that require either 5V or 3.3V, or even just 3.3V power supply voltages.

#### **4.1.2.3 12V Automotive Standard**

This standard came about because of the nominal battery voltage of the lead-acid batteries used in automobiles, which is 12V. Although not an official standard, its widespread use across the world has made it a *de facto* standard for automotive electronics. While electricity in automobiles started with powering rudimentary electrical systems, with the advancement of electronics, it was only natural for the integration of more complex electronics into automobile systems. This means that a wide array of electronic devices that are designed to utilize the nominal 12V that is provided by an automobile's battery have become available, including microprocessors, logic circuits, and other various circuitry.

#### **4.1.2.4 Impact of Voltage Standards**

It has been made clear by Sections 4.1.2.1, 4.1.2.2, and 4.1.2.3 that these standards have had a direct impact on the availability of electrical devices and components that are available on the consumer market. This means that the Bike System's design will be relatively confined to one of the power supply voltage standards. While a system could be made to utilize many different supply voltages, it is impractical to implement many different power supplies to provide these different voltages to a circuit. However, there are situations where it is necessary to provide many different supply voltages for the proper operations of a circuit, such as with FPGA circuits.

The impact on the Bike System's design will be in the design of the power subsystem and with the selections of parts. The power subsystem must be designed to be able to supply the chosen voltage, and be able to meet the standard. In the parts selection, the part must be chosen to where they are compatible with the provided supply voltage. There are also power dissipation concerns when it comes to power supply selection. As a higher voltage will result in a higher dissipation of power for the same load via Ohm's Law. In general, a lower power supply voltage leads to lower power losses in the resistances of components, which means more efficient systems.

### **4.1.3 Software Standards**

When designing the algorithm and logic of the software for the Bike System, there are certain standards that were taken into consideration. In this section, both established standards and *de facto* standards that were considered is discussed.

### 4.1.3.1 C Programming Language

The programming language chosen that was chosen for the software aspect of the Bike System is the C programming language. The International Standard, *ISO/IEC 9899*, “specifies the form and establishes the interpretation of programs written in the C programming language” [citation]. This international standard includes rules for interpreting and representing the programs written in C. It also includes specific representations for the input and output data that are used and produced by C programs.

This international standard does contain specifications for the mechanisms of any form of data processing within the C programs. Also, *ISO/IEC 9899* does not specify any constraints or limitations on the complexity or processing size of the C program.

### 4.1.3.2 Software and Systems Engineering

The international standard, *ISO/IEC/IEEE 29119*, details 5 steps or sub-standards for the life cycle of the software development of the Bike System. This standard also entails the standards and expectations for software testing. Figure 49 shows the stages of the software development life cycle.

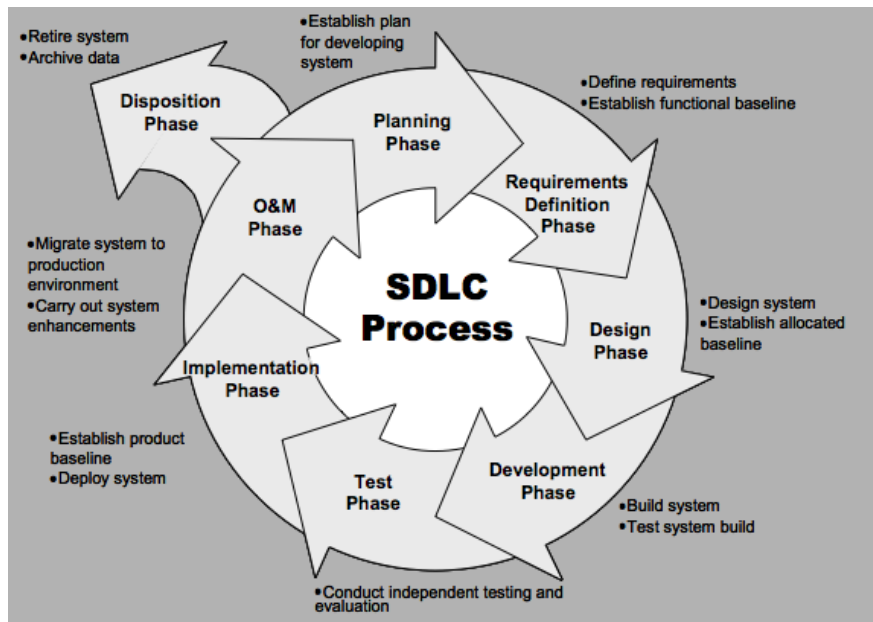


Figure 49: Software Development Life Cycle<sup>[21]</sup>

These 5 standards within the *ISO/IEEE 29119* series are:

- ISO/IEC 29119 – 1: Concepts and Definitions
- ISO/IEC 29119 – 2: Test Processes
- ISO/IEC 29119 – 3: Test Documentation
- ISO/IEC 29119 – 4: Test Techniques
- ISO/IEC 29119 – 5: Keyword Driven Testing

The software development of the Bike System is not very complex, and it is the current expectation that not all of these sub-standards will apply to the design of the Bike System. The basis or goal of the *ISO/IEC/IEEE 29119* International Standard is to ensure there is proper documentation and testing of the software being created and used.

#### **4.1.3.3 ISO/IEC 29119-2: Test Processes**

This standard specifies three (3) test processes that can be used to govern, manage, and implement software testing. These three test processes are the organizational test process, test management process and the dynamic test process.

##### **4.1.3.3.1 Organizational Test Process**

Within the organizational test process, the testing policy and testing strategies are created. The testing policies and strategies implemented will be decided upon by the four group members collectively. The final decisions will not be made by the programmer solely.

##### **4.1.3.3.2 Test Management Process**

The Test Management Process is divided into three main parts:

- Test Plan

This Test Plan process describes the planning of multiple tests for multiple factors. Some of the tests that will be planned are reliability test plan and acceptance test plan

- Test Status

The Test Status process contains the monitoring and control of the Test Plan created in the step before. This step is where anomalies and undesired results can be monitored. Based off of any undesired or unplanned results, changes can be noted to be made to the algorithm design to make corrections.

- Test Completion

The main role of this final step is to ensure all of the testing processes were performed correctly. This step also includes ensuring that the entire organization or group was aware of the final results and any testing incidents.

##### **4.1.3.3.3 Dynamic Test Process**

The Dynamic Test Process includes the specific test processes (and test cases) relating to the environment in which tests were carried out. This test process relates directly to the test completion phase of the Test Management Process.



#### **4.1.3.4 ISO/IEC 29119-3: Test Documentation**

Following the three major parts of the Test Process phase, is the Test Documentation. This *ISO/IEC 29119-3* standard outlines the documentation that should be produced during the testing processes detailed in *ISO/IEC 29119-2*. There are also three major parts to this standard. They are the Organizational Test Process Documentation, the Test Management Process Documentation, and the Dynamic Test Process Documentation.

##### **4.1.3.4.1 Organizational Test Process Documentation**

Within the Organization Test Process, documentation of the test policies created by the group and the strategies agreed upon is to be made.

##### **4.1.3.4.2 Test Management Process Documentation**

Documentations specifically outlines the test plan will be made. As the tests proceed, the test status documentations will be updated. Documentation relating the outcomes of the test and its completion will also be defined.

##### **4.1.3.4.3 Dynamic Test Process Documentation**

This Dynamic Test Process Documentation is the most important within this *ISO/IEC 29119-3* international standard. The specifications relating to the test design, test cases used, and the testing procedure will be required. Reports of the test data used, and the testing environment(outlined by the test environment requirements) will also be assembled to make sense of the test plans that were initially created. *ISO/IEC 29119-3* also specifies proper documentation for the logs of the test execution and testing incident reports.

#### **4.1.3.5 ISO/IEC 29119-4: Test Techniques**

The *ISO/IEC 29119-4* standard specifies the design for the test cases and testing methods implemented within the software design stage. Test cases can be designed to test either the functional aspects of the software or the internal structure of the software.

##### **4.1.3.5.1 Functional Test Techniques**

The purpose of functional test techniques and test cases is to ensure that the code is actually doing what it is supposed to do. In relation to the Bike System, this would include testing to ensure that the sensors are being read correctly and the metrics needed are being computed correctly. Scenario testing and Syntax testing are both carried out under this technique.

##### **4.1.3.5.2 Structural Test Techniques**

The purpose of this type of technique is to uncover flaws within the logic of the algorithm and the code. This is not limited to testing the flow of data within the code. The Bike System's code can be optimized through structural testing.

### 4.1.3.6 ISO/IEC 29119-5: Keyword Driven Testing

The *ISO/IEC 29119-5* standard describes where the test is executed using drivers to read the keyword specified and then execute the code corresponding to that keyword. This mainly applies to the automation of testing execution, which is not applicable to the software design of the Bike System. It is not an expectation that any of our testing will be automated.

## 4.1.4 Communication Standards

The RC522 RFID Module has the capability to communicate with the selected microcontroller via three communication protocols. They are: Universal Asynchronous Receiver Transmitter (UART), Serial Peripheral Interface (SPI), and Inter-Integrated Circuit (I2C).

Pin	Interface type		
	UART (input)	SPI (output)	I <sup>2</sup> C-bus (I/O)
SDA	RX	NSS	SDA
I2C	0	0	1
EA	0	1	EA
D7	TX	MISO	SCL
D6	MX	MOSI	ADR_0
D5	DTRQ	SCK	ADR_1
D4	-	-	ADR_2
D3	-	-	ADR_3
D2	-	-	ADR_4
D1	-	-	ADR_5

*Figure 50: MFRC522 MC Detecting Digital Comm Interfaces Pinout*

At first glance of Figure 10, the easiest communication protocol to use to relay information from the RC522 RFID module to the selected microcontroller would be the Inter-Integrated Circuit (I2C) since it allows for data to both be written to and read from the RC522 RFID module; however, there are some limitations and adjustments that must be made if the RC522 RFID Module is to communicate with the selected microcontroller via Inter-Integrated Circuit (I2C). In order to activate the Inter-Integrated Circuit communication mode on the RC522 RFID Module, a physical pin to the microcontroller located on the RC522 RFID Module must be physically disconnected. In order for this to be successfully done, the integration process would involve drilling a hole in the printed circuit board on the RC522 RFID module. This process would allow for a large probability of damaging in the part to the effect that it would not be able to be used anymore and would have to be reordered. If time were not such a valuable resource in this project, this would be the route chosen for the communication protocol used to communicate with the RC522 RFID Module. It is for this reason that the Universal Asynchronous Receiver Transmitter (UART) and Serial Peripheral Interface (SPI) communication

protocols will be used to write information to and read information from, respectively, the RC522 RFID Module.

#### **4.1.4.1 Universal Asynchronous Receiver Transmitter (UART)**

A universal asynchronous receiver transmitter (UART) is a module, integrated circuit, or software/logic specified piece of equipment used to communicate serial data to another universal asynchronous receiver transmitter. For two universal asynchronous receiver transmitters communicating in full duplex, meaning that both modules are sending and receiving serial data simultaneously, only two wires are required. As mentioned in the name, universal asynchronous receiver transmitters communicate asynchronously which means that they communicate without a shared clock. Instead, the beginning and end of a packet being sent or received has start and stop bits, respectively. With this convention, along with the understanding that both universal asynchronous receiver transmitters must be operating with the same baud rate, allows for the universal asynchronous receiver transmitters to communicate without a common clock. Baud rate is a measurement of how many bits are being sent per second. A typical data transmission via universal asynchronous receiver transmitter will consist of the following settings:

- **Start Bit**  
A start bit signifies the beginning of a transmission. Typically, the transmission wire (TX) will be held at a logic high level until the beginning of the transmission where it is driven low, signifying the beginning of a transmission. There is typically only one start bit.
- **Data Bits**  
The data bits are the data being transmitted. There can be between 5 to 9 data bits depending on the number of parity bits being used. Typically, there are 8 data bits in a transmission. Also, the least significant bit is sent first across the wire.
- **Parity Bit or Bits**  
The parity bit or bits is an optional configuration. Parity bits are used for error checking when receiving a packet. There can be either 0, 1, or 2 parity bits.
- **Stop Bit or Bits**  
The stop bit or bits is used to signify the end of a data transmission. Since the transmission wire is usually held high when not in use, once the receiver detects that the transmission has been held high for either 1 or 2 bits after detecting a start bit, this signifies the end of a transmission and the transmission line is held high until next start bit is detected.

Also, the range for which data can be sent and received ranges from 7.2 to 1228.8 kBd (kilobaud). The most typical baud rates are 9600 and 115200 baud.

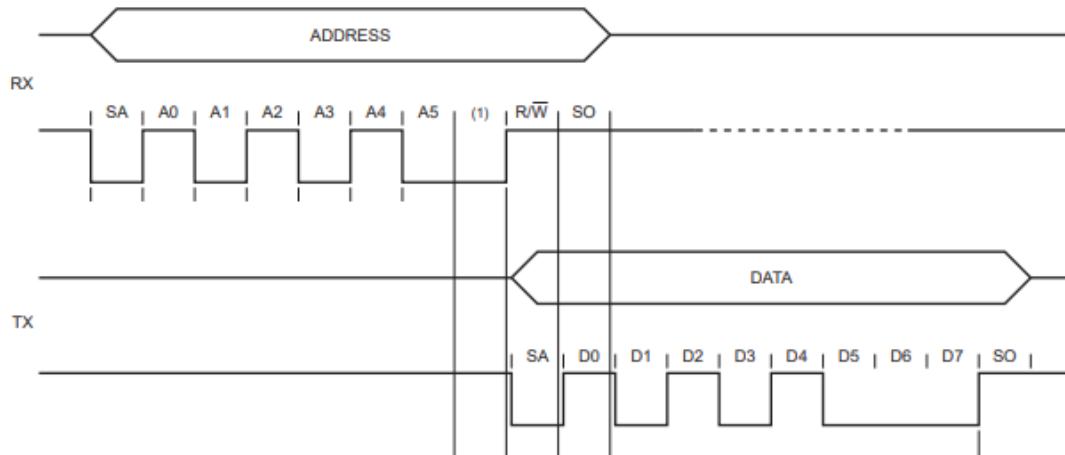


Figure 51: Typical UART packet reception and transmission diagram

In Figure 51, a typical packet transmission and reception can be observed. On the TX line, a data packet 10 bits long is transmitted. There is one start bit, eight data bits, and one stop bit. Also, in Figure 51, a typical reception packet is observed. On the RX line, a packet of 10 bits is received. In this packet, there is a start bit, five address bits, one reserved bit, a bit signifying whether the address received is to be written to or read from, and a stop bit.

#### 4.1.4.2 Serial Peripheral Interface (SPI)

Serial Peripheral Interface communication, unlike the universal asynchronous transmitter receiver communication, requires a common clock between the two devices communicating, which makes it a synchronous communication protocol. Serial peripheral interface communication works on the principle of master-slave relationship. This means that the master, in this application the selected microcontroller, commands the slave, in this application the RFID module, to either send or receive data from a specific address in the slave's memory. At the very minimum, serial peripheral interface communication requires 3 wires to work. In the case where serial peripheral interface communication could work with only 3 wires, there would only be one master and one slave. Theoretically, there can be an unlimited number of slaves in a serial peripheral interface communication network. The limiting factor is the number of bits available on the CSEL line. In serial peripheral interface communication, there are 4 lines used when there is more than one slave. They are:

- MOSI (Master Out, Slave in)  
This is the wire for the master to transmit data to the slave.
- MISO (Master In, Slave Out)  
This is the wire for the slave to transmit data to the master
- SCLK  
This is the wire used for the clock signal.
- SS/CS

SS/CS stands for “slave select / chip select.” This is the wire used to signal which slave the master wants to send data to.

The speed at which serial peripheral interface communication takes place depends on the master, in this application the microcontroller clock. If the master is able to reliably output a clock signal oscillating at 25 MHz, then the serial peripheral interface communication will take place at 25 MHz.

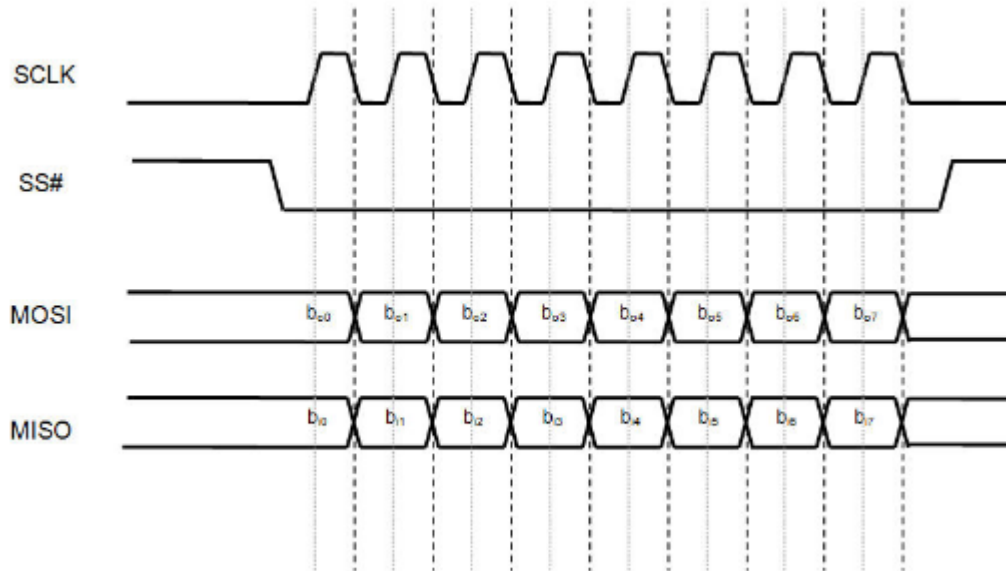


Figure 52: Typical SPI communication frame

As can be observed in Figure 52, this master and slave are communicating in full duplex, meaning that the master is simultaneously sending data while receiving data also. It can also be implied from Figure 52 that there could be possibly two slaves in this serial peripheral interface communication network as the SS# line can only represent a logic 0 or 1.

## 4.2 Design Constraints

A popular saying among engineers is “there is no free lunch,” which means that there are always some constraints that result in a price to be paid, or some trade-offs to doing something. This section describes the constraints that were face in the design of the Bike System.

### 4.2.1 LED Array

The regulated output from the rectification stage is 3.3V nominal. To ensure the lifespan of the LED is maximized, the voltage and current need to be tightly controlled.

## **4.2.2 Locking Mechanism**

Existing systems are application specific and a custom design is required to get the automatic lock implemented into the system. Knowledge in material science and mechanical engineering are required to ensure tolerances and clearances of moving parts do not jeopardize the electrical system or structural components within the housing.

### **4.2.2.1 Cable & Reel**

In order to realize the optimal design of implementing an inertial reel to control the securing cable, a seat belt assembly from an automobile will be used in place of a custom length steel cable and inertial reel. The cost of the seat belt assembly is less than what it would cost to design and build a custom cable and reel assembly. The size and location of the mounting plate of seat belt assembly may need to be altered to fit the space requirements of the bike system.

### **4.2.2.2 Linear Solenoid**

The seat belt assembly locking mechanism is designed to be pressed by a person and the stiffness of the spring could pose a problem. The solenoids researched may not be able to generate enough force to release the lock. A lever system may need to be implemented to increase the push force of the solenoid.

### **4.2.2.3 Manual Override**

Lock mechanisms are designed for specific applications and finding a lock and key from a different system is not realizable for this bike system as it would increase the cost and time requirement of the project. Using a seat belt assembly from a car limits the ability to implement a manual override to unlock the bike system. Creative engineering is required to design a reliable system that only the user can access.

## **4.2.3 Bike System Enclosure**

The material used to construct the enclosure will not be practical for actual use of the bike system. Materials such as wood and plastic will be compared to construct the enclosure.

## **4.2.4 Time Constraints**

One of the greatest enemies to any engineering project is time, and the Bike System is no exception to this. Many successful products can undergo many years of development before they are released, and with continuous product improvement plans in place for many years after. Unfortunately, the Bike System does not have the luxury of having this kind of time allotment. The Bike System must be completed in the course of two semesters, with the majority of the design portion being within the first semester, and the assembly and integration done in

the second. This means that there is a tight time budget for the Bike System project.

The impacts of these time constraints are limiting the amount of time to research solutions to the various problems that the Bike Systems faces, limiting the time that can be put towards optimizing the design, and severely limits the amount of functionality and additional features that can be added to the Bike System. This requires the design team to carefully budget it's time to make sure that the design goals specified in Section 2 are met.

A specific example of how this constraint impacted the project is the inability to meet stretch goals. The stretch goals listed in Section 2 are features that the Bike System's design team would have like to have included in the Bike System. These goals of GPS, Bluetooth, and mobile app integration would take up far too much time in design and development to meet the deadline set for the project. One of the main factors for this need for time is due to a lack of experience, which is discussed in Section 4.2.5.

## **4.2.5 Experience Constraints**

Many of today's greatest products were developed by teams of engineers that have a massive amount of cumulative experience. Many companies are comprised of many engineering disciplines that all cooperate together to achieve the company's goals. While the design team does have some access to those that are experienced in the fields that relate to the Bike System, this is not the same as having the direct access to use this experience in the design of the Bike System.

The main impacts of this constraint are lacking in experience means more time has to be spent in researching and learning various topics and methods that relate to the Bike System, making mistakes that require things to be redone; redesigned; or dropped entirely, and decreasing the efficiency and optimization of solutions proposed for the Bike System. This constraint also compounds with the time constraint discussed in Section 4.2.4, as lacking in experience adds more time to a project. This eats up some the of precious little time that there has been allotted to the project.

A specific example of how this constraint impacted the project is in the creation of the schematics and board layouts. While circuit theory and electronics concepts are covered in depth throughout the courses taken, the actual circuit design and the laying out of a board are not covered in such detail. This means that the design team does not have much experience in the actual laying out of a circuit board, and lead to needing to spend time to learn how to use the programs that are needed to layout the board. This resulted in some mistakes being made, such as a hole being the wrong size, and a loss in time to correct these mistakes.

## 4.2.6 Resource Constraints

The stereotype of the broke college student usually rings true, and the Bike System's design team is no exception to this. Most companies have access to large resources and have the ability to invest a substantial amount of capital into the development of their products. Additionally, for those companies working in the government/defense sector, often times the government provides grants to these companies to perform the initial research, prototyping, and proof of concepts before awarding a contract to the company that demonstrates the best product. Large companies also have access to other resources than money. They also have the ability to get access to items that have yet to hit the market or are still in development, they can leverage their capital to have custom IC solutions made, and access to tools and machinery that aid in product development. Large companies can also bring on subject matter experts (SMEs) and individuals experienced in specific areas to make up for any lapses in experience for a project, which is how these companies can overcome their own experience constraints discussed in Section 4.2.5.

Being comprised of meager college students, the Bike System's design team does not have access to the vast resources that are at the disposal of companies that usually design and manufacture products, such as the Bike System. The impact of this constraint becomes clear. With only a very limited amount of funds available parts selection had to be done very carefully, which compounded with the time constraints discussed in Section 4.2.4. The need for careful selection was because the parts had to be thoroughly researched to ensure a high probability that the part ordered would meet the requirements of the Bike System, as ordering other parts proves to be costly.

A specific example of how this constraint impacted the project was delaying in circuit testing. The components that the circuit were comprised of were all surface mount devices (SMDs) of varying package types and sizes. This means that these parts could not be simply 'breadboarded' for circuit testing, as this would have required expensive adapters for each component. The solution was to buy cheap blank copper printed circuit boards (PCBs) to hand carve lands and traces for the SMD components, as depicted in Figure 62.



## 5. Bike System Design

The previous sections that detailed the technology, parts selection, standards, and constraints culminate to the actual design of the Bike System. This section details the overall design aspect of the Bike System, broken up into various subsections.

### 5.1 Hardware Design

This section covers the hardware aspect of the Bike System's design, broken into the various hardware subsystems.

#### 5.1.1 Power Subsystem Design

The power subsystem design is a critical subsystem, since all other subsystems will receive their power from this subsystem. In Sections 3.1 and 3.2 the various technologies and components related to the Bike System's power subsystem were discussed in detail and how they could be utilized in power system designs. This section details the design process for the power subsystem and how things covered in 3.1 and 3.2. Figure 53 shows the Bike System's power subsystem diagram.

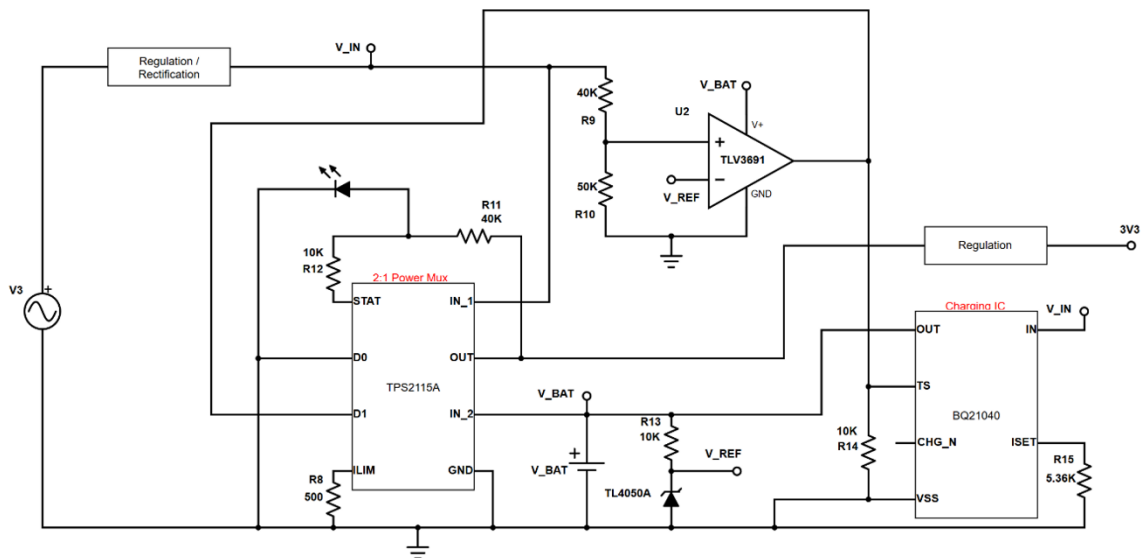


Figure 53: Power Subsystem Diagram<sup>(1)</sup>

The overall operation of the Bike System's power subsystem is taking either the regulated 5V created by the dynamo or the 3.7V from the Li-ion battery, then routing it to the output regulator to supply 3.3V to the rest of the Bike System's circuitry. An LED will illuminate when the battery is in use.

### 5.1.1.1 Power Input Stage

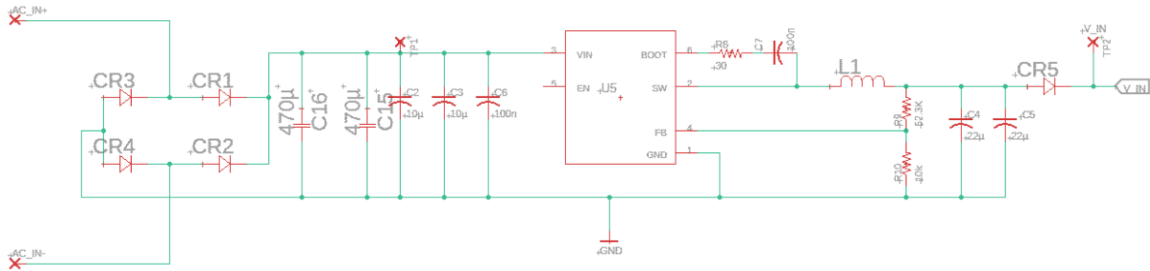


Figure 54: Power Input Stage Circuit<sup>(1)</sup>

The input power stage will consist of the rectification and regulation of the input power, represented by the “Rectification/Regulation” functional block in Figure 53, with the schematic picture in Figure 54. Additionally, there is a reverse voltage protection provided by the diode CR5 in Figure 54. Input power will be provided by a dynamo that generates power from the spinning of the bike tire. This type of power generation results in an alternating current (AC) voltage, see Figure 55 for the dynamo’s output waveform.

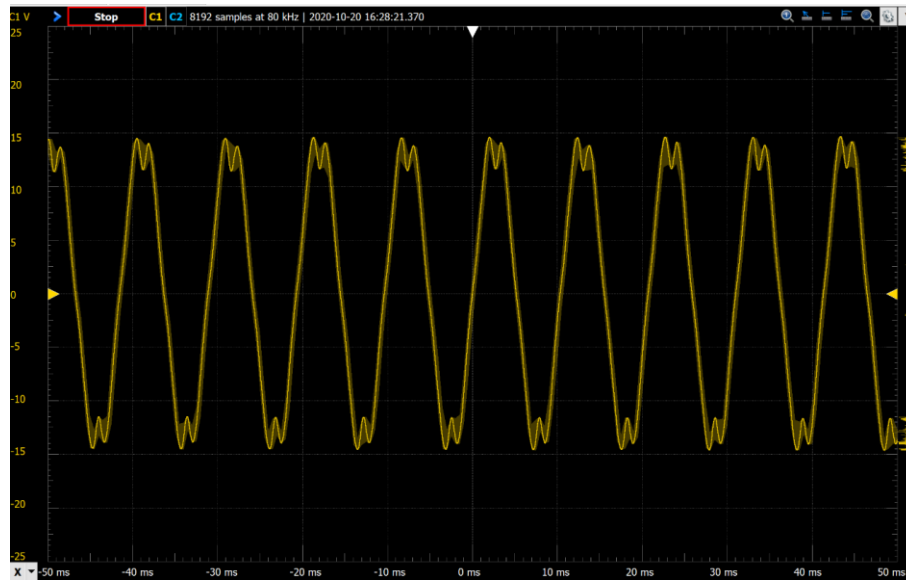


Figure 55: Dynamo Output

The AC voltage generated from the dynamo is not useable with most electronics, which usually require a direct current (DC) voltage. The most common method to take this AC voltage and convert it to a DC voltage is by rectifying the AC signal by the use of diodes. The process of rectification essentially takes the negative voltage portion of the signal, and flips it to make it positive, see Figure 56, left. Figure 56 shows full-wave rectification, where the whole wave is used and made into a unidirectional current signal. Full-wave rectification will be accomplished by a full-wave bridge rectifier, shown in Figure 56, top right. A bridge rectifier is built by putting an array of diodes (Figure 56, top right, shows schottky diodes). These diodes “flip” the negative portion of the wave form by routing the negative voltage

into a positive orientation with respect to the load. This means that the load will experience only a positive voltage throughout the entire waveform, which is what rectification is.

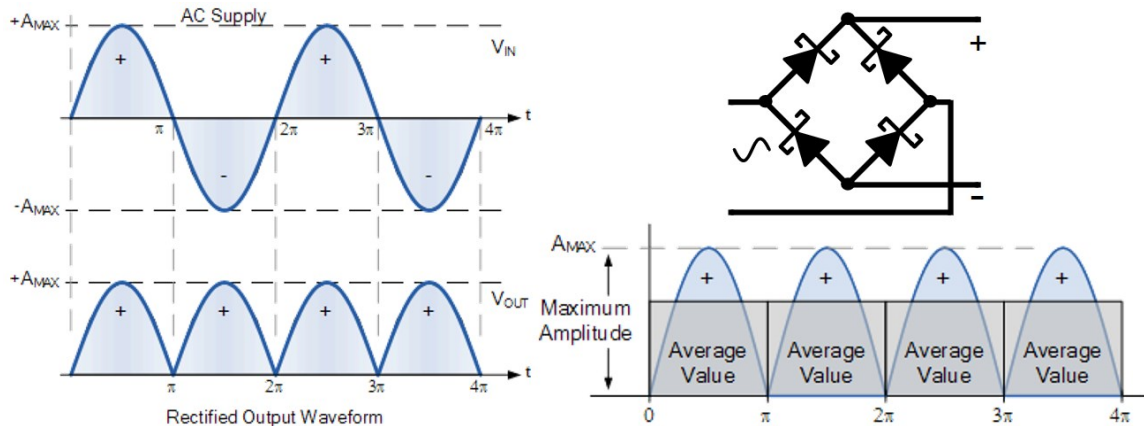


Figure 56: Voltage Rectification<sup>[15]</sup>

Although the rectified voltage is no longer alternating current from positive to negative, there is a substantial amount of variation from the average value, see Figure 56, bottom right. These variations are referred to as voltage ripple, or the AC component of the signal. Most electronic devices cannot function correctly, or at all, when accepting a large amount of ripple at their supply lines. This means the rectified voltage must be smoothed out, or thinking of it another way, the varying voltage component of the rectified signal must be filtered out. This is done by the use of capacitors, which act to smooth the voltage variations, since they determine the rate of change for voltage. Alternatively, the capacitors can be thought of as filters that filter out the AC component of the signal, leaving only the DC component. Figure 4 shows the results of rectifying and smoothing/filtering the dynamo's output, shown in Figure 55. Comparing the waveform shown in Figure 56, bottom right, and Figure 4 the effect of rectification and filtering is clear. However, there is still a noticeable ripple even after the filtering.

A full-wave rectifier was implemented in the power subsystem circuit, shown in Figure 54. The diodes are represented as CR1 – CR4, with the AC voltage generated by the dynamo coming from the left. Capacitors C2, C3, C6, C15, C16 serve to smooth out the ripple voltage from the rectification process, so that the voltage is relatively stable when it arrives at the regulation stage.

Voltage regulation is needed to deal with the remaining voltage ripple from the input voltage, as well as the variations in the voltage level as the bike tire's rotational speed changes. The effectiveness of a 5V regulator on the waveform shown in Figure 4, is shown in Figure 57.



*Figure 57: Input Voltage After Regulation*

From Section 3.2.1.4, the voltage regulator chosen was the TPS56339 (U5 in Figure 54) for the first stage of regulation. Due to the varying nature of the voltage generated from the dynamo, supported by waveforms depicted in Figures 55 and 4, the input of the rectifier needed to support a wide range of input voltages. Regulating the input voltage to 5V was decided based on the characteristics of charging a Li-ion battery. While a Li-ion battery nominally provides a voltage of 3.7V, the voltage required to charge the battery is 4.2V. To accommodate this need, a regulator was chosen to output a voltage of 5V.

Referencing Figure 54, the passive components that comprise the voltage regulation circuit are used to set the output voltage, the current ripple, and voltage current. The output voltage is set by the voltage divider network that is connected to the FB (feedback) pin. This pin also is a part of the control feedback to ensure the output is stable. The voltage and current ripples are determined by the inductor and output capacitor values, respectively.

The diode (CR5) serves to prevent the power provided from the USB connection from Section 5.1.1.3 to feed back into the 5V regulator, but allows power to flow to the rest of the Bike System when the USB is not providing power. The penalty of this is the small voltage drop across the diode; however, this voltage drop was minimized by utilizing a Schottky diode, which has a lower voltage drop than a traditional PN junction diode.

### 5.1.1.2 Power Switching Stage

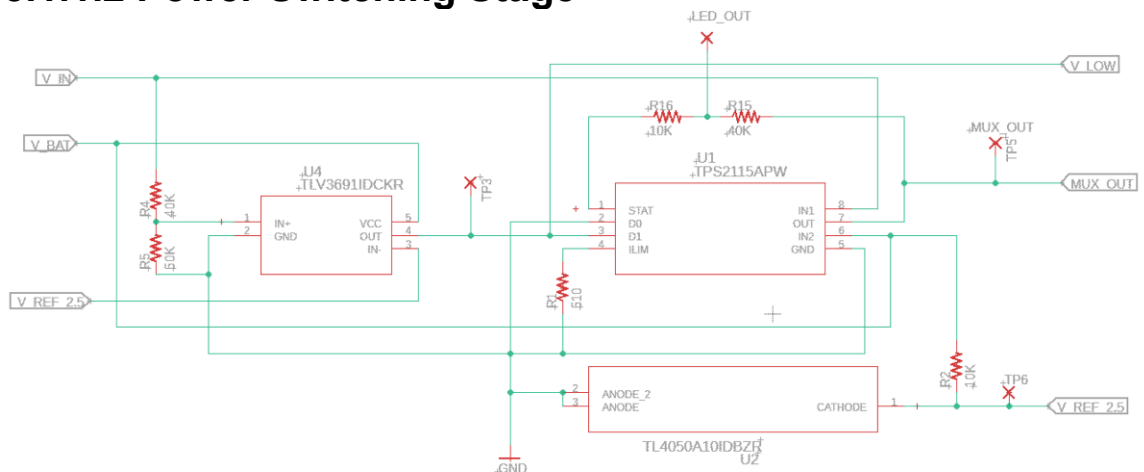


Figure 58: Power Switching Stage Circuit

The power switching stage is very important in the successful operation of the Bike System. This is because it is at this stage that the two power sources, from the dynamo and the battery, are switched between. The threshold for switching between the power sources is 4.5V at dynamo input line. This is determined by a comparator circuit, discussed later in this section. In Figures 58 and 53 the power switching stage is comprised of the power mux IC and the open drain comparator (U1 and U4 in Figure 58, respectively). In the circuit diagram, the power mux has two input pins (IN\_1 and IN\_2) where the two power sources are fed to (represented as V\_IN and V\_BAT in Figure 58). The power from one of these two input pins is then routed to the output pin of the mux (OUT) to be fed to the following stages (represented as MUX\_OUT in Figure 58).

There is a functional pin (ILIM) that sets the maximum current that can pass through the mux. In the current configuration a 500Ω resistor is put between this pin and ground. This resistance value sets a max current of 1A at the output, which is the same max current specified for the voltage regulator in the input stage as specified in Section 3.2.1.4. The STAT pin is used to determine the mode of operation of the power mux, whether it is routing power at the IN\_1 pin, or the power at the IN\_2 pin to the output pin OUT.

The STAT pin gets pulled low when pin IN\_1 is routed to the output pin, and is “Hi-Z” when IN\_2 is routed to the output pin. “Hi-Z” means high impedance, and can usually be treated as an “open” or no connection. In essence, the STAT pin either acts as a ground or as an open wire. Referencing the schematic diagram in Figure 58, the resistor network and LED connected between the output pin, the STAT pin, and ground serve to indicate when the battery is in use (IN\_2 routed to the output). When IN\_1 is routed to the output, meaning STAT is pulled low, the voltage at the anode of the LED is pulled lower than the required voltage drop for the LED. This means that the LED will not be lit, indicating the battery is not in use. When IN\_2 is routed to the output, meaning STAT is Hi-Z, the voltage at the anode of the LED

is sufficient to push the LED into conduction. This means the LED will be lit, which indicates the battery is in use.

Referencing Figure 58, the resistor values for the voltage divider were determined using the voltage divider equation provided in Section 3.1.1.3.1, by capitalizing on the fact that a typical red LED requires a minimum voltage drop of around 1.7V in order to be pushed into conduction, using the assumption that the STAT pin is either ground (0V) or open ( $R \rightarrow \infty$ ), and the voltage at the output of the power mux will change between 5V and ~3.7V.

To prevent the LED from conducting, and therefore illuminating, the voltage divider needed to have an output of around 1V. Using the voltage divider equation, where  $V_{in}$  is the power mux output voltage (which would be 5V at this time) the resistor values that could be used to accomplish this were 40K $\Omega$  and 10K $\Omega$  for  $R_1$  and  $R_2$ , respectively (R15 and R16, respectively in Figure 58). Although any combination of resistor values could have been used to get 1V, these values were chosen since they are already used elsewhere in the design and to reduce the power dissipated by the resistors. Once the STAT pin goes Hi-Z (when the battery is being used) the diode only sees the 40K $\Omega$  resistance in series with it. This resistance value can be show to allow enough current to pass through the diode to drive it into conduction (or make it illuminate) by the following equation:

$$I_d = \frac{V - V_d}{R}$$

Where  $I_d$  is the current passing through the diode,  $V$  is the voltage from the output of the power mux (which would be ~3.7V at this point in time),  $V_d$  is the diode voltage drop, and  $R$  is the resistance.

What determines which input is routed to the output pin is determined by selection control line pins (D0 and D1). Table 28 shows the logic table for how the inputs pins are routed.

*Table 28: Power Mux Logic Table*

D0	D1	OUT
Low	High	IN_1
Low	Low	IN_2

“High” and “low” are defined as TTL values, so a “high” signal is any voltage over 2V, and a “low” signal is any voltage under 0.7V. To achieve a low the control line pin can simply be tied to ground. Since pin D0 is low for either operation, the D0 pin is permanently tied to ground to always keep it low. Pin D1 is pulled either low or high via the open-drain comparator, represented by the signal  $V\_LOW$  in Figure 58.

An open-drain comparator either outputs high (whatever the comparators supply voltage is) or ties its output to ground. The comparator outputs high when the voltage at noninverting terminal (denoted by a “+”) is higher than the inverting terminal (denoted by a “-”). A voltage reference, represented as V\_REF\_2.5 in Figure 58, sets a voltage of 2.5V and applies that voltage to the inverting terminal of the comparator. The voltage divider at the noninverting terminal of the comparator sets the voltage at the noninverting terminal to 2.5V when 4.5V is reached by the dynamo’s input line. What this does is set the threshold for triggering the comparator to go low when 4.5V is reached at the dynamo’s input line. Thus, when the dynamo’s input line goes below 4.5V, the voltage at the noninverting terminal of the comparator goes below 2.5V (lower than the inverting terminal) and causes the output of the comparator to go low. This switches the output of the mux to be that of IN\_2.

One concern raised in Section 3.1.1.5 was the issue of oscillations of a comparator’s output due to noise on the signals at the inputs of the comparator. The solution in Section 3.1.1.5 was the use of hysteresis. The comparator chosen (TLV3691) has a 17 mV hysteresis value built in, which address this issue in the Bike System’s power subsystem and prevents unwanted oscillations at the output of the comparator.

### 5.1.1.3 Charging and Battery Stage

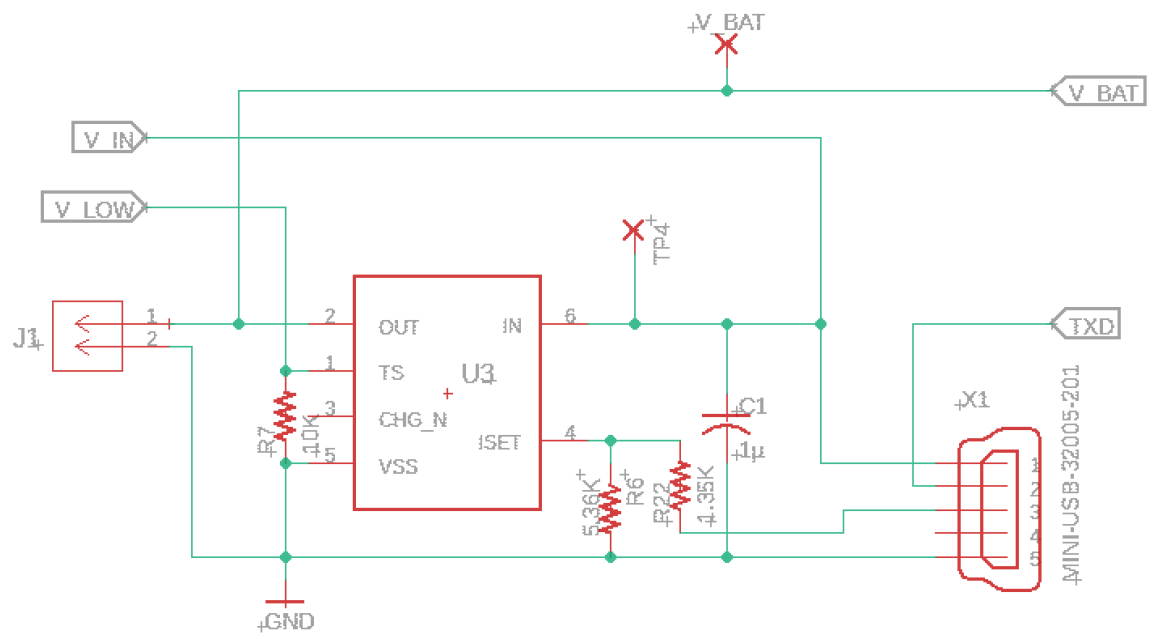


Figure 59: Charging and Battery Stage Circuit

Referencing the schematic diagram of the power subsystem depicted in Figure 53 and the circuit shown in Figure 59, the battery and the battery charging stage of the power subsystem are comprised of the battery charging circuit and the battery.

In Figure 59, the battery is represented by J1 (the jack that the battery will plug into). The charger's output to the battery is represented by V\_BAT in Figure 59.

The battery charging circuit consist of the battery charging IC (BQ21040, U2 in Figure 59) selected in Section 3.2.1.6, the necessary passive components, and a USB mini connector for external power. The passive components include a capacitor (C1 in Figure 59) for some passive filtering of the supply line recommended by the IC's datasheet, a resistor to set the battery charging current limit (R6 in Figure 59), and a resistor for the temp sense pin (R7 in Figure 59).

The resistor value that is used to limit the battery charging current was chosen to be 5.4K $\Omega$  to limit the current to 100mA. This calculation was obtained from the battery charging IC's datasheet, with the given equation:

$$R_{ISET} = \frac{540}{I_{OUT}}$$

For the temperature sense (TS) pin on the battery charging IC it serves two functions. First, the datasheet specified to use a 10K $\Omega$  when the battery does not support temperature sense, such as the one used in the Bike System's design. Second, the TS pin serves as an output enable. When the TS pin is pulled low, the charging IC is disabled. This function can be used to turn of the charging IC to when the regulated input voltage from the dynamo is not sufficient to power the rest of the Bike System. This is done to help prevent the charging IC from attempting to charge the battery when there is not enough voltage being generated by the dynamo.

The TS pin can be pulled low by using the open source comparator, U4 in the circuit shown in Figure 60. This comparator signal is represented by V\_LOW in Figure 59. This is the same comparator that is used to command the power mux to switch between IN\_1 and IN\_2 pins being routed to the OUT pin. This means that when the regulated voltage generated by the dynamo dips below a certain voltage level, the input power is switched to the battery, and the battery charging IC is disabled.

The USB mini connector allows for external power to be applied to the Bike System in order to charge the battery and power the Bike System without needed to actually ride the bike. This is because the other source of power used to charge the battery is generated by the dynamo, which requires the bike wheel to be in motion.

The battery is connected directly to the power mux's IN\_2 pin, which is then routed to the output pin, as described in Section 5.1.1.2. The battery also directly powers the voltage reference IC (U2 in Figure 60), selected in Section 3.2.1.5, and the comparator. The issue that comes from powering devices directly from a battery



are the changing voltage levels as the battery is charging and discharging. This is one of the reasons why an output regulator is needed (see Section 5.1.1.4).

However, the voltage reference has been designed to maintain a set voltage over a varying voltage. This is because the voltage reference has a range of current that will guarantee the correct reference voltage. This current is established and maintained by the 10KΩ resistor in series with it. The 10KΩ value was chosen based on the expected voltages at the top of the resistor (in reference to the circuit in Figure 60), and the current was calculated based on that voltage range. The voltage range is expected to vary from 3.5V (the battery voltage with little charge remaining) to 4.2V (Li-ion battery charging voltage). The resistance is found by the following equation:

$$R = \frac{V - V_{ref}}{I_{ref}}$$

Where R is the resistance needed to maintain the reference current, V is the voltage seen by the resistor,  $V_{ref}$  is the reference voltage, and  $I_{ref}$  is the current through the voltage reference. The maximum current threshold to ensure proper operation for this particular part is 65μA, so 100μA was chosen for  $I_{ref}$  to accommodate this requirement. Using this value, the minimum expected voltage V of 3.5V, and the reference voltage  $V_{ref}$  of 2.5V, R was shown to be 10KΩ.

Unlike the voltage reference, the comparator function will vary directly proportionally to the supply voltage provided to it. This is because the comparator's high output voltage is essentially the same as the supply voltage. To overcome any issues with this the components connected to the output of the comparator had to be selected carefully. The voltage supplied to the comparator is expected to vary from 3.5V – 4.2V. This means that the high output from the comparator will vary by the same voltage, and the components connected to the comparator output need to be able to use this voltage. The components connected to the comparator's output are the control lines for the power mux and the TS pin of the charging IC.

The datasheets for the power mux (TPS2115A) and charger IC (BQ21040) specify TTL voltage thresholds for the control lines, which has a minimum voltage of 2V to read high. This means that the minimum voltage that the comparator voltage high would satisfy this requirement.

### 5.1.1.4 Power Output Stage

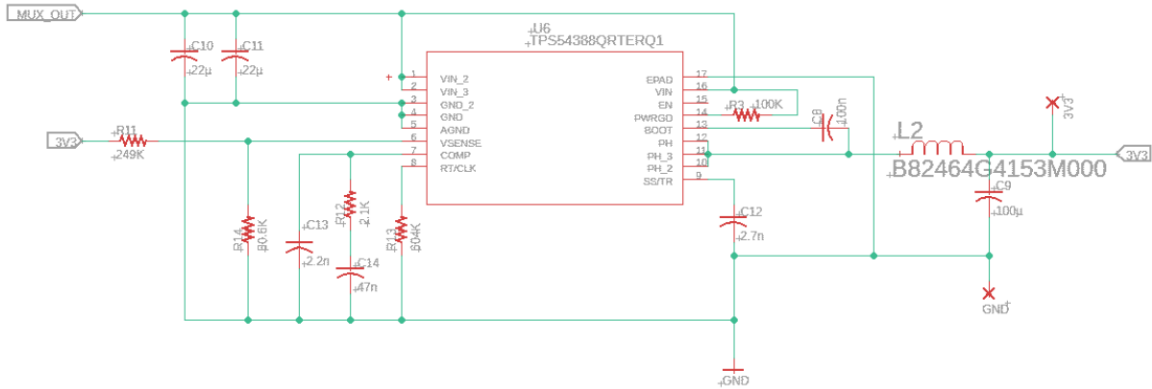


Figure 60: Power Output Stage Circuit<sup>(1)</sup>

The power output stage consists of the 3.3V voltage regulator (U6 in Figure 60). The need for this output regulator is twofold. First, the voltage outputted by the power mux (MUX\_OUT) will either be the 5V from the regulated output from the dynamo, or the nominal 3.7V from the battery. Since the voltage varies so widely there is a need to regulated this voltage to a stable output that can be used by other electronics. The second reason is that even if the power mux is running exclusively from the battery, the voltage from the battery is not completely stable. This is because as the charge state of the battery changes, the voltage from the battery will change as well. The is another reason for regulation. The voltage generated from the dynamo is already regulated, so it would be a usable voltage. However, this voltage is not as reliable as the battery (the bike needs to be in motion with sufficient speed to generate the power), it needs to be fed into another regulator to ensure that it gets stepped down to the 3.3V regulated output voltage.

The circuit of passive components around the second voltage regulator are used to set the various parameters and features of the regulator. The resistors at the  $V_{SENSE}$  pin form a voltage divider that is used as part of the control feedback loop and to set the output voltage (3V3 in Figure 60) to 3.3V. The passive components connected the COMP pin are used for frequency compensation to the modulated signal that controls the switching within the internals of the IC.

### 5.1.1.5 Power Subsystem Layout

After the creation of the schematic shown in Figures 54 and 58 – 60 (overall in Figure 89), the board layout could begin. Due to the relative simplicity of the design, a two-layer board was all that was needed. Figure 61 show the layout of the board. The through-hole terminals on the left side of the board shown in Figure 61 are used to route power to the rest of the Bike System's subsystems via wires soldered directly to the board. Various test points, denoted with the reference designator TP shown in Figure 61, were added to help with the testing of the Bike System's power subsystem, detailed in Section 5.1.1.6.

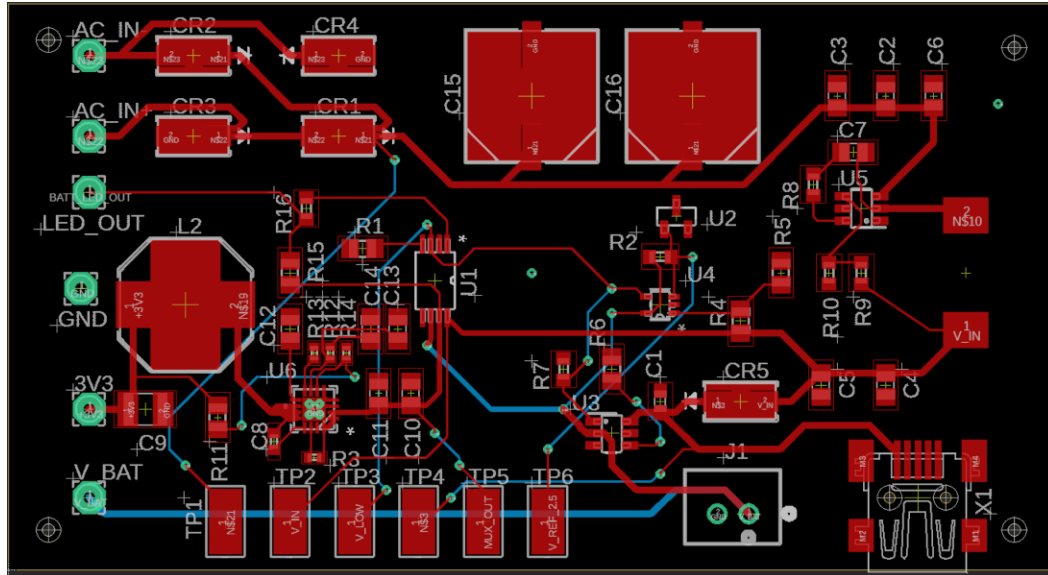


Figure 61: Power Subsystem Board Layout

### 5.1.1.6 Power Subsystem Testing

The testing of the Bike System's power subsystem was accomplished in two phases. The first phase was the breadboard testing of the parts to ensure that they would work together as designed. The second phase of testing was the testing of the parts installed on the PCB that was designed in Section 5.1.1.5.

Since all of the components ordered were small SMDs (service mount device), there was a need for an additional test board used in conjunction with the breadboard (see Figure 62). This board was hand carved from a bare copper PCB and components were also hand soldered to the board. Transformer wire was used as jumper wire, since it has a small diameter and is insulated.

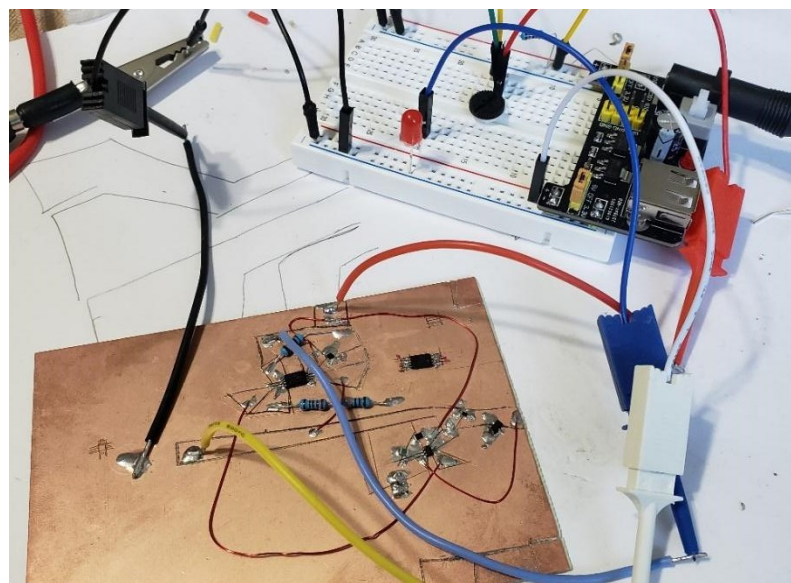


Figure 62: Breadboard Testing

The second phase of testing was carried out by utilizing the test points included in the board layout, see Figure 61 in Section 5.1.1.5. These points allow for voltage measurements at key stages in the circuit, such as the regulated voltages, input power from the dynamo, etc., which allow the easy determination of functionality. This must be done after the assembly of the circuit board by hand. It is important to test a board after assembly for a few reasons, one is the chance of having a faulty product from the manufacture. Figure 63 shows the assembled board being tested.



*Figure 63: Assembled Power Subsystem Testing*

While manufacturing processes for electrical components have matured, and many include testing before leaving the factor, there is still the possibility of having a part that is 'dead-on-arrival.' Another reason for testing after assembly, is the chance of component damage during installation. This can happen from electro static discharge (ESD) or from heat. Most ICs have ESD protections built in, but these have a limit if the components are mishandled. Heat damage can occur during the soldering process. As electrical components become smaller and smaller, the amount of heat the packages can handle also decreases. The relatively large dual in-line package (DIP) components of the past had more thermal mass, and could handle more heat for longer. Small components, however, do not have the luxury of a high thermal mass to deal with this heat. A rapid change in temperature due to a soldering iron or hot air can cause thermal shock to the component, which can result in physical damage to the component.

### 5.1.1.7 Senior Design II Changes

The major changes made to the power subsystem during Senior Design II were updating the battery-in-use LED indicator circuit and adding an additional output voltage of 5V. The new 5V output was implemented by adding a boost converter.

The battery-in-use LED indicator circuit was changed by the STAT pin gets pulled low when pin IN1 is routed to the output pin, and is “Hi-Z” when IN2 is routed to the output pin. “Hi-Z” means high impedance, and can usually be treated as an “open” or no connection. Effectively, the STAT pin either acts as a ground or as an open wire. Referencing the schematic in Fig. 5, resistor R25, MOSFET Q3 and a LED (represented as the BAT\_LED signal in Fig. 5) create a circuit that serves to indicate when the battery is in use (IN2 routed to the output). Resistor R25 serves as a pull-up resistor and pulls the gate of the Q3 up when the STAT pin goes to “Hi-Z”, which cause Q3 to act like a closed switch. This causes the LED connected between the drain of Q3 and the 3.3V rail (not shown in Fig. 5) to illuminate, indicating to the user that the battery is in use. When IN1 is routed to the output, meaning STAT is pulled low, the voltage at the gate of Q3 will be low and Q3 will act as an open switch. This means that the LED will not be lit, indicating the battery is not in use. See Figure A4 in the Appendix section A.3 at the end of this document.

### 5.1.2 LED Array Design

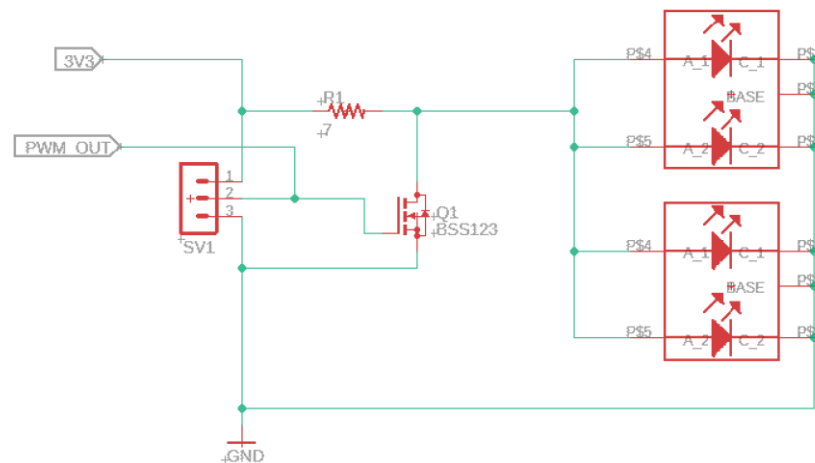


Figure 64: LED Schematic

Figure 64 shows the schematic for the LED array design. The PWM\_OUT signal from the microcontroller is fed to the transistor (Q1) to control the brightness of the LEDs and reduce power usage. The resistor (R1) is used to limit the current passing through the LEDs.

The LED system will be used as a source of light to illuminate the area around the rider as well as serve as a deterrent from motor vehicles. The brightness, or

luminous flux of the LED must be able to light approximately 5 – 10 feet in front of the rider and be visible for cars on the road. Efficiency is the most important aspect of this design and the LED array will be scaled down if necessary, to ensure all components within the system have sufficient power.

The LED structure will consist of a  $n \times m$  array where  $n$  corresponds to the number of LEDs in series and  $m$  corresponds to the number of parallel strings. The LEDs will be mounted on the handle bars of the bike to provide lighting, increase visibility during hours of darkness and, as protection from motor vehicles. The datasheet indicates the LED has a 3V forward voltage at 40mA. Enough voltage must be delivered to satisfy the forward voltage of the LED and a constant current is required from the power supply which will be described in the LED driver section. There is 3.3V at the output of the rectification stage and configurations that require more voltage would need an amplifier to increase the voltage to the desired level. The number of LEDs used in the system reflect on the total illumination of the area around the rider. If the number of LEDs in the array is to be scaled down, the total illumination of the area should be recalculated to ensure adequate lighting based on the references mentioned in Figures 47 and 48.

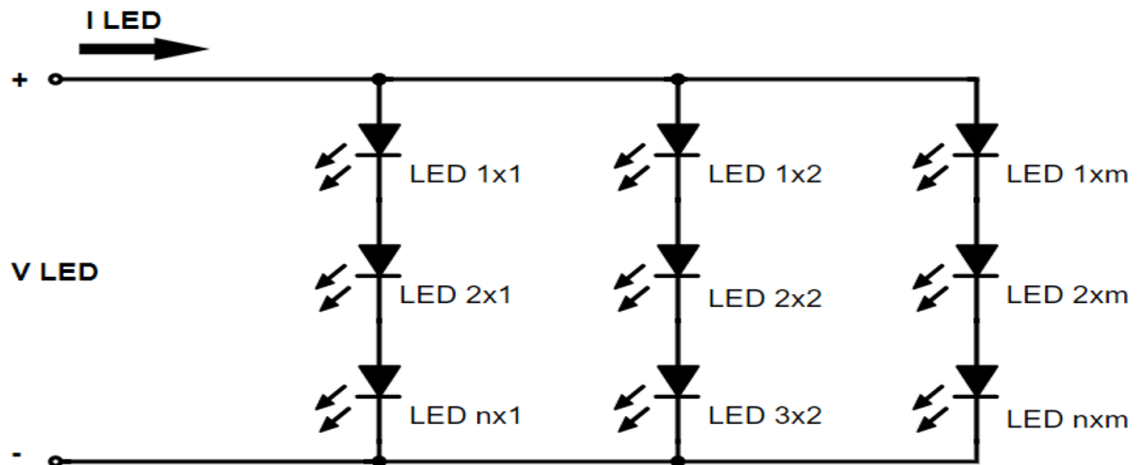


Figure 65:  $n \times m$  LED Array with  $m$  Parallel Strings of  $n$  LED's in Series<sup>(1)</sup>

### 5.1.2.1 Different Configurations Comparison

The bike system is portable and power constraints must be designed with maximum efficiency to decrease the demand from the generator and battery. The power requirement will be the same for all configurations as the circuit must follow Ohm's law. A larger total voltage requirement corresponds to a smaller total current for the array. An array of 10 LEDs will consume approximately 600mW with a current of 20mA flowing through each LED with a nominal forward voltage of 3V. Since this is a portable system, large voltages should be avoided. Configuration 3 consists of all 10 LEDs in series and would require approximately 30V to satisfy the forward voltage requirement for each LED. Configuration 4 should be avoided as well as each parallel string of 5 LEDs would need 15V from the supply and battery. Configuration's 1 & 2 provide the best results for the voltage to current

relationship of the circuit. Figure 65 illustrates configuration 1 as the ideal design for this system. Depending on the LED chosen, the forward voltage required to allow current to flow through the LED will range from 2.7V to 3.6V. The output from the rectification stage will be regulated at 3.3V which will provide enough forward voltage for each LED. The array can be scaled down to 8 or 6 LEDs if the power budget is tighter than expected.

Table 29: LED Configurations

Configuration	1	2	3	4
n X m Array	1X10	2X5	10X1	5X2
Total Forward Voltage	3V	6V	30V	15V
Total Current	200mA	100mA	20mA	40mA
Total Power	600mW	600mW	600mW	600mW

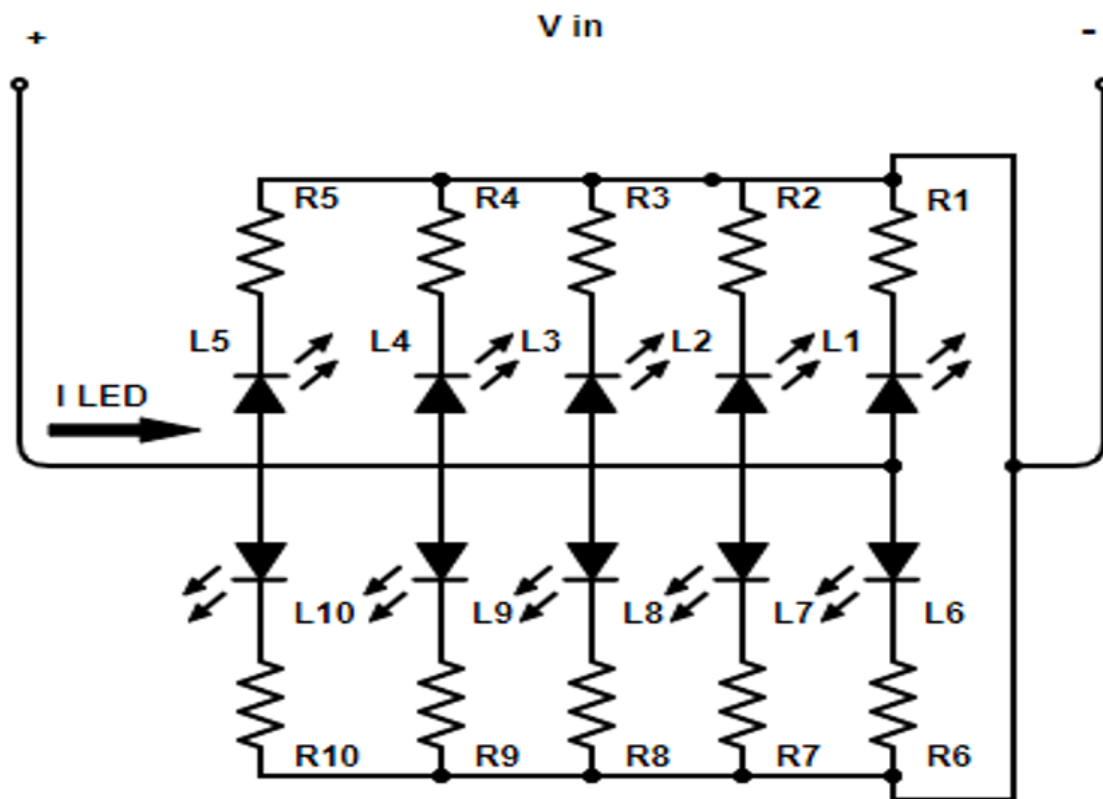


Figure 66: Ideal LED Array Configuration 1<sup>(1)</sup>

### 5.1.2.2 LED and Illumination Calculations

In the following sections, the calculations used to determine the amount of light required to act as a deterrent from motor vehicles will be shown in detail. The

calculations for the resistance values will be used to obtain the optimal voltage and current relationships. Illuminance of the LED decreases at a rate of  $\frac{1}{d^2}$  and must be accounted for in the design of the lighting system. Illuminance is the measure of luminous flux per unit area and is characterized by the equation:

$$Lux(lx) = \frac{Lumens(lm)}{Distance(m)^2}$$

The measured distance from the ground to the handle bars of the bike is:

$$h = 42" = 1.0668 m$$

The minimum and maximum distance to an area in front of the bike is:

$$l_{min} = 5ft = 1.524m, l_{max} = 10ft = 3.048m$$

The distance from the handle bars to  $l_{min}$  and  $l_{max}$  is:

$$d = \sqrt{h^2 + l_{min,max}^2}$$

$$d_{min} = \sqrt{h^2 + l_{min}^2} = 1.86m, d_{max} = \sqrt{h^2 + l_{max}^2} = 3.23m$$

The datasheet for the LED indicates the luminous intensity as:

$$\phi_{v-LED} = 21 lm$$

Lux is the illumination of an area and is calculated as:

$$Lux = \frac{\phi_{v-LED}}{d^2}$$

$$\frac{\phi_{v-LED}}{d_{min}^2} = \frac{21}{1.524^2} = 9.04lx$$

$$\frac{\phi_{v-LED}}{d_{max}^2} = \frac{21}{3.23^2} = 2.01lx$$



According to Figure 48 in the standards section, public areas with dark surroundings are illuminated to 20-50 lx. The distance the 21lm LED can illuminate at 5ft and 10ft respectively is:

$$d_{x1} = \sqrt{\frac{21 \text{ lm}}{20 \text{ lx}}} = 1.02\text{m}, \quad d_{x2} = \sqrt{\frac{21 \text{ lm}}{50 \text{ lx}}} = 0.648\text{m}$$

To calculate the number of LEDs required to light an area in front of the bike to 20-50 lx:

$$\# \text{ of LEDs} = \frac{20\text{lx} \times d^2}{21 \text{ lm}}$$

For a distance of 5ft in front of the bike:

$$\frac{20\text{lx} \times 1.86\text{m}^2}{21\text{lm}} = 3.3 \text{ LEDs}, \quad \frac{50\text{lx} \times 1.86\text{m}^2}{21\text{lm}} = 8.24 \text{ LEDs}$$

For a distance of 10ft in front of the bike:

$$\frac{20\text{lx} \times 3.23\text{m}^2}{21\text{lm}} = 9.9 \text{ LEDs}, \quad \frac{50\text{lx} \times 3.23\text{m}^2}{21\text{lm}} = 24.84 \text{ LEDs}$$

It is not ideal for a bike to have between 10 and 25 LEDs on it. With the maximum distance of 5ft, between 3 and 8 LEDs will be used.

The nonlinear V-I characteristics of the LED is described by the general equation:

$$i_{LED} = I_{sat} \left( e^{\frac{q \times v_{LED}}{k \times T}} - 1 \right)$$

Where each parameter is defined as:

$$i_{LED} = \text{Forward Current}$$

$$I_{sat} = \text{Saturation Current}$$

$$v_{LED} = \text{LED Terminal Voltage}$$

$$q = \text{Magnitude of Electron Charge } (1.602 \times 10^{-19})$$

$k = \text{Boltzmann's Constant } (1.38 \times 10^{-23})$

$T = \text{Absolute Temperature } (273K)$

### 5.1.2.2.2 LTPL-P00DWS57 High Power LED

The illuminance can be calculated for the high power LED which contains two LEDs that emit a total of 21 lumens at 40mA with a distance of 36 inches or 0.9144 meters from the ground, as:

$$\text{Lux}(lx) = \frac{21 \text{ lumens}}{(0.9144 \text{ m})^2} = 25.12 \text{ lx}$$

The illuminance with 75mA flowing through the LED is calculated as:

$$\text{Lux}(lx) = \frac{37 \text{ lumens}}{(0.9144 \text{ m})^2} = 44.25 \text{ lx}$$

Based on the references from Figure 48, illuminance of 25.12lx at 40mA is slightly higher than the lower threshold of 20lx for a public area with dark surroundings. The illuminance of 44.25lx is just under the upper threshold of 50lx for a public area with dark surroundings. The high power LED array should be effective in emitting enough light to serve as a deterrent from motor vehicles.

$V_{in}$  is the input voltage from the rectification section and is equal to 3.3V nominal. From Ohm's law, the resistance required to achieve the lower limit of 40mA through the LED is calculated as:

$$R_{LED} = \frac{V_{in} - V_{LED}}{I_{LED}}$$

$$R_{LED} = \frac{3.3V - 3V}{40mA} = 7.5\Omega$$

The resistance required to achieve the upper limit of 75mA through the LED is calculated as:

$$R_{LED} = \frac{3.3V - 3V}{75mA} = 4\Omega$$

Each LED requires a range of resistor values of 4 Ohm to 7.5 Ohm assuming all LEDs are identical. The difference in the resistance values for the upper and lower limit for current through the LED is very small in that a small change in the resistance would correspond to a big change in the current through the LED. Adjustments in the resistance values may be required during experimental trials to obtain a uniform lighting solution.

### 5.1.2.2.3 LED Resistor Calculations

$V_{in}$  is the input voltage from the rectification section and is equal to 3.3V nominal. From Ohm's law, the resistance required to achieve the lower limit of 40mA through the LED is calculated as:

$$R_{LED} = \frac{V_{in} - V_{LED}}{I_{LED}}$$

$$R_{LED} = \frac{3.3V - 3V}{40mA} = 7.5\Omega$$

The resistance required to achieve the upper limit of 75mA through the LED is calculated as:

$$R_{LED} = \frac{3.3V - 3V}{75mA} = 4\Omega$$

Each LED requires a range of resistor values of 4 Ohm to 7.5 Ohm assuming all LEDs are identical. The difference in the resistance values for the upper and lower limit for current through the LED is very small in that a small change in the resistance would correspond to a big change in the current through the LED. Adjustments in the resistance values may be required during experimental trials to obtain a uniform lighting solution.

### 5.1.2.3 LED Power Supply

Current must be regulated to ensure longevity and proper function of the LED array. Depending on the LED chosen, a range of constant voltages of 2.7V - 3.6V is required to power each LED. Three different design options will be discussed in the following sections.

#### 5.1.2.3.1 Buck-Boost Converter

A buck-boost DC/DC converter was explored to drive the LED array. The buck-boost converter illustrated in Figure 67 would take a range of unregulated voltages and step down the voltage in the buck section of the converter. The boost section

would they supply the desired current to drive the LED array based on the parameters of L1, C1, and RL which is the equivalent resistance of the LED array.

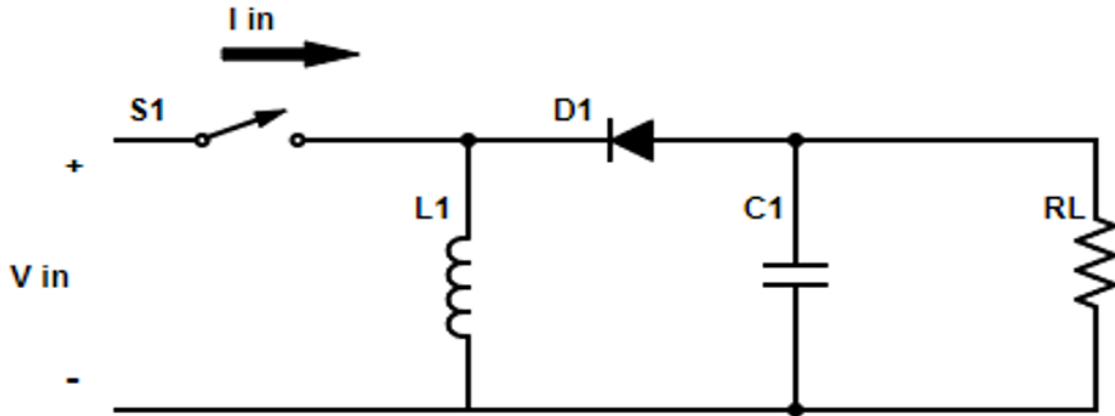


Figure 67: Buck Boost Converter<sup>(1)</sup>

Using the Webench® power designer tool on TI's website, the schematic in Figure 68 would accept input in the range of 0.5V – 5.5V and output 2.2V – 5.5V with up to 3.7A. The LED array would only require about 400mA in configuration 1 and this circuit would cover the requirements.

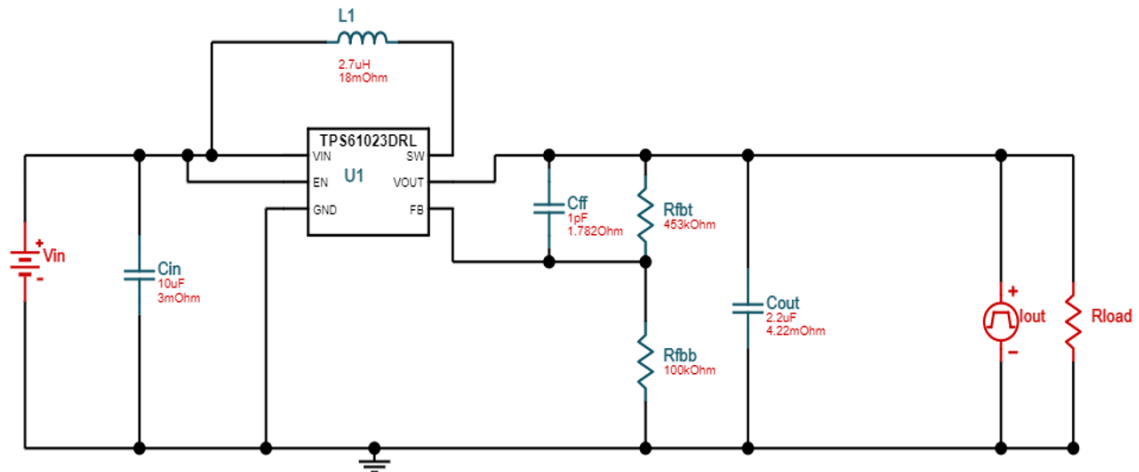


Figure 68: Integrated Buck-Boost LED Driver<sup>(1)</sup>

### 5.1.2.3.2 CMOS Common-Gate Current Source

The common gate amplifier illustrated in Figure 69 has a large output resistance which allows the circuit to behave as a constant current source.  $V_{DD}$  would be supplied from the rectification stage and  $V_I$  would come from the microcontroller PWM signal.

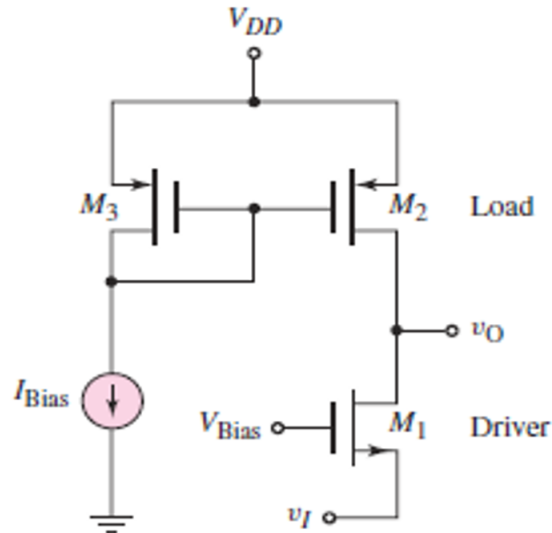


Figure 69: Common-Gate Amplifier

### 5.1.2.3.3 Feed from Output Regulator

A NMOS device will be used to control the LED array with the PWM signal from the microcontroller. The biasing voltage will come from the 3.3 output of the rectification stage and the array will connect to the output of the MOSFET.

### 5.1.2.4 Pulse-Width Modulation

Pulse Width Modulation (PWM) is a control technique used to produce analog results from a digital sources. The Pulse Width Modulation signal is defined by the frequency of said signal and the duty cycle.

The figure below (Figure 70) shows the comparison amongst the varying duty cycles. The duty cycle is a representation of how long the signal is in an ON state. Similarly, it also represents the amount of time that the signal is in an OFF state. The percentage seen in the duty cycle is the percentage of the total time it takes to fully complete one cycle. For example, in the 50% duty cycle shown in Figure 70, the amount of times that the signal is in an ON state at 3.3 volts is the same amount of times that the signal is in an OFF state (at 0 volts).

Although it is a small feature, we plan to utilize Pulse Width Modulation to change the luminance of the display; namely, dimming the backlight of the LED(s) found in the display. Pulse Width Modulation can also be used to dim the LED lights that will be mounted on the Bike System. The LED lights are addressed in another section.

We plan to control the variations of the duty cycle by the means of programming that will be loaded onto the microcontroller.

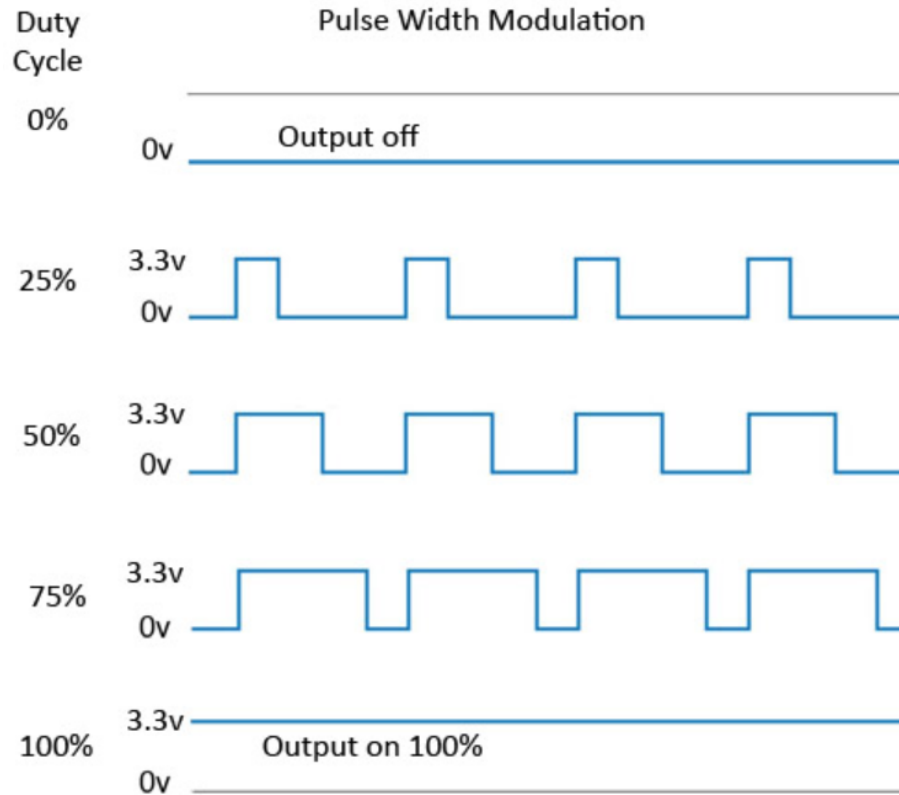


Figure 70: Duty Cycle comparison

#### 5.1.2.4.1 LED and Automated Locking Mechanism

On the MSP430G2553, Timer0\_A3 is a 16-bit timer that can support multiple PWM outputs. The design for each driver will incorporate a PWM signal to help save on energy consumption. The LEDs will be pulsed at 1000Hz and the ACLK will be configured to 32kHz in up-mode a period set to  $T = 0.001$  seconds. One of the available input/output pins will be used for each the LED and automated lock.

### 5.1.3 Microcontroller Design

In this section, the various data transmission methods and common communication protocol interfaces will be discussed. These factors ultimately influenced the decision in choosing the best fit microcontroller for the auxiliary components of the Bike System.

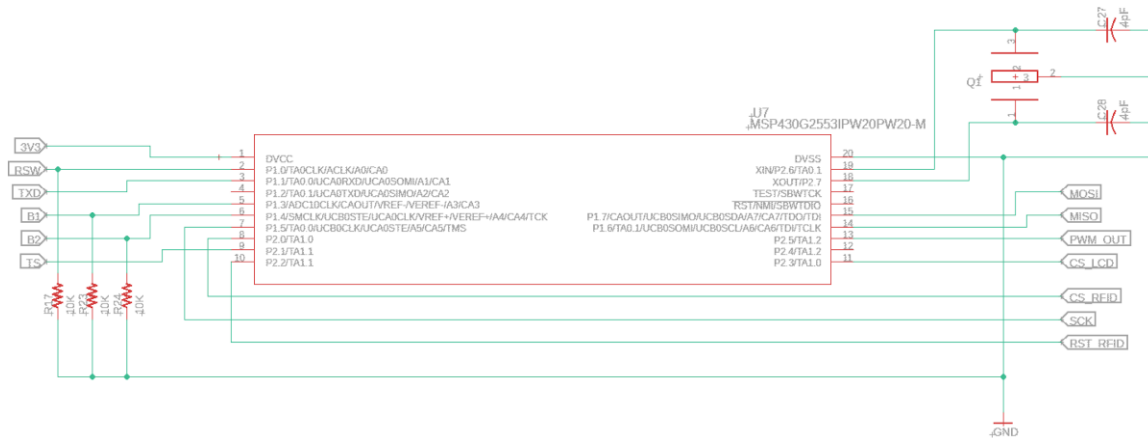


Figure 71: Microcontroller Circuit

Figure 71 shows the schematic for the microcontroller design, and consists of the microcontroller (U7), a crystal oscillator (Q1), and pull-down resistors (R17, R23, and R24). The crystal oscillator is used to provide an accurate timing reference for the use of generating clocks and timers by the microcontroller. The pull-down resistors are used in conjunction with the reed and UI button switches, whose signals are represented by RSW, B1, and B2; respectively; on the left of Figure 71. Since the input from the reed switch will be a logic high (3.3V), the resistor is there to ensure that the logic high is maintained at the microcontroller's input pin, and to ensure that the pin is pulled down to low (0V) when logic high is no longer being applied.

In addition to the RSW and button signals, there are many other different signals interfacing with the microcontroller. The TXD signal is used for programming the microcontroller via backchannel UART, the TS signal is the input from the temperature sensor, the MOSI and MISO lines are used for SPI communication with the LCD and RFID module, SCK is the clock for the SPI communication, the CS signals are used for selecting between the LCD and RFID on the SPI lines, and the PWM\_OUT is used for outputting a PWM signal for the LED lighting subsystem.

### 5.1.3.1 Data Transmission

The process of transmitting or transferring data from one digital device to another is known as data transmission. Data transmission can be done using either of two methods: serial transmission and parallel transmission. The visualization of the differences between serial and parallel data transmission can be seen in Figure 72.

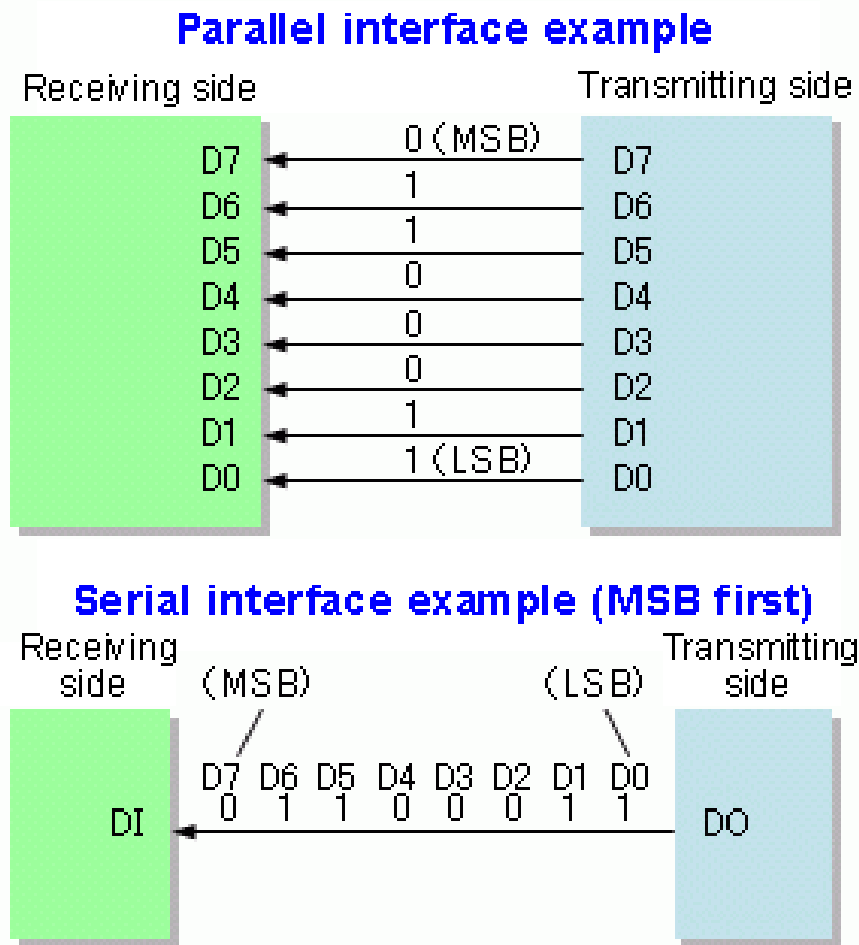


Figure 72: Example of parallel transmission vs serial transmission

### 5.1.3.1.1 Serial Transmission

In serial transmission communications, data is sent over the channel or computer bus one bit at a time in order. Essentially, data bits are only continuously sent if the previous data bit has been received.

This simple process makes serial communications for data transmissions very reliable. In this type of data transmission, it is not possible to have corrupted data as a result of bits arriving at the destination device out of order.

### 5.1.3.1.2 Parallel Transmission

In parallel transmission communications, data bits are sent simultaneously over the channel or computer bus. This type of data transmission is a lot faster than serial transmission since it allows data bits to be all sent at the same time. In parallel transmission protocols, there is no waiting time to send the next bit while waiting on the previous bit to reach the destination device.



The largest concern with parallel transmission protocols is the risk of having corrupted data since there is always a chance of bits arriving out of order. This risk can be reduced with the use of a parity bit. The tradeoff of using parallel communication protocols is having data being transmitted very quickly at the expense of the likelihood of it being corrupted data.

### **5.1.3.2 Microcontroller Communication Protocols**

Due to the major difference between serial and parallel communication protocols, we chose to focus on having components that utilize serial data transmission. Although it might be a little slower when compared to parallel transmission protocols, we wanted to minimize or completely eliminate the risk of having corrupted data bits sent. In this section, the most common serial microcontroller protocols are discussed.

#### **5.1.3.2.1 Serial Protocol Interface (SPI)**

Serial Protocol Interface is a synchronous serial communication protocol that utilizes a clock. The data transmitted is read on either the rising or falling edge of the clock signals. This protocol is full duplex. Therefore, the data being transferred or transmitted is sent without interruption. This means that the data is not broken up into frames or packets.

The basis of the Serial Protocol Interface is the use of a master device and its MOSI (Master Out Slave In) and MISO (Master In Slave Out) data lines. The other devices are referred to as “slaves” and they can be daisy chained if necessary.

#### **5.1.3.2.2 Inter-Integrated Circuit Communication (I2C)**

Inter-Integrated Circuit Communication is also a synchronous serial communication protocol. Two data lines or wires are used within this protocol: the serial data line (SDA) and the serial clock line (SCL). Data is transmitted in parts known as messages. These messages are further broken down into frames.

This type of communication uses a bus topology. The microcontroller is usually assigned as the master device in this set up. In Inter-Integrated Circuit Communication, the master is the device that initiates all transmissions and possess the capability to read and write to all other devices within the network. The master, which is the microcontroller in this case, is also responsible for the clock signals.

As previously stated, data messages are broken up into frames to be sent. Each data message has a start condition and a stop condition to indicate the beginning and the end of the message. This way, the destination device will know whether it has received the whole message once it has received the stop condition.

### 5.1.3.2.3 Universal Asynchronous Receiver and Transmitter

The Universal Asynchronous Receiver and Transmitter (UART) is not a communication protocol in the traditional sense like SPI and I2C discussed above. It is an actual physical circuit existing within a microcontroller. This communication is unlike SPI and I2C since it is asynchronous. This is due to the fact that both the receiver and transmitter have their own clock signal. As a result, it is not a given nor an expectation that the rising and falling edges of these two clock signals are synced with each other.

The Universal Asynchronous Receiver and Transmitter can be set up to be either half-duplex or full duplex depending on the application. Due to the asynchronous nature of UART, start bits and stop bits are added to the beginning and end of the data packets being transferred. These bits operate in a similar fashion to the start condition and stop condition of I2C.

## 5.1.4 LCD Design

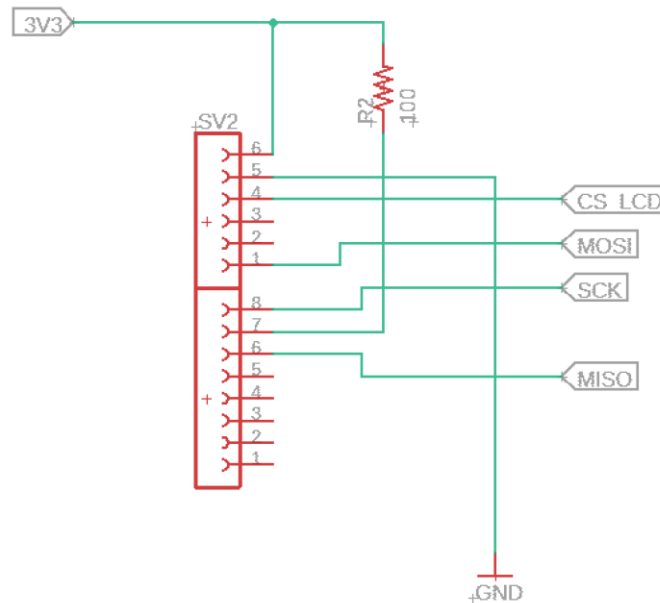


Figure 73: LCD Schematic

This section details the LCD design. The LCD will be interfaced with the microcontroller via the SPI communication protocol. Figure 73 shows the schematic for the LCD design, where the LCD module will plug into the SV2 connector. The signals are for interfacing with the microcontroller via SPI, and the resistor is to set the LCD brightness. Refer to Figure 71 in Section 5.1.3 for the microcontroller pinout, and refer to Section 5.2.1.1 for the software design for the LCD.

### 5.1.4.1 LCD Design Testing

The display is a vital part to the Bike System design. This display is where the rider, or user of the Bike System, will be able to see the ambient temperature readings, the average distance travelled thus far, and the average speed of the rider's trip thus far.

In order to make sure that the microcontroller is properly connected and interfacing correctly with the display chosen, the programmer will utilize a test program to output "TESTING" to the screen of the display.

The Figure 74 shows the breadboard testing for the LCD module. The pins were connected in as it is shown in Table 74. The main function of this testing was to test the connection and ensure the display was receiving proper power.

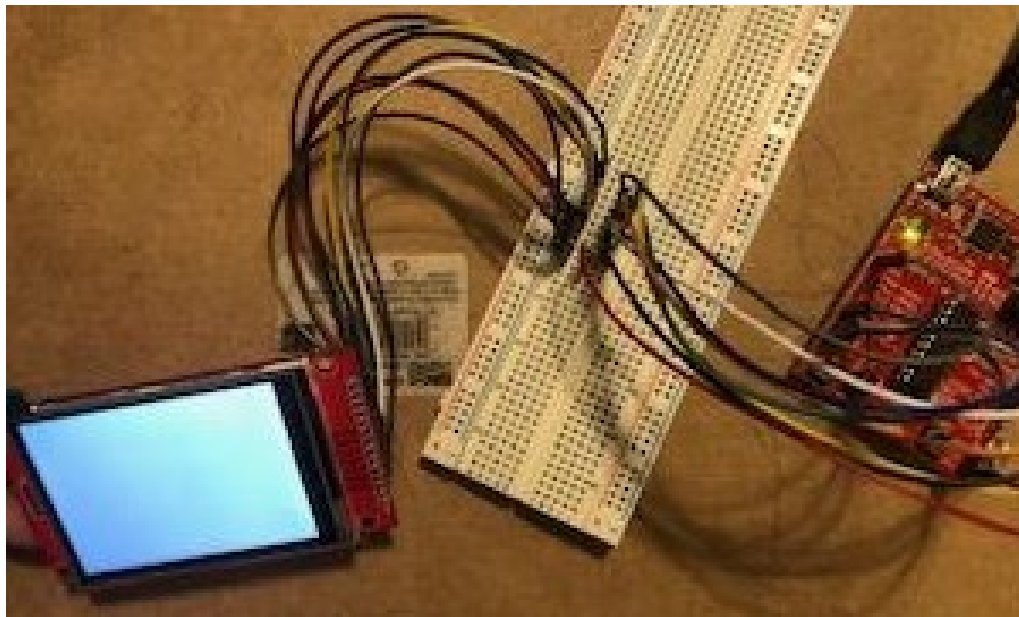


*Figure 74: LCD Breadboard testing*

### 5.1.5 Sensors Design

This section covers the design of the sensors used in the Bike System design. These sensors will interface with the microcontroller and provide data to it. See Figure 71 in Section 5.1.3 for the schematic.

### 5.1.5.1 Temperature Sensor Design and Testing

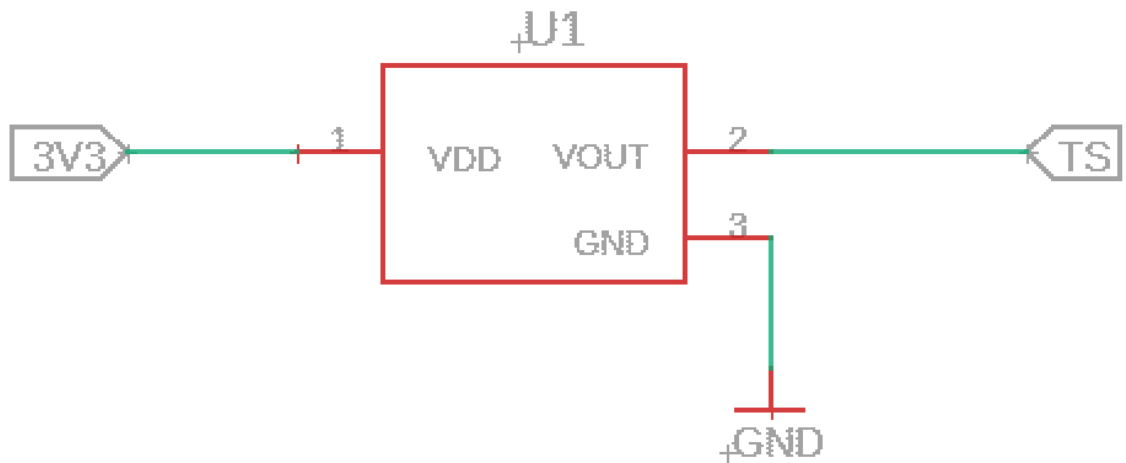


Figure 75: Temperature Sensor Schematic

Figure 75 shows the schematic for the temperature sensor. The TS signal on the right of Figure 75 is fed to the microcontroller's analog-to-digital converter (ADC). This carries a voltage signal that is related to the temperature, and is converted to a digital signal via the ADC so that it can be processed by the microcontroller.

The breadboard testing for the LM35AH temperature sensor was tested on the breadboard to ensure that the temperature sensor was working with MSP430G2553 microcontroller as expected.

### 5.1.5.2 Hall Sensor Design and Testing

The Hall Sensor design was done with the APS11700 Micropower Hall Effect Switch at its center. The APS11700 Micropower Hall Effect Switch is a relatively simple part with only three pins: input voltage, ground, and the output analog voltage. Two design choices were made when implementing the APS11700 Micropower Hall Effect Switch. They are the inclusion of the 10 kilohm resistor and the 0.1 microfarad capacitor. First, the 10 kilohm resistor was added between the input voltage pin and the output analog voltage to act as a current limiting element. Second, the 0.1 microfarad capacitor was added between in the input voltage pin and ground to act as a filtering component for electromagnetic interference.

Similar to the RFID Module testing, the Elegoo Uno Rev3 development board was used as the microcontroller element. There is only one difference between the above design and the testing design; that is the exclusion of the filtering capacitor. Also, an LED was driven from the microcontroller to show when the ADC reading dropped below a certain value, signifying the presence of a magnet.

When there is no permanent magnet present to actuate the APS11700 Micropower Hall Effect Switch. Since there is no permanent magnet present, the LED is not driven high.

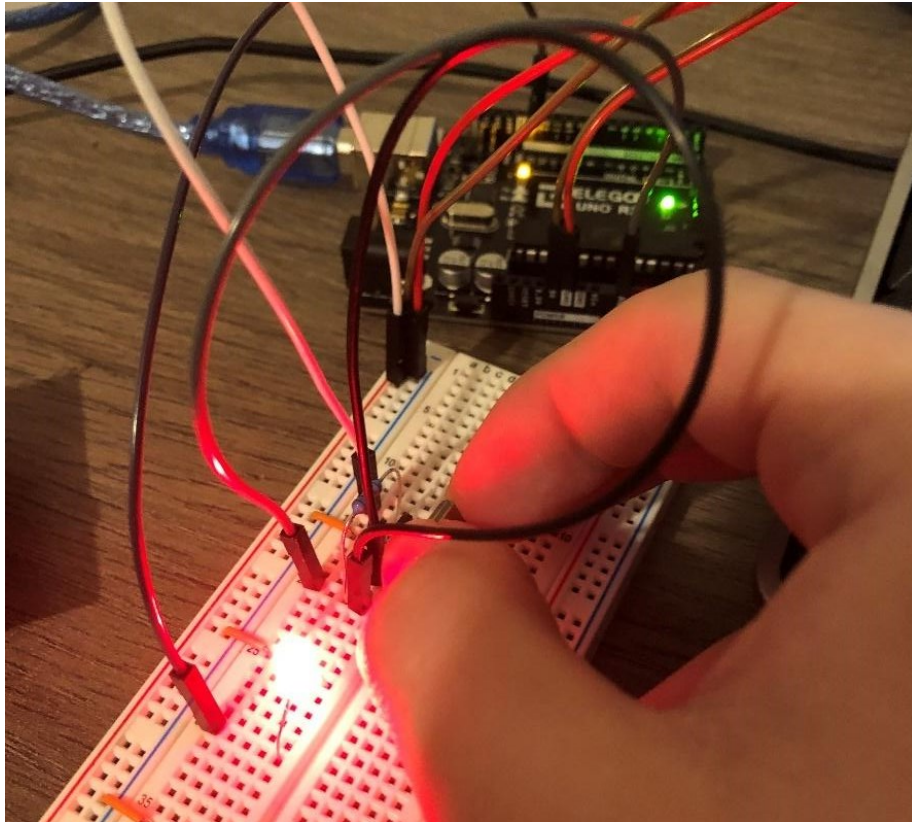
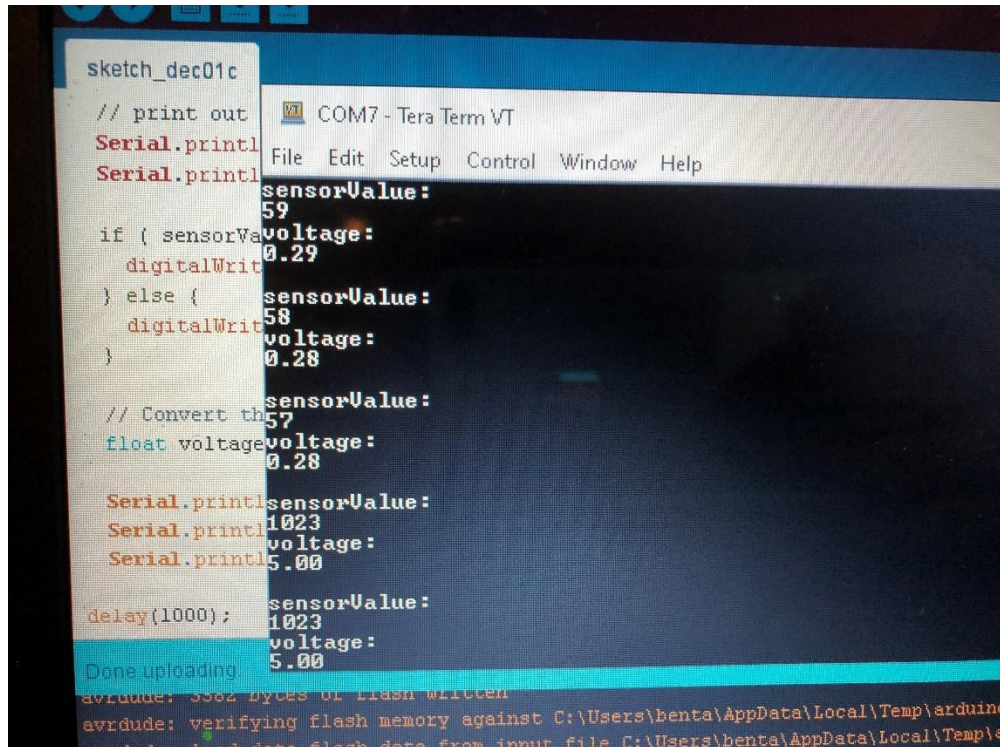


*Figure 76: Hall Sensor with actuating permanent magnet present*

In Figure 76, it can be observed that when the permanent magnet acting as the actuator is present, the output analog voltage propagates to the ADC onboard the microcontroller, which causes the LED to be driven high, signifying the presence of a magnet. This test proves that the APS11700 Micropower Hall Effect Switch is functional. It should also be noted that the magnet needed to be, at the maximum, about 18 millimeters away from the APS11700 Micropower Hall Effect Switch before the ADC reading dropped to a value that signified that a magnet was present.



```
sketch_dec01c
// print out
Serial.println
Serial.println
if ( sensorValue > 1023 ) {
  digitalWrite(LED_BUILTIN, HIGH);
} else {
  digitalWrite(LED_BUILTIN, LOW);
}
// Convert the sensor value to voltage
float voltage = sensorValue * 0.00488;
Serial.println(sensorValue);
Serial.println(voltage);
Serial.println(5.00);
delay(1000);
Done uploading.
avrdude: 3362 bytes of flash written
avrdude: verifying flash memory against C:\Users\benta\AppData\Local\Temp\arduino...
avrdude: load data flash data from input file C:\Users\benta\AppData\Local\Temp\...
```

Figure 77: Terminal Output When Magnet was Present vs. Not Present

In Figure 77, the ADC readings onboard the Elegoo Uno Rev3 development board can be observed. The first three readings are from the scenario when the permanent magnet is present. The last two readings visible on the terminal are when there was no permanent magnet present. The possible ADC values range from 0 to 1023, as specified in the code.

### 5.1.5.3 Reed Switch Design

There are not many design choices to make when designing with a Reed Switch. The Reed Switch can be symbolized as a normally open (NO), two pin switch that is only actuated by a permanent magnet. In the application of this part, a digital high signal will be driven to the input side of the Reed Switch and once actuated by a permanent magnet, the normally open (NO) Reed Switch will close and will allow the digital high signal to pass through the output. The output of the Reed Switch will be connected to a GPIO port on the microcontroller and, once actuated, will read a digital high signal for a short duration of time. This method is advantageous over using the Hall Sensor as it does not require a constant power source.

Testing the Reed Switch involved only a multimeter and a permanent magnet. To prove that the Reed Switch works, only the characteristic of continuity is required. As such, two leads from the multimeter were connected to either side of the Reed Switch with the continuity setting set. Once a permanent magnet was brought close enough to the Reed Switch, the contacts inside the Reed Switch actuated, and the multimeter signified that the connection was continuous, proving that the Reed

Switch being tested is functional. It should be noted that the distance from which the permanent magnet being used was able to actuate the contacts inside the Reed Switch was less than that of the Hall Sensor. At a maximum, the Reed Switch actuated with the same magnet used to test the Hall Sensor from about 15 millimeters away, 3 millimeters less than that of the Hall Sensor. To lengthen this distance, a stronger permanent magnet is required.

## 5.1.6 RFID Module Design

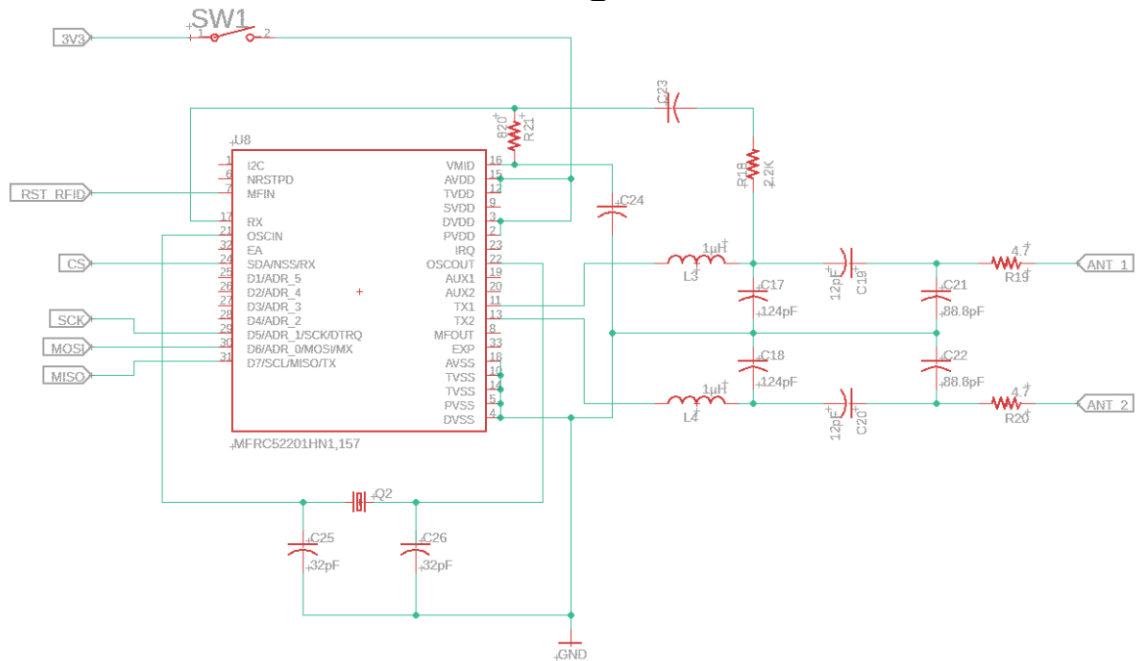


Figure 78: Schematic of RFID Module Design

Figure 78 shows the schematic for the RFID module design. It consists of the RFID IC (MFRC522, U8), passive components, a crystal oscillator (Q2), and a momentary on switch (SW1). The passive components are used for EMC filtering and impedance matching. The crystal oscillator is used to generate a 27.12 MHz signal that is used by the RFID IC to generate the 13.56 MHz operation frequency by taking the oscillator signal and cutting it in half. The momentary on switch is used to apply power only when the user of the Bike System needs to unlock the bike. This is done to save power. The signals on the left of Figure 78 come from the microcontroller, and are used to interface the RFID IC via SPI protocol.

The process of designing the RFID Module for this project involved tuning the resistor, capacitor, and inductor values listed in the MFRC522 datasheet, specifically the application section, to optimize the antenna characteristics. According to a reference note listed in the MFRC522 datasheet, the design of the antenna can be optimized for different data transmission rates based on the hardware, specifically inductance and capacitance values, used to layout this design on a printed circuit board. Due to the uncertainty of whether or not this

design will use an existing antenna or an antenna will have to be laid out on the printed circuit board, the resistor, inductor, and capacitor values have been omitted as these values will fluctuate based on that design choice.

The heart of the RFID Module design is the MFRC522 integrated circuit. The MFRC522 is a 32-pin package that communicates with both the microcontroller unit and the contactless RFID transponder. The MFRC is able to communicate via universal asynchronous transmitter receiver (UART), inter-integrated circuit (I2C), and serial peripheral interface (SPI) buses; however, the input/output configurations of these avenues are limited. For example, a universal asynchronous transmitter receiver (UART) is only able to be used as a communication method with which to input data to the MFRC522 from the microcontroller. The serial peripheral interface (SPI) is only able to be used as a communication method with which to output data from the MFRC522 to the microcontroller. Lastly, the inter-integrated circuit bus can be used to both input and output data from the MFRC522 to and from the microcontroller, respectively.

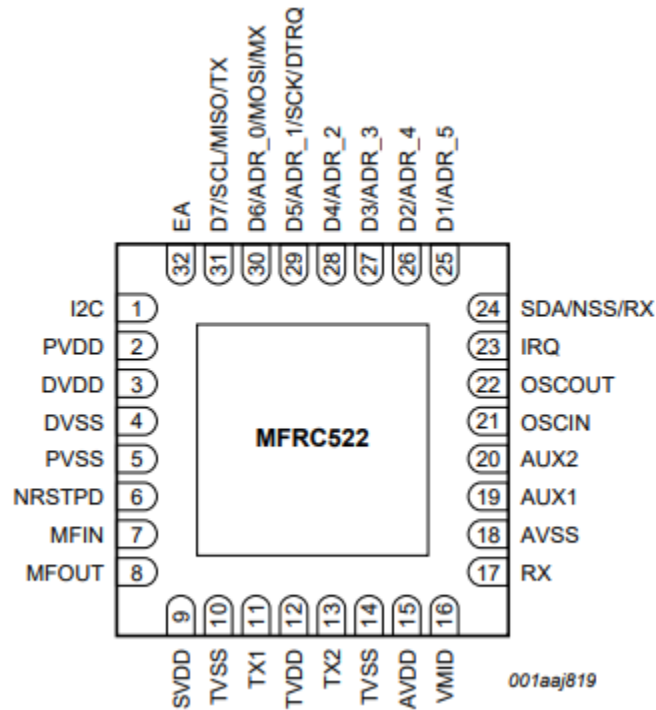


Figure 79: MFRC522 Pin Map

Because of this serial communication limitation, it will be most convenient, from a hardware perspective, to communicate with the MFRC522 IC from the selected microcontroller via an inter-integrated circuit (I2C) bus since it can handle both input and output. However, from a software perspective, the most convenient option for a communication bus is a serial peripheral interface (SPI) bus since there are existing libraries that can be applied to this project, thus saving time and effort. The aforementioned downside will be negligible since for this project's application, the microcontroller does not need to write any data from the MFRC522, but instead



only read the unique identification (UID) hex value encoded on the RFID transponder when one is scanned.

In an effort to keep the design as low power as possible, one of two avenues will be pursued. First, a switch will be designed to enable the 3.3V that the MFRC522 needs. The idea behind this method is that the MFRC522 IC does not need to be powered at all times, but only when the user needs to scan their RFID transponder. So, he will press a switch that enables power to flow from the power supply circuit to the RFID module and then he will be able to scan his RFID card. The start-up time for the MFRC522 is negligible as it only requires 50 microseconds at most to boot up; this is the case for if the oscillator is also powered down. The second method by which to keep the design power efficient is to utilize the onboard soft power-down mode on the MFRC522. In this state, the MFRC522 IC only draws 10 microamps at 3.3V, which is equal to 33 microwatts. The primary benefit to pursuing this avenue is that it does not require any additional hardware; instead, there is a bit inside the CommandReg register in the MFRC522 that the microcontroller can toggle to set the MFRC522 IC in a low power mode. In this soft power-down mode, the current sinks are turned off, digital input pins keep their functionality, and digital output pins keep their state. Also, all registers, including the CommandReg register and configuration registers, keep their content as well as the FIFO buffer.

### **5.1.6.1 RFID Testing**

Initially, the MSP430G2553 development board was used to test the RC522 RFID module. The Energia IDE, version 1.8.10E23, was used to attempt to program the RC522 RFID module, but this attempt failed due to a lack in maintenance in the compilation software provided by Energia. Every attempt to upload code to the MSP430G2553 failed due to an upload error. The Energia IDE was chosen as the IDE to test the RC522 RFID module since there are existing libraries available for use through <https://github.com>, a free and open source code sharing community. After failing to upload code to the MSP430G2553 via the Energia IDE, the decision was made to test the RC522 RFID Module with the Elegoo Uno Rev3 development board. In order to program the Elegoo Uno Rev3 development board, the Arduino IDE, version 1.8.13, was used. Once again, the decision to use the Elegoo Uno Rev3 development board was made to use the existing libraries relevant to the RC522 RFID Module on <https://github.com>. The user on GitHub whose code was used to test the RC522 RFID Module is a user by the name of "miguelbalboa." The code used from miguelbalboa's library did three things:

- Read the unique identification (UID) hex value from each RFID transponder and printed it to the terminal
- Gave the ability to set a master tag that when scanned, allowed for the scanning of additional tags to be granted access privileges
- Read the unique identification (UID) hex value from unrecognized RFID transponders and denied access.

All pins on the RC522 RFID Module were used except for the “IRQ” pin since no interrupts were required for testing. Furthermore, for the application of this module in the project, interrupts will not be necessary since the microcontroller will not need to interrupt the RC522 RFID Module during its operation. It is also worth noting that the center of the embedded antenna on the RC522 RFID Module is at the dot surrounded by lines that appear to be propagating radially.

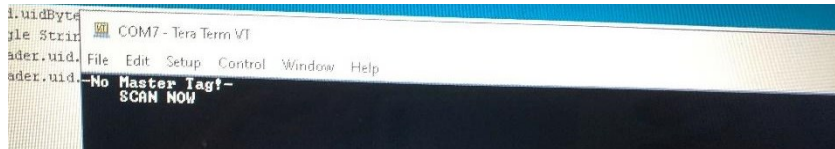


Figure 80: User being prompted to scan a Master Tag

In Figure 80, the output from the terminal can be observed. This is the output from the terminal when first uploading the code to the Elegoo Uno Rev3 development board. At this stage of testing, it has not yet been proven that the serial peripheral interface (SPI) bus being using to read data from the RC522 RFID Module is functional as this text is programmed in code and is not an output of the RC522 RFID Module.



Figure 81: Setting a Master Tag

In Figure 81, a Master Tag is set. It can be observed that the unique identification (UID) hex value of the particular RFID transponder used is “56 DF 6F 29.” Because of the code used, once the Master Tag is set; it cannot be undone.

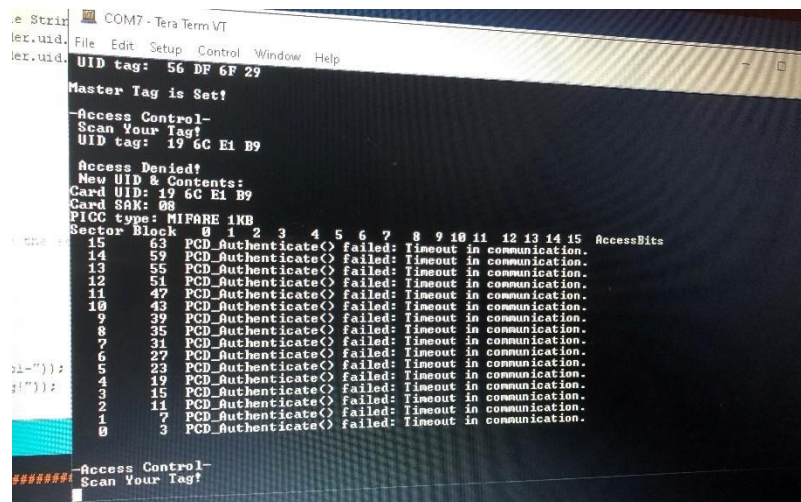


Figure 82: Denial of access

In Figure 82, it can be observed that a tag with the unique identification (UID) hex value of “19 6C E1 B9,” was scanned. Since this RFID transponder is not the Master Tag and it has not been granted access by the Master Tag, it is both recognized by the RC522 RFID Module and is denied access. Furthermore, it can be observed that the RC522 RFID Module reported additional information such as the type of card attempting to be used, in this case an RFID transponder of type MIFARE 1K, as well as attempting to read the memory on the RFID transponder itself.

```

10 43 PCD_Authenticate() failed: Timeout in communication.
19 39 PCD_Authenticate() failed: Timeout in communication.
08 35 PCD_Authenticate() failed: Timeout in communication.
07 31 PCD_Authenticate() failed: Timeout in communication.
06 27 PCD_Authenticate() failed: Timeout in communication.
05 23 PCD_Authenticate() failed: Timeout in communication.
04 19 PCD_Authenticate() failed: Timeout in communication.
03 15 PCD_Authenticate() failed: Timeout in communication.
02 11 PCD_Authenticate() failed: Timeout in communication.
01 07 PCD_Authenticate() failed: Timeout in communication.
00 03 PCD_Authenticate() failed: Timeout in communication.

Access Control-
Scan Your Tag!
UID tag: 56 DF 6F 29

Program mode:
Add/Remove Tag
UID tag: 19 6C E1 B9

Tag Added!

Access Control-
Scan Your Tag!
#####

```

Figure 83: Adding a tag after the Master Tag is scanned

In Figure 83, it can be observed that after the Master Tag, with unique identification (UID) hex value “56 DF 6F 29,” another tag, with unique identification (UID) hex value “19 6C E1 B9,” was added. This signifies that the newly scanned tag can be used to access the RC522 RFID Module until it is removed by the Master Tag.

As a result of the above testing, it has been proven that the RC522 RFID Module is indeed functional. It should be noted that testing with the RC522 RFID Module was performed with the Elegoo Uno Rev3 development board using only the serial peripheral interface (SPI). As a result of this condition, on the RC522 RFID Module’s ability to be read from was tested. Further testing is required to verify the RC522 RFID Module’s ability to be written to. Such testing would require the use of either a universal asynchronous transmitter receiver (UART) or inter-integrated circuit (I2C) bus.

### 5.1.6.2 Senior Design II Changes

In senior design 2, many changes were made to the integration efforts taken to ensure that the RFID would function as intended. The changes are as follows:

- A custom antenna was designed.
- The circuitry to support the custom antenna was designed.
- 8 male header pins were implemented.

Each of the aforementioned bullet-points will be described in detail in the following paragraphs.

The first step in designing the RFID system was to design an antenna with characteristics suitable for the MFRC522 IC. It is recommended in [27] to design an antenna with an estimated inductance between 300nH and 3 $\mu$ H and a resistance between 0.3 and 8 $\Omega$ . As such, a 3-turn coil (antenna) embedded on a printed circuit board was designed and manufactured. Upon testing the antenna, it was recorded that the antenna had an inductance of 1.951 $\mu$ H at 13.56 megahertz, a resistance of 2.6 $\Omega$ , and an assumed capacitance of 0.1pF at 13.56 megahertz. The next step was to calculate the value of a damping resistor needed to decrease the Q-factor of the antenna to a value between 30 and 35. According to the formula in [27] regarding how to calculate the correct Q-factor, the resistance value of 1.47 $\Omega$  was chosen. The layout of the 3-turn coil (antenna) can be found as A5 in section A.3.

The next circuit that was designed was the electromagnetic compatibility (EMC) cutoff filter which was designed to have a cutoff frequency of 14.5 megahertz as this is the frequency past which the amplitude of the output signal decreases by 3 decibels. It is recommended in [27] that the EMC cutoff frequency be between 14.1 and 14.5 megahertz as this will ensure that reception bandwidth is maximized.

After the EMC compatibility (EMC) cutoff filter was designed, the next circuit to be designed was the matching circuit. The purpose of the matching circuit is to match the input impedance of the antenna to the output impedance of the TX1 and TX2 pins on the MFRC522 IC. The matching circuit includes two sets of capacitors named C1 and C2. As recommended in [27], the formulas used to calculate the values of C1 and C2 can be found as A6 in section A.3.

After the values for C1 and C2 were solved, the EMC cutoff filter, matching network, damping resistor, and antenna series equivalent circuits were simulated using RFSim99, a free open-source software suggested by NXP Semiconductors, and an S11 port measurement was taken with the center of the Smith Chart normalized to 50 $\Omega$ . The simulation circuit and simulation output can be found as figures A7 and A8, respectively, in section A.3.

The last circuit to be designed was the receiver circuit because its parameters depend on the component values in the EMC cutoff filter, matching network, damping resistor, and antenna. The two capacitor values, CVMID and CRX, were predefined in [27] as 100nF and 1nF, respectively. The two resistor values form a voltage divider and depend on the voltage level across one of the capacitors in the EMC cutoff filter with respect to ground. The entire RFID circuit schematic can be seen in section A.3 as figure A9.

## **5.2 Bike System Software Design**

The Bike System's software will be implemented onto or loaded onto the microcontroller chosen. The software that will be written will take in inputs from the sensors and produce outputs onto the display for the user to read and interpret.

### **5.2.1 Software Functionality**

The software for the Bike System main functions include reading the data from certain sensor to display them directly onto the screen like the ambient temperature and use in computations to find out the other metrics like speed and distance traveled. This software environment that will be used to write, compile, and load the code onto the microcontroller is Code Composer Studio (CCS).

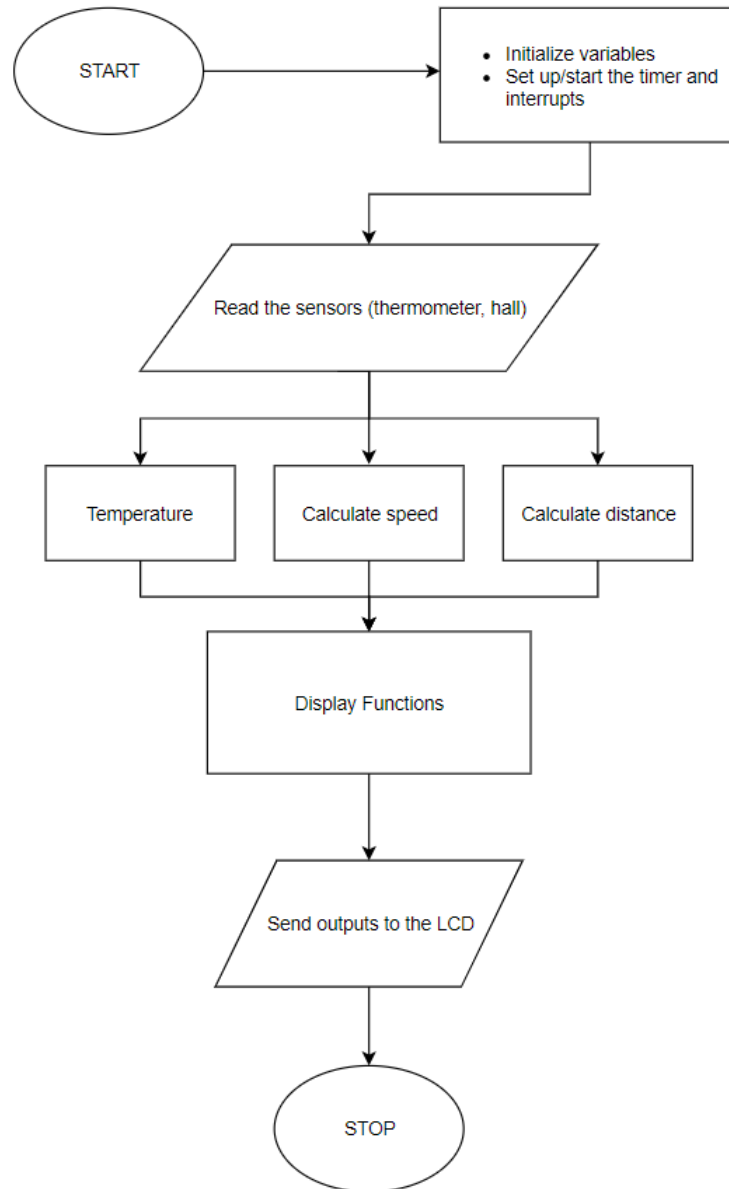


*Figure 84: Algorithm Logic Flowchart*

### 5.2.1.1 Use Case Diagram

The Use Case diagram seen in Figure 85 below shows the expected behaviors of the Bike System and what the intended relationships between the system and the user are. This type of Unified Modeling Language (UML) diagram does not seek to explain or specify the exact processes of how these tasks will be done. This Use Case diagram is purely behavioral.

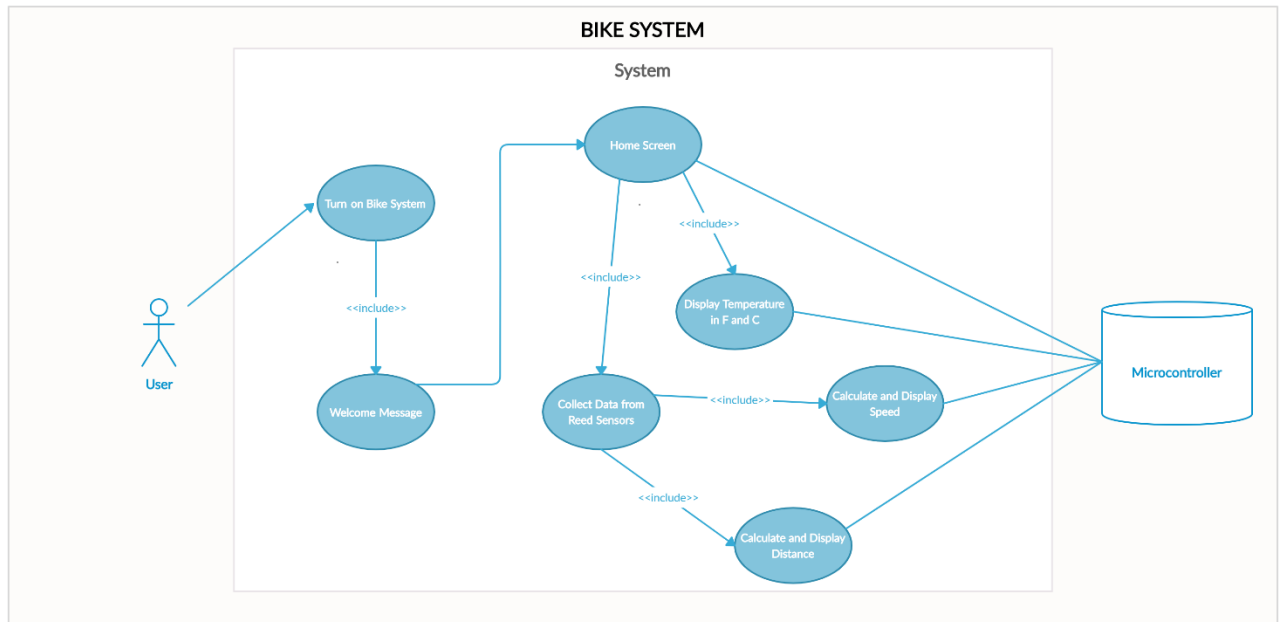


Figure 85: Use Case UML Diagram

### 5.2.1.1 LCD Display

The function of this device is to simply display the outputs being sent from the microcontroller. Namely, the values for the ambient temperature, speed, and distance traveled.

#### 5.2.1.1.1 User Interface Illustration

In this section, the possible illustration of the user interface is discussed. These prototypes were not drawn to the exact size of the LCD screen. The dimensions of the screen were scaled to produce both the welcome screen and home screen shown in this section.

To create the user interface illustrations in this section, the web-based prototyping tool, Figma, was used. This is a very popular software design tool amongst UX/UI developers. Its beginner friendly format and free version made it the ideal prototyping and wireframing tool for the Bike System.

In Figure 86, the simple welcome message displayed is illustrated. Ideally, the welcome screen will be very close to this design in simplicity. Similarly, in Figure 87, the battery level and Bike System label are kept to adhere to some level of uniformity within the design. In this home screen prototype, the ambient temperature is displayed in both Fahrenheit and Celsius. The details of “Today’s Trip” are also displayed boldly enough for the user to see within any difficulty.

We opted to have the distance traveled displayed in three measurements since depending on the length of the trip, one measurement might be too small to be understandable, for example, if the user traveled a distance of 6 feet, it would be

counter intuitive and uninformative to display that information as 0.00114 miles. For similar reasons, the average speed during the trip is displayed to the user in both miles per hour (mph) and in kilometers per hour (kmh).

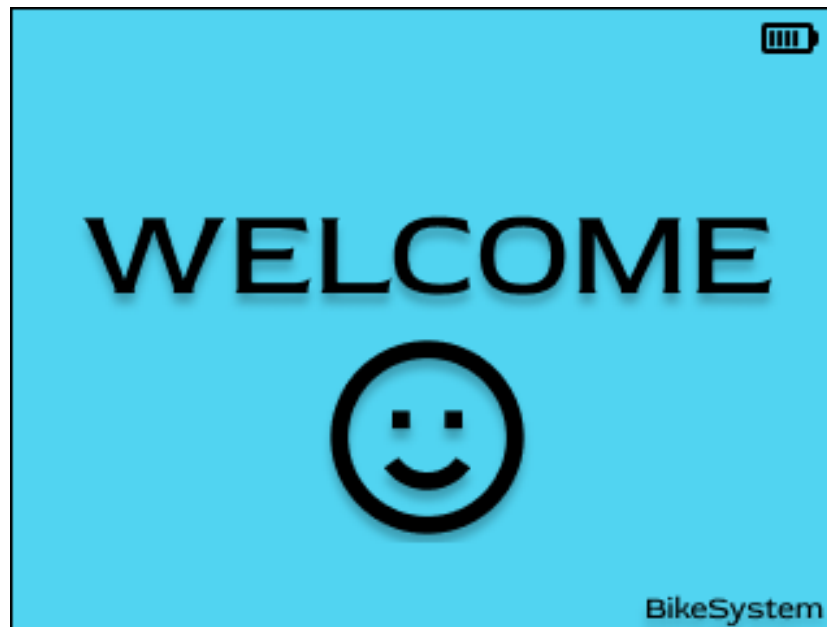


Figure 86: *Prototype of Welcome message*

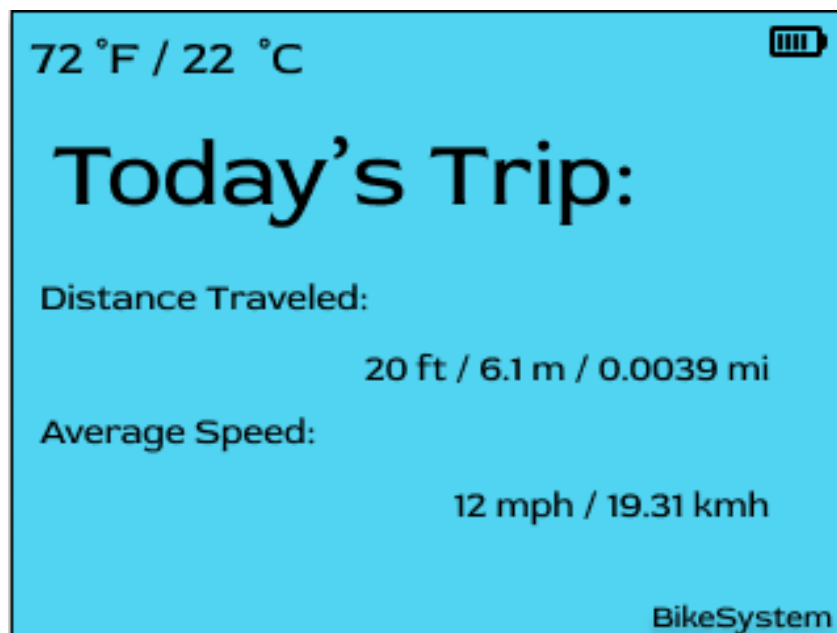


Figure 87: *Prototype of Home Screen*

### 5.2.1.2 Algorithm Description

The code for the Bike System will be broken down into three main subsections: reading inputs, computing the data, and outputting said data to the display for



viewing by the user. All constants, such as the wheel size of the bicycle, and all variables will be explicitly defined.

### 5.2.1.3 Display Function

The purpose of this device is to display the information generated to the user.

- Start
- Print Welcome message
- Print the ambient temperature
- Print the average distance traveled thus far
- Print the average speed thus far
- Stop

### 5.2.1.4 Temperature Calculation

The purpose of this function is to continuously read the ambient temperature in degrees Celsius and calculate the corresponding temperature in degrees Fahrenheit.

- Start
- Convert degrees Celsius to degrees Fahrenheit using the formula:
  - $^{\circ}\text{C} * (9/5) + 32 = ^{\circ}\text{F}$
- Send the temperature in both degrees Celsius and degrees Fahrenheit to the display
- End

#### 5.2.1.4.1 Distance Calculation

The purpose of this function is to continuously record the distance traveled by the user in the current trip.

- Start
- Collect input data from Reed sensors
- Send the distance in miles, feet, and meters to the display.
- End

#### 5.2.1.4.2 Speed Calculation

The purpose of this function is to continuously read and calculate the speed that the user is travelling at.

- Start
- Timer set to 0
- Start timer
- Use result from Distance calculation function
- Send the speed to the display
- End



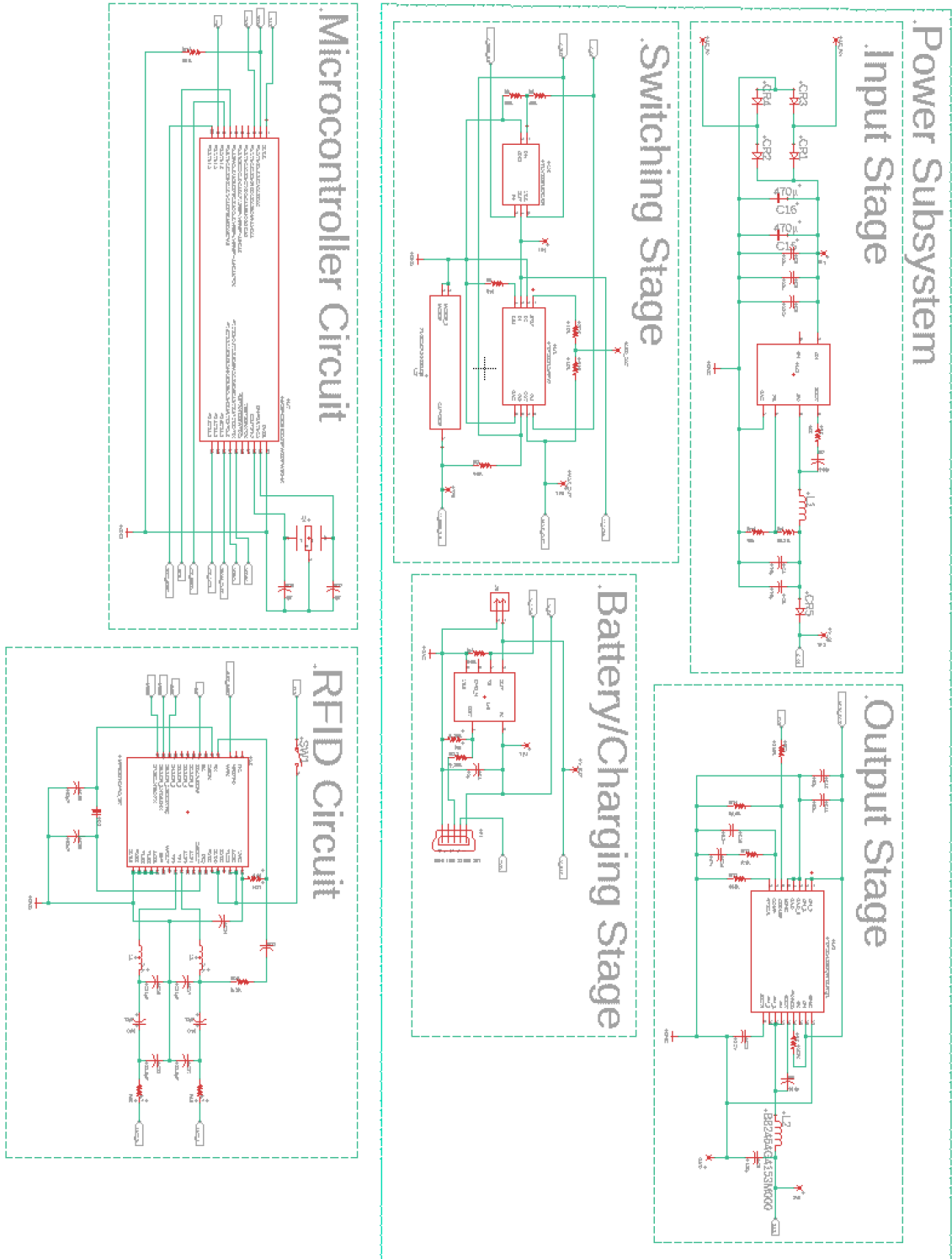


Figure 89: Bike System Main Board Overall Schematic

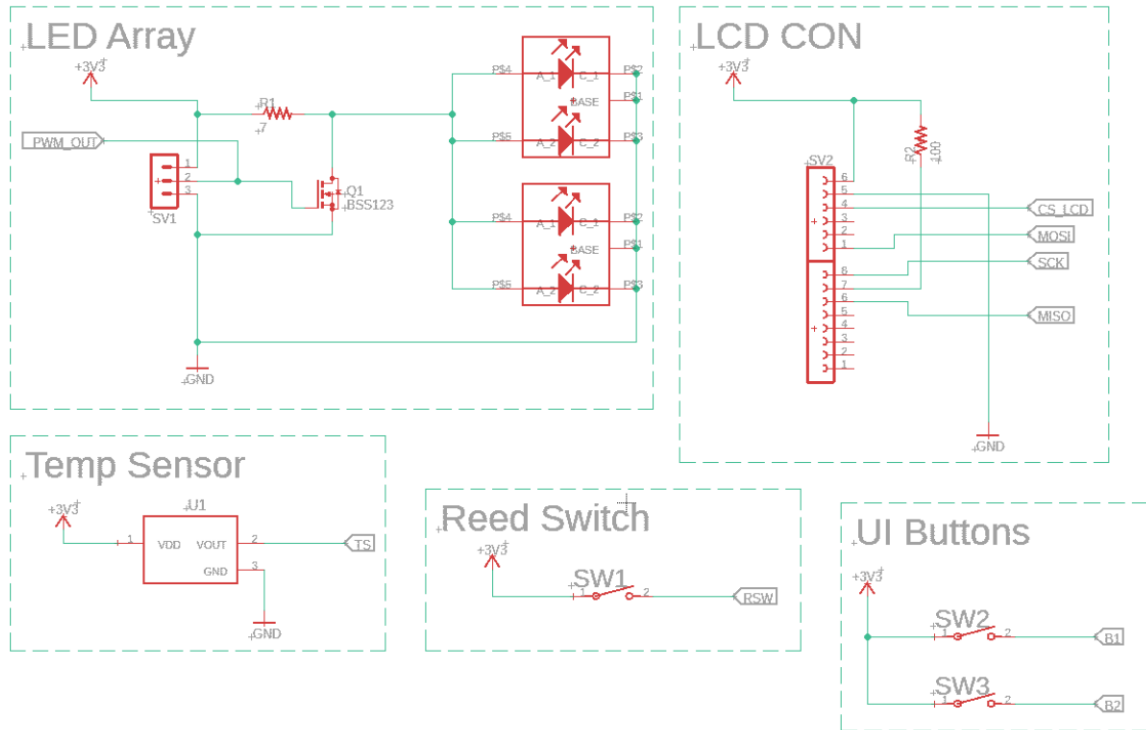


Figure 90: Bike System Secondary Board Overall Schematic

## **7. Administration**

This section contains all the management-related details of the Bike System. The projected financial plans and project milestones are discussed in detail. This section also talks about the main software tools used for project management within the group.

### **7.1 Project Milestone**

The milestone dates were set with the due dates of the documentation versions in mind. These milestones also revolved around the schedule of the team members and their respective responsibilities. Majority of the milestones in Senior Design I directly related to the research and development of certain components and technologies required.

*Table 30: Milestones*

<b>No.</b>	<b>Task</b>	<b>Date</b>
<u>Senior Design 1</u>		
1	Initial Project Idea	09/18/2020
2	Role assignment	09/22/2020
3	Refined Project Idea	10/02/2020
4	First Draft	11/13/2020
5	Technology and Parts Research	11/13/2020
6	Document Review Meeting with Lei Wei	11/18/2020
7	Order main parts	11/19/2020
8	Testing of parts	11/23/2020
9	Second Draft	11/29/2020
10	Document Review Meeting with Lei Wei	12/02/2020
11	Final Draft	12/08/2020
<u>Senior Design 2</u>		
12	Assemble Prototype	01/29/2021
13	Testing and redesign	02/12/2021
14	Finalize Prototype	03/21/2021
15	Peer Review	04/21/2021
16	Final Documentation	04/21/2021
17	Final Presentation	04/21/2021

### **7.2 Software Tools**

The key to success for the Bike System project included proper team collaboration and team cohesion. In order to achieve this, certain communication and

development software tools were chosen. These tools are discussed in this section.

## **7.2.1 Communication**

In order to ensure that team collaboration went as smoothly as possible given the current state of the pandemic and COVID-19 restrictions, these tools were selected. It was paramount to have reliable platforms for sharing ideas and information, assigning tasks, and conducting progress reports. It was also important to utilize tools that made this collaboration easy – not create too much of a hassle to actually use.

### **7.2.1.1 Zoom**

The team utilized zoom for meetings in the early stages of the project since that was the most familiar communication platform at the time. After a few meetings, it became obviously apparent that this type of communication platform was hindering the performance of the team. Spending the time to create new zoom meetings at odd times and having trouble with team members being stuck in zoom waiting rooms were creating unwanted breakdowns in communication.

### **7.2.1.2 Discord**

This communication platform was what the team adopted and is still continually using. Discord gave the team the ability to make a free, private server to share an information. Unlike Zoom, the team was able to “drop in” to a meeting calls at any time. We were also able to see when other team members were online or offline. Multiple text channels were created within this discord server to organize the team’s information. There were specific channels for: (i) contact information for everyone in the team, (ii) helpful links or notes to content being covered, (iii) links to external websites for the Bike System’s files such as the Google Drive, and (iv) meeting notes and attendance. The discord server’s feature of recording date and time of every message sent was also very useful.

### **7.2.1.3 Google Drive**

In the early stages of the planning and development of the Bike System idea, the team used google drive to save and store documents that were being collaborated on. Since most of our communication has been transitioned over to the Discord server, the Bike System’s google drive is being used to save larger files such as datasheets, a spreadsheet of current expenses for each team member, final versions of documentation, and other miscellaneous items.

## **7.2.2 Development**

In this section, the development tools used to bring the Bike System project idea to a completion and realization is discussed.

### 7.2.2.1 Autodesk Eagle

The Printed Circuit Board (PCB) design is a huge requirement of the Bike System project. This software tool was free to use with the student education license version. Autodesk's Eagle allowed the team to fully create PCB schematics and layouts. The design rule checker and auto router that this software tool provides made the final design step much easier.

### 7.2.2.2 Code Composer Studio (CCS)

The Texas Instruments MSP430G2553 microcontroller was chosen early on in the project's life cycle. As a result, the integrated development environment that the team would be using was already known. Code Composer Studio (CCS) is the IDE preferred when working with Texas Instruments microcontrollers. One of the main reasons for this is the fact that a lot of documentation already exists for common troubleshooting errors and debug applications.

## 7.3 Estimated Budgeting and BOM

The Table 30 below shows the breakdown of the overall cost of the Bike System project. As requirements change or problems arise, changes will be made, and the overall cost will be adjusted accordingly. Table 31 shows a breakdown of the smaller, miscellaneous parts and their corresponding references.

This project is being self-financed by the group members.

*Table 31: Financial Budget and Expenses*

Item	Price / Unit	Quantity	Price Estimate
Bicycle	NA	1	Already acquired
Microcontroller	\$9.99	1	\$9.99
Hall Sensor	\$5.99	6	\$35.94
Dynamo	\$20.24	1	\$20.24
LCD	\$13.99	1	\$13.99
LED lights	\$15.92	2	\$31.84
Safety Harness	\$10.99	1	\$10.99
Seat Belt Assembly	\$20.00	1	\$20.00
Temperature Sensor	\$31.13	3	\$93.39
Lithium-Ion Battery	\$21.49	1	\$21.49
Stainless Steel Cable	NA	33' x 1/8"	\$19.88
Housing Lock	\$25.66	1	\$25.66
Housing Fabrication	\$15.00	1	\$15.00
Final PCB w/ Integrated Circuit	\$16.80	1	\$16.80
RFID Module	\$12.79	1	\$12.79
Circuit Components	NA	NA	\$98.15
<b>Total</b>			<b>\$446.15</b>

Table 32: Breakdown of Circuit Components

Item	Price	Reference
TLV3691IDCKR	\$3.66	Comparator, U4
B120-13-F	\$3.87	Diode, CR1-5
TL4050A25QDBZT	\$7.74	V reference, U2
TPS2115APW	\$8.40	Power Mux, U1
CRCW080540K0FKEA	\$0.57	Res, R4, R15
PTN0805E5002BST1	\$3.35	Res, R5
GRT188C8YA105ME13D	\$4.81	Cap, C1
ZXMN2A14FTA	\$4.73	N-MOS
BQ21040DBVR	\$3.57	Battery IC, U3
7843330560	\$8.01	Ind, L1
CRCW060352K3FKEA	\$0.31	Res, R9
CRCW060310K0FKEA	\$0.31	Res, R2, R7, R16
C0805C104M5RACTU	\$0.64	Cap, C6 - C8
C2012X7S1A226M125AC	\$6.44	Cap, C4, C5, C10, C11
RC0603FR-0730RL	\$0.31	Res, R8
GRM21BR61E106MA73L	\$1.72	Cap, C2, C3
C0805C473J3GACTU	\$2.16	Cap, C14
C2012C0G1H272J060AA	\$1.48	Cap, C12
CRCW040280K6FKED	\$0.33	Res, R14
CRCW0402100KFKED	\$0.33	Res, R3
TPS54388QRTERQ1	\$9.06	V reg, U6
GRM32ER60J107ME20L	\$3.20	Cap, C9
CRCW04022K10FKED	\$0.33	Res, R12
CRCW0402604KFKED	\$0.33	Res, R13
CL21C222JBFNNE	\$0.97	Cap, C13
B82464G4153M000	\$3.74	Ind, L2
UCL1V471MNL1GS	\$3.60	Cap, C15, C16
CRCW08055K36FKEA	\$0.57	Res, R6
CRCW0805510RFKEA	\$0.57	Res, R1
CRCW0805249KFKECC	\$0.54	Res, R11
10033526-N3212MLF	\$1.48	Conn, X1
Micro JST PH 2.0	\$6.99	Conn, J1
TPS56339DDCR	\$4.13	V Reg, U5
<b>Total</b>	<b>\$98.15</b>	



## **8. Conclusion**

While the Bike System might not sound all that impressive on the surface, there are many facets to the Bike System that required intricate design work. This is true for many modern engineered products that are taken for granted, and these products often present unique challenges. An example of this a computer vs an electric toothbrush. While a computer is going to certainly be more complex than an electric toothbrush, the toothbrush must consider limited power requirements since its battery powered, fit a certain small form factor, be water proof/resistant, etc. These challenges require a different design mindset and innovating thinking in order to be overcome. The Bike System is similar in the way that it presents unique challenges to the design team that required some thinking 'outside-the-box.'

The unique challenges presented during the development of the Bike System, and learning how to overcome those design challenges, is one of the most significant takeaways that this project had to offer. By tackling these challenges, the design team was able to grow as engineers. This was accomplished by allowing the team to step out from the theoretical material covered in classes, and learn what its truly like to design a product. When designing the Bike System, the design team was faced with a variety of standards and constraints that guided the decisions made, from the parts selection to the actual design itself. Through the process of the careful research and parts consideration, the team was able to apply their theoretical knowledge to find practical solutions to the challenges and problems that the Bike System presented.

Regardless of the feasibility of the Bike System as a consumer product, the design team learned many valuable lessons, such as working within standards and constraints, how to take an abstract problem and come up with a practical solution, and working as a team to surmount all the obstacles along the way to achieve a working product. These lessons will be carried forward into the careers of the members of the design team and have help make them capable engineers, ready to take one any engineering challenges that lie ahead of them.



## Appendix

### A.1 References

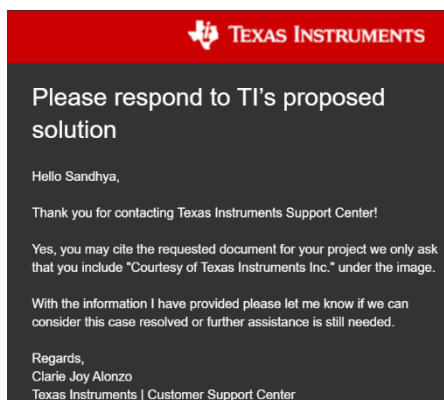
- [1] Generator Figure. Retrieved 10 October 2020 from <https://www.toppr.com/guides/physics/electromagnetic-induction/ac-generator/>
- [2] Swagatam (2019). Dynamo Figure. Retrieved 10 October 2020 from <https://www.homemade-circuits.com/bicycle-dynamo-battery-charger-circuit/>
- [3] (2016). Switching Regulator Figure. Retrieved 10 October 2020 from [https://techweb.rohm.com/knowledge/dcdc/dcdc\\_sr/dcdc\\_sr01/696](https://techweb.rohm.com/knowledge/dcdc/dcdc_sr/dcdc_sr01/696)
- [4] Zener I/V Plot. Retrieved 10 October 2020 from <http://www.learningaboutelectronics.com/Articles/Zener-diode-IV-characteristics-curve>
- [5] Whelan, Brendan. Bandgap Reference. Retrieved 10 October 2020 from <https://www.analog.com/en/technical-articles/how-to-choose-a-voltage-reference.html>
- [6] Shamieh, Cathleen. Battery Picture. Retrieved 10 October 2020 from <https://www.dummies.com/programming/electronics/how-batteries-work/>
- [7] Dynamo Picture. Retrieved 13 October 2020 from <https://havefunbiking.com/nokias-pedal-powered-charger-plans-influence-bike/>
- [8] Hub Dynamo Picture. Retrieved 13 October 2020 from <https://us.huntbikewheels.com/products/hunt-search-29-dynamo-disc-wheelset>
- [9] Chain Dynamo Picture. Retrieved 13 October 2020 from <https://www.aliexpress.com/item/32623236134.html>
- [10] "Different Types of Batteries and Their Uses" (2019). Retrieved 31 October 2020 from <https://components101.com/articles/different-types-of-batteries-and-their-uses>
- [11] Lowrider Dynamo Picture. Retrieved 1 November 2020 from [https://www.toplowrider.com/Dynamo-Generator-Bicycle-12V-6W\\_p\\_8300.html](https://www.toplowrider.com/Dynamo-Generator-Bicycle-12V-6W_p_8300.html)
- [12] QFN Size Reference. Retrieved 1 November 2020 from [https://en.wikipedia.org/wiki/Flat\\_no-leads\\_package#/media/File:28\\_pin\\_MLP\\_integrated\\_circuit.jpg](https://en.wikipedia.org/wiki/Flat_no-leads_package#/media/File:28_pin_MLP_integrated_circuit.jpg)
- [13] TSSOP Size Reference. Retrieved 1 November 2020 from [https://www.distrelec.biz/Web/WebShopImages/landscape\\_large/t/if/TSSOP-8.jpg](https://www.distrelec.biz/Web/WebShopImages/landscape_large/t/if/TSSOP-8.jpg)
- [14] Comparator Picture. Retrieved 1 November 2020 from <https://en.wikipedia.org/wiki/Comparator#/media/File:Opamp105.gif>
- [15] Rectifier Picture. Retrieved 1 November 2020 from <https://www.electronicstutorials.ws/power/single-phase-rectification.html>

- [16] "Logic Signal Voltage Levels." Retrieved 1 November 2020 from <https://www.allaboutcircuits.com/textbook/digital/chpt-3/logic-signal-voltage-levels/>
- [17] Claycomb, Timothy and Kay, Art (2014). "TI Designs - Precision: Verified Design; Comparator with Hysteresis Reference Design" Comparator Oscillations Picture. Retrieved 1 November 2020 from <https://www.google.com/url?sa=t&rct=j&q=&esrc=s&source=web&cd=&ved=2ahUKEwio1MnCh6jtAhUxRjABHbclAO0QFjAAegQIAxAC&url=https%3A%2F%2Fwww.ti.com%2Flit%2Ftidu020&usg=AOvVaw368P1IBljJQQ8KK9gu3xY1>
- [18] Hysteresis Plot. Retrieved 1 November 2020 from <https://www.analogictips.com/analog-comparators-and-hysteresis/>
- [19] Hall Sensor Reverence. Retrieved 1 November 2020 from <https://www.electronics-tutorials.ws/electromagnetism/hall-effect.html>
- [20] RFID Reverences. Retrieved 1 November 2020 from <https://www.atlasrfidstore.com/rfid-insider/near-field-vs-far-field-rfid-antennas> and <https://www.mdpi.com/2079-9292/8/2/129/htm>
- [21] Software Devolvement Image. Retrieved 15 November 2020 from [https://itlaw.wikia.org/wiki/System\\_Development\\_Life\\_Cycle#Overview](https://itlaw.wikia.org/wiki/System_Development_Life_Cycle#Overview)
- [22] ISO Standard for C. Retrieved 15 November 2020 from <https://www.iso.org/standard/74528.html>
- [23] Halogen Lamp. Retrieved 13 November 2020 from [https://en.wikipedia.org/wiki/Halogen\\_lamp](https://en.wikipedia.org/wiki/Halogen_lamp)
- [24] Buck-Boost Converter. Retrieved 13 November 2020 from <https://ieeexplore.ieee.org/abstract/document/7533493>
- [25] PWM. Retrieved 18 November 2020 from [http://homepage.cem.itesm.mx/carbajal/Microcontrollers/ASSIGNMENTS/readings/ARTICLES/barr01\\_pwm.pdf](http://homepage.cem.itesm.mx/carbajal/Microcontrollers/ASSIGNMENTS/readings/ARTICLES/barr01_pwm.pdf)
- [26] LED Info. Retrieved 20 November 2020 from <https://ieeexplore.ieee.org/abstract/document/6480835> and <https://ieeexplore.ieee.org/abstract/document/6978439>
- [27] Antenna Design Guide for MFRC52x, PN51x and PN53x, AN1445, Rev. 1.2, NXP Semiconductors, 2010.

## A.2 Copyrights

Other than the exceptions below (which are annotated in the above document), all images were of the public domain and free to use.

- (1) Webench® was used for regulator designs, and Scheme-it® was used for generating simple circuit diagrams as per the Service agreement: "...TI grants you permission to download, reproduce, display, and distribute TI Services solely for non-commercial or personal use...", see <https://www.ti.com/legal/terms-of-use.html> and the response from TI below.



- (2) Images free to use per: <https://creativecommons.org/licenses/by-sa/4.0/>
- (3) Images used from this site may be used for "personal use," see <https://www.rohm.com/terms-and-conditions> and the snippet from the terms:

Protection of intellectual property rights  
Information, text, graphics, images, photographs, and the like relating to products, services, and technology posted on this website (hereinafter collectively referred to as "Content") are protected by copyright law and various other treaties, laws, and other relevant restrictions.  
Guests may only use the Content for personal use and other purposes within the scope permitted by laws, treaties, and the like. Use exceeding those described above (including duplication, alteration, transmission, distribution, and transfer) is strictly prohibited without the express written consent of ROHM.  
Except for the above, this website does not constitute a license for customers to rights of any kind relating to copyrights, patent rights, trademark rights, or other intellectual property rights relating to the Content. If conditions of use for particular sections of the Content are individually indicated, the conditions in question shall take precedence. Trade names, trademarks, and emblems of ROHM or third parties used on this website are protected by trademark law, the Unfair Competition Prevention Law, and other regulations. These may not be used without the express permission of the rights holders.

- (4) Images used from this site may be used for "non-commercial" use, see [https://www.analog.com/en/about-adi/landing-pages/001/terms\\_of\\_use.html](https://www.analog.com/en/about-adi/landing-pages/001/terms_of_use.html) and a snapshot of the terms of service:

ADI grants you a revocable, non-transferable, non-exclusive license to view, print out or download a single copy of the ADI Information, solely for internal non-commercial or informational use provided that you do not remove any copyright, trademark or other proprietary notices. Other than the foregoing limited single copy license, no transfer of any other rights is made or intended with respect to the ADI Information and the ADI Site. ADI may terminate this single copy license at any time for any reason, including for any breach of these terms of use, or breach of any other ADI agreement or policy. Upon termination you will immediately destroy all ADI Information in your possession or control.

## A.3 Senior Design II Changes and Figures

This section covers the major changes and additions made during the course of Senior Design II and relevant figures. One of the most important additions would be the finalized board layouts for the three boards that were utilized. See Figures A1 – A3.

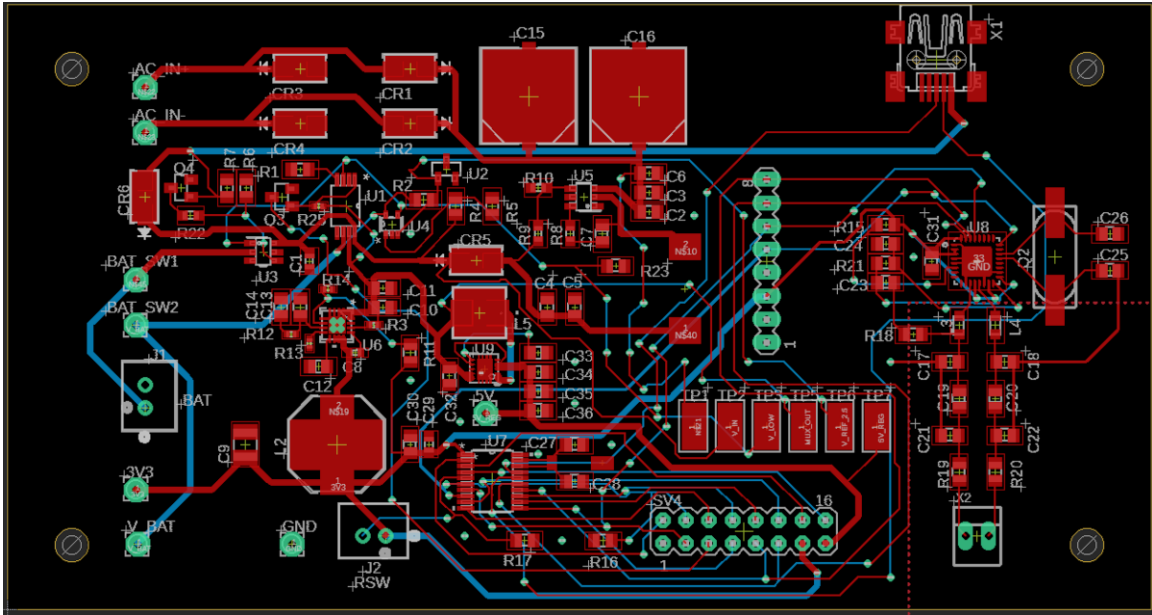


Figure A1. Main Board Layout

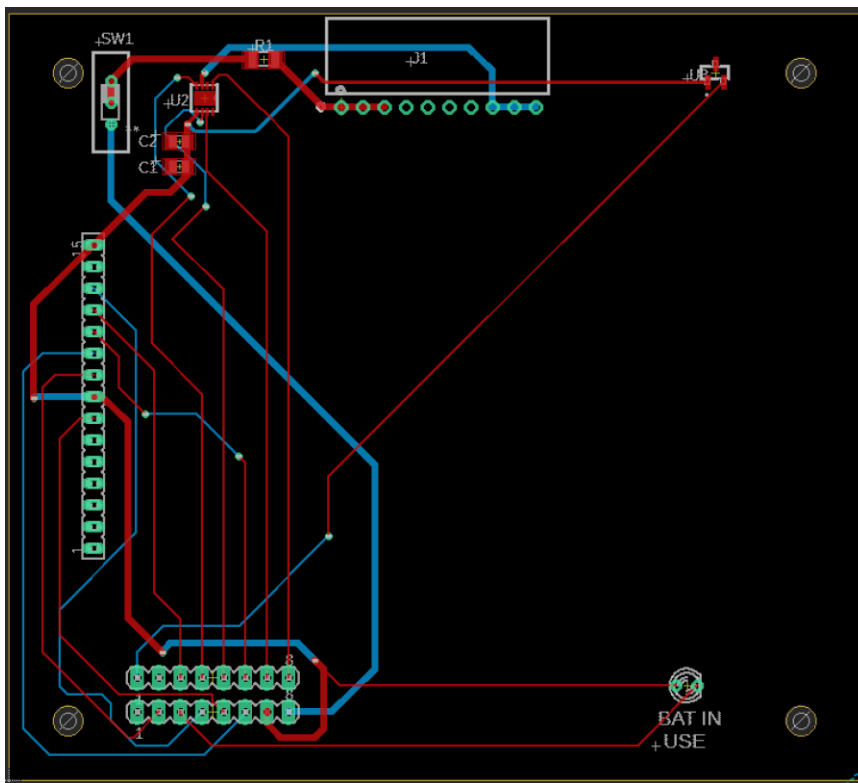


Figure A2. LCD Board Layout

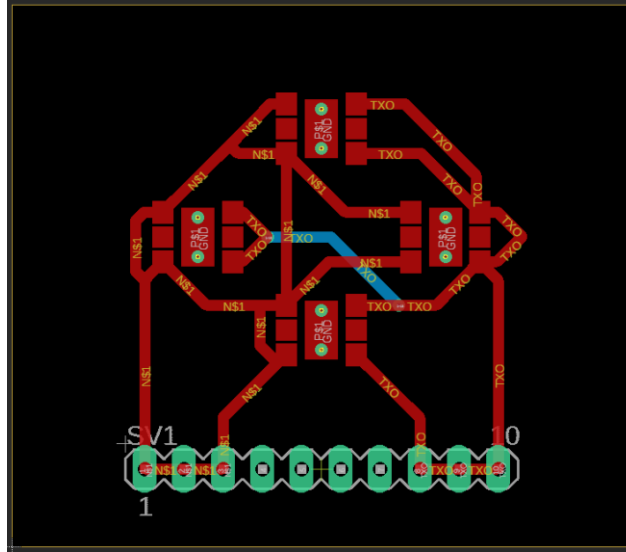


Figure A3. LED Board Layout

# Switching Stage

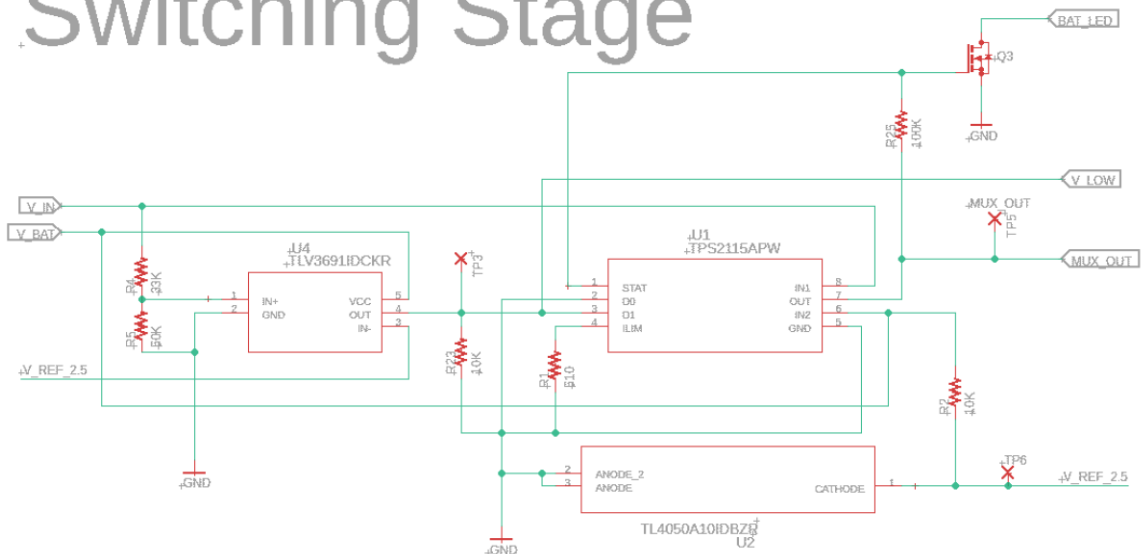


Figure A4. Power Subsystem's Updated Switching Circuit

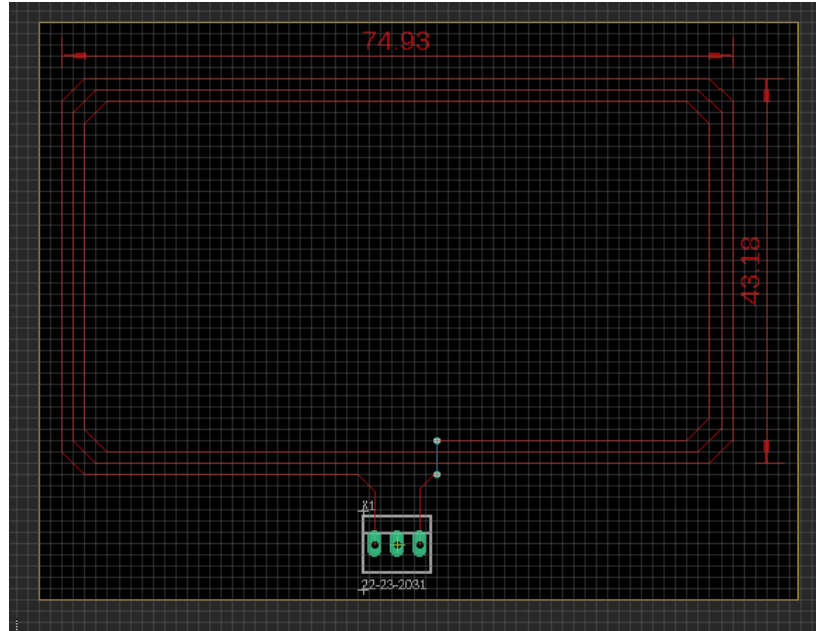


Figure A5. Antenna Layout

$$C_1 \approx \frac{1}{\omega \cdot \left( \sqrt{\frac{R_{tr} \cdot R_{pa}}{4}} + \frac{X_{tr}}{2} \right)}$$

$$C_2 \approx \frac{1}{\omega^2 \cdot \frac{L_{pa}}{2}} - \frac{1}{\omega \cdot \sqrt{\frac{R_{tr} \cdot R_{pa}}{4}}} - 2 \cdot C_{pa}$$

Figure A6. RF Matching Circuit Equations

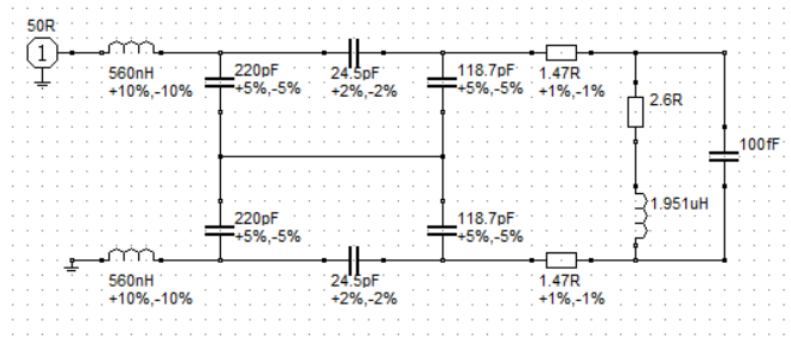


Figure A7. RF Simulation Circuit



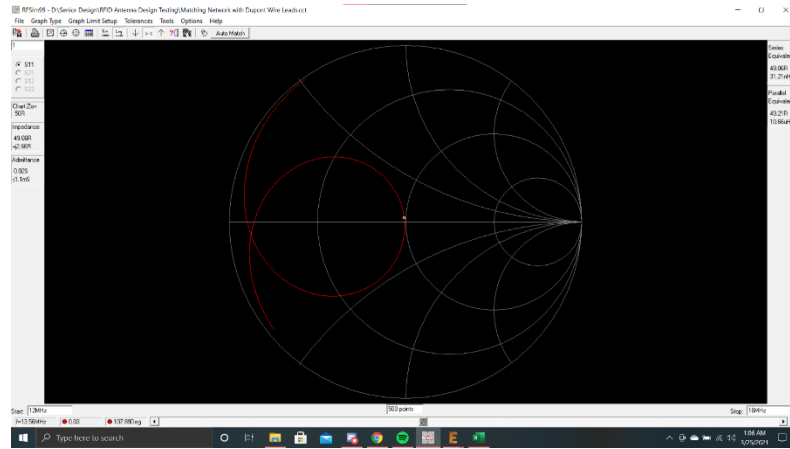


Figure A8. Smith Chart

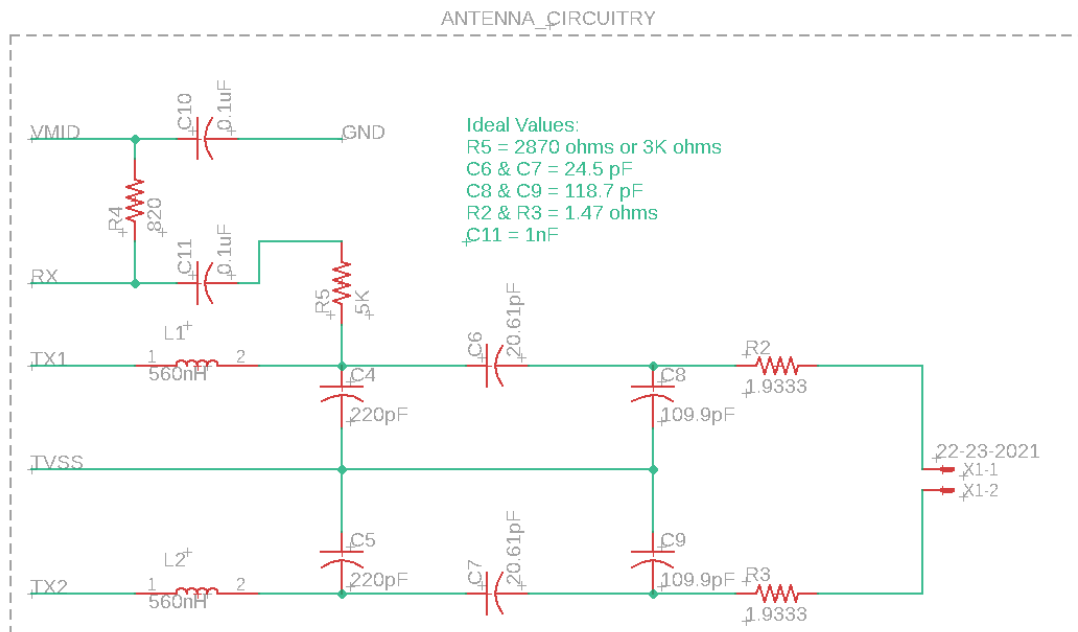


Figure A9. RFID Matching Network Schematic

## A.4 Source Code

-  tests.h
-  typedefs.h
-  msp.h
-  msp.c
-  main.c
-  lcd.h
-  lcd.c
-  graphics.h
-  graphics.c
-  fonts.h
-  config.h